

Tapping beam recognition and measurement with infrared camera

Optimisation of an industrial process using an thermal imaging camera and computer vision algorithms

JØRGEN NILSEN

SUPERVISOR

Sondre Sanden Tørdal

University of Agder, 2021

Faculty of Engineering and Science

Department of Engineering Sciences

Abstract

This thesis presents the research and development of an application for recognition and measuring of a ferrosilicon tapping beam using an Infrared (IR) camera. Ferrosilicon production is a highly endothermic process, requiring large amounts of energy to operate; thus, the need for increased efficiency is constant. Using an IR camera for non-intrusive measurements of the tapping beam and developing computer vision algorithms that can identify distinctive process parameters are investigated in this project. Today a video stream from an IR camera overlooking the tapping area at Elkem Thamshavn is directly displayed in the tapping control room with no form of warning labels or data logging. Thus, the motivation for this research is derived from the need for more direct feedback on the tapping beam to the on-site human operators and data logging for the metallurgists. Developing a system that can detect temperature, the shape of the tapping beam and alert operators of unwanted situations is set as the main goals for this project.

An application that connects the IR camera to a series of algorithms written in Python and publishes the resulting data to a web-based Human Machine Interface (HMI) is developed and tested on an NVIDIA Jetson Nano single-board computer with an Optris IR camera. It incorporates OpenCV, NumPy, Numba, SQLite database, and GStreamer as computing and data communication tools. With testing on a tapping beam test stand, where the molten ferrosilicon is replaced with warm water; the application has proven to give feedback on the beam shape, temperature and status of the tapping beam through the web-based HMI.

Preface

The work presented in this master's thesis has been performed as the final project in a two-year master's degree in Mechatronics at the University of Agder, Department of Engineering Sciences. It covers multiple elements within Mechatronics; programming of single-board computers, computer vision, camera technology and application development. The project has demanded dedication, resilience and structure, which have been challenging and highly rewarding.

Elkem has contributed to the project with the necessary equipment and expertise on the tapping process and production of ferrosilicon. Throughout the conduction of this master's project, multiple meetings have been held with the representatives at Elkem and arising questions have been quickly dealt with, and the correct information evoked. This has resulted in a project that complies with the challenges that are of interest for Elkem to solve and the requirements from the university regarding content and field of research.

And finally, a special thank you to the supervisor on this project, Sondre Sanden Tørdal, for valuable assistance and guidance.

Grimstad, Norway 2019-05-27



Jørgen Nilsen

Table of Contents

	Page
1 Introduction	2
1.1 Brief history of Elkem and silicon production	2
1.2 Motivation	3
1.3 Project scope and objectives	4
1.4 Limitations	5
1.5 Source code repository	5
1.6 State-of-the-art	6
2 Theory	8
2.1 Production of ferrosilicon	8
2.1.1 Producing ferrosilicon	8
2.1.2 Furnace construction	9
2.1.3 Electrical arrangement	10
2.2 Tapping process	13
2.2.1 Human operators	13
2.2.2 Tapping timeline	14
2.3 Infrared thermal camera	15
2.3.1 Infrared radiation	15
2.3.2 Infrared camera	16
2.4 Software tools and packages	18
2.4.1 Python	18
2.4.2 Numerical Python	18
2.4.3 Numba compiler	19
2.4.4 OpenCV	21
2.4.5 GStreamer	21
2.4.6 Flask application	22
2.4.7 GitLab	22
2.5 Computer vision	24
2.5.1 Locating features	24
2.5.2 Detail enhancement with histogram equalisation	26
2.5.3 Model fitting and data filtering	28
RANSAC basics	29
2.5.4 Edge detection	30
2.6 Project management and development	33
2.6.1 Gantt chart	33
2.6.2 Task management	33

3	Method	35
3.1	Implementation and use of thermal infrared camera	35
3.1.1	Optris PI400i thermal camera	35
3.1.2	Hardware integration	36
3.1.3	Software integration	36
	IR Imager Direct-SDK on Windows OS	37
	IR Imager Direct-SDK on Ubuntu OS	37
	Receiving data from the IR camera	38
3.2	Computer vision algorithms	39
3.2.1	Tappingbeam detection	39
3.2.2	Detail enhancement and binarization	40
	Equalising the histogram	40
	Creating a binary image	41
3.2.3	Data-filtering and model-fitting	42
3.2.4	Temperature calculation	43
3.2.5	Tapping beam algorithms	43
3.2.6	Application structure and data flow	46
3.3	Database and Human Machine Interface	47
3.3.1	SQLite database	48
3.3.2	Flask web interface	50
3.4	Tapping beam test stand	51
4	Results	53
4.1	Computer vision algorithms	53
4.1.1	Overall results	53
4.1.2	Template matching	53
4.1.3	Histogram equalisation and detail enhancement	54
4.1.4	Binary image	55
4.1.5	Inlier detection with RANSAC	56
	Just-In-Time compilation	57
4.1.6	Beam shape classification	57
4.2	Human Machine Interface and database	58
4.2.1	Overall results	58
4.2.2	SQLite database	59
4.2.3	Temperature data	59
5	Discussion and further work	60
5.1	Position of IR camera at Elkem Thamshavn	60
5.2	Detection of tapping beam	60
5.3	Application structure	61
5.4	Jetson Nano performance	62
6	Conclusion	63
A	Administrative	68
A.1	Project description	69
A.2	Gantt chart	70
B	System	72
B.1	System charts	73
B.1.1	Tapping process timeline	73
B.2	Datasheets	74
B.2.1	Optris PI 400i	74

B.2.2	IR Camera application flowchart	76
B.2.3	Synthetically developed images	77
B.3	Human Machine Interface	79
B.3.1	Flask web-HMI homepage	79
B.4	Database file	80
B.4.1	Temperature table	80
B.4.2	Image data table	81
C	Code	82
C.1	Computer vision algorithms	82
C.1.1	mainRealTime.py	82
C.1.2	IRCamera.py	86
C.1.3	FeatureTracking.py	92
C.1.4	BeamDetector.py	95
C.1.5	RansacFit.py	100
C.1.6	Database.py	106
C.2	Human Machine Interface	110
C.2.1	mainFlask.py	110
C.2.2	home.py	111
C.2.3	base.html	115
C.2.4	home.html	117

List of Figures

1.1	Drawing of a silicon furnace [5].	3
1.2	Drawing of the tapping process [5].	3
1.3	IR camera installed at Elkem Thamshavn oven nr. 2 [6].	4
1.4	Thermal image from the tapping beam at Elkem Thamshavn oven nr. 2 [6].	4
2.1	Process block of the Ferrosilicon process	8
2.2	System overview of the ferrosilicon process [5].	9
2.3	Furnace construction[10].	10
2.4	Electrical arrangement of electrodes.	11
2.5	Section view of a Söderberg electrode	12
2.6	Operators working in the tapping area at Elkem Salten [13].	13
2.7	The electromagnetic spectrum [15].	15
2.8	A typical microbolometer [17].	16
2.9	Working principle of a bolometer [18].	16
2.10	Readout circuit for a uncooled microbolometer array [18].	17
2.11	Python logo [19].	18
2.12	Process for compiling Python code with the JIT decorator [22].	19
2.13	OpenCV logo[23].	21
2.14	Gstreamer overview [24].	21
2.15	Flask "Hello world!" example.	22
2.16	Git workflow [26].	23
2.17	Coordinates used in template matching. $T(x', y')$ is the coordinates locally to the template and $I(x, y)$ is the coordinates locally to the larger image.	25
2.18	Example picture for template matching.	25
2.19	Template image extracted from figure 2.18.	25
2.20	Applied template matching.	26
2.21	Effects of histogram equalisation [27].	26
2.22	Normal histogram and the cumulative histogram [27].	27
2.23	Histogram equalised image [28].	27
2.24	Data set containing both inliers and outliers [29].	28
2.25	Least-squares linear fitting on the dataset [29].	28
2.26	RANSAC compared to least-squares [29]. Note that the least-squares linear fitted line is biased by the blob of outliers.	29
2.27	Illustration of the RANSAC principle. Where the data is presented in the \mathbb{R}^2 -domain.	29
2.28	Sampled horizontal 1D-vector of an image	30
2.29	One dimensional convolution of a Gaussian filter and it's partial derivative.	31
2.30	Convolution with a Gaussian partial derivative filter [31].	32
2.31	TeamGantt example [32].	33
2.32	Trello example	34

3.1	Optris PI 400i thermal camera with standard O29 lens [36].	35
3.2	Optris PI 400i thermal camera, USB and PIF input terminals [36].	36
3.3	Optris PI 400i thermal camera connected to a computer running either Linux Ubuntu or Windows 10.	36
3.4	General application structure for cross-platform compatibility.	37
3.5	Application layout.	39
3.6	Grayscale input image for the template matching.	40
3.7	Template for the input image.	40
3.8	Resulting example image from <code>TemplateMatching()</code>	40
3.9	Histogram equalised image.	41
3.10	Binary image.	42
3.11	Horizontal sampling of the tappingbeam to detect shape.	44
3.12	Convolution with a derivative-Gaussian filter and absolute value on the result.	45
3.13	Edge detection algorithm example.	46
3.14	Application structure and data flow.	47
3.15	Application sequence and data flow.	47
3.16	Application layout.	50
3.17	HMI label for optimal tapping beam profile.	51
3.18	HMI label for split tapping beam.	51
3.19	HMI label for stopped tapping beam.	51
3.20	HMI label for free pouring tapping beam.	51
3.21	HMI label for inverted tapping beam.	51
3.22	Top view of the test stand.	51
3.23	Camera view of the test stand.	51
3.24	Grayscale thermal image from the test stand.	52
4.1	Input thermal image to the template matching.	54
4.2	Isolated tapping beam image returned from template matching.	54
4.3	Histogram equalised image.	54
4.4	Unequalised histogram of figure 4.2.	55
4.5	Histogram of the equalised image in figure 4.3.	55
4.6	Unequalised cumulative histogram of figure 4.2.	55
4.7	Cumulative histogram of the equalised image in figure 4.3.	55
4.8	Resulting binary image	56
4.9	Effects of JIT-compilation with increasing computational load.	57
4.10	Observation of a split tapping beam at the plant in Thamshavn.	58
4.11	Synthetically created image of a divided tapping beam.	58
4.12	HMI video stream.	59
4.13	HMI status labels.	59
4.14	HMI temperature graph made with Chart.js	59
5.1	Suggested application structure	62
B.1	Tapping process manual operations timeline.	73
B.2	Optris PI 400i datasheet, page 1.	74
B.3	Optris PI 400i datasheet, page 2.	75
B.6	Database temperature data.	80
B.7	Database image data.	81

List of Tables

3.1	Optris PI 400i general specifications [36].	35
3.2	NVIDIA Jetson Nano specifications [37].	36
3.3	Optris SDK API comparison [38].	37
4.1	Average load and performance while running <code>mainRealTime.py</code> on the Jetson Nano.	53
4.2	Detected inliers from binary image in figure 4.8.	56
4.3	Optimised parameters for the RANSAC linear model.	56
4.4	Average execution time of the RANSAC-function, with and without JIT-compiling.	57
4.5	Number of detected edges	58
B.1	Synthetically developed image number 2.	77
B.2	Number of detected edges in image number 2.	77
B.3	Synthetically developed image number 3.	77
B.4	Number of detected edges in image number 3.	77
B.5	Synthetically developed image number 4.	77
B.6	Number of detected edges in image number 4.	77
B.7	Synthetically developed image number 5.	78
B.8	Number of detected edges in image number 5.	78

List of Abbreviations

- AC** Alternating Current. 8, 10, 12
- AI** Artificial Intelligence. 3, 61
- API** Application Programming Interface. 36
- BGR** blue, green and red. 39
- BOF** Basic Oxygen Furnace. 6
- DLL** Dynamic-link Library. 37, 38
- dpkg** Debian package. 37
- HMI** Human Machine Interface. 4, 5, 21, 22, 43, 46, 48–50, 58, 61, 63, 64
- HTML** Hypertext Markup Language. 50, 58
- IR** Infrared. 4–7, 15–17, 21, 35–39, 43, 46–48, 50, 51, 53, 54, 58, 60, 61, 63
- JIT** Just-In-Time. 19, 20, 53, 57, 62
- NumPy** Numerical Python. 18, 19, 36, 40, 43, 57, 62
- OOP** Object-oriented programming. 18
- OpenCV** Open Source Computer Vision Library. 21, 24, 36, 39, 53, 60–63
- PER** Plan, Execute and Reflect. 33
- PIF** Industrial Process Interface. 35, 36
- PLC** Programmable Logic Circuit. 35, 36
- R&D** Research and Development. 2, 6
- RANSAC** Random Sample Consensus. IV, 28–30, 42, 43, 56, 57, 60, 61, 63, 64
- ROI** Region of Interest. 7, 44, 54, 60, 63
- SAF** Submerged Arc Furnace. 3, 8, 9
- SDK** Software Development Kit. 36, 37
- UN** United Nations. 2
- USB** Universal Serial Bus. 35, 36, 53, 61
- VPN** Virtual Private Network. 60

List of Nomenclature

Constants

π Pi 3.141592

Units

V Volts

Hz Hertz

s Second

m Meter

ϵ Emissivity

η Fill factor

C Celsius

K Kelvin

Introduction

1.1 Brief history of Elkem and silicon production

Elkem was founded in 1904 by the industrial entrepreneur Sam Eyde, with the intention of developing technology and industry based on the natural resources in Norway. Over 110 years, Elkem has played a vital role in the development of the Norwegian process industry and technology. Covering aluminium production, the invention of the Söderberg electrode and the position as a world-leading producer of silicon and other special alloys [1]. Today, Elkem consists of three business divisions. Silicones, a fully integrated silicones producer. Silicon Products, a provider of silicon, ferrosilicon, foundry alloys, micro-silica and related speciality products. And finally, Carbon Solutions, a supplier of electrode paste and speciality products to the ferroalloy, silicon and aluminium industries [2].

Sustainable development is central to Elkem's production strategy and a defining factor in conducting their business and production development. New technology is implemented for developing products of higher quality and increasing production efficiency. Using less energy to create the best possible products. Elkem has developed its sustainability goals in line with the principles of the United Nations (UN) Global Compact, supporting the ambitions of the Paris climate agreement and the UN Sustainable Development Goals [3].

Silicone-based materials and products are particularly common and essential in embedded electronics, the healthcare industry, industrial processes and energy production. In 2013, 2.1 million tonnes of silicone products were sold on a global basis, yielding a turnover of \$11 billion and around \$40 billion in downstream added value [4]. The silicone production industry maintains a high focus on innovation and implementation of new technology, investing approximately 4% of the global turnover into Research and Development (R&D) [4].

1.2 Motivation

In the process industry, the implementation and development of new technology have always been a defining feature and a necessity for increasing production efficiency, quality and plant safety. Elkem has since its origin placed a focus on technology, with the development of the Söderberg electrode as an example. With the advancements in computer science, Artificial Intelligence (AI), and sensor technology; information and process data availability allows for a higher level of understanding and real-time status on previously immeasurable operations. Many parameters in the production of Elkem's products are not directly measurable due to high temperatures in and around the furnace. Traditional sensors that need to be in direct contact with the measuring medium will not survive over extended periods. Non-intrusive measurements, measure process parameters without disturbing the process and are the appropriate method for extracting information from a ferrosilicon furnace.

Ferrosilicon is produced in a Submerged Arc Furnace (SAF), where raw material is added from the top, and the three electrodes reduce the mass down to the resulting molten ferrosilicon. The resulting alloy is retrieved through a spout on the side of the furnace, in a process called tapping. When tapping is initiated, the hole above the spout into the furnace, is manually opened by drilling. The molten alloy is then poured into a ladle; a vessel that transports the molten alloy. The process of tapping molten metal into the ladle is a fairly non-complex task but provide valuable information about the furnace operation and the produced ferrosilicon.

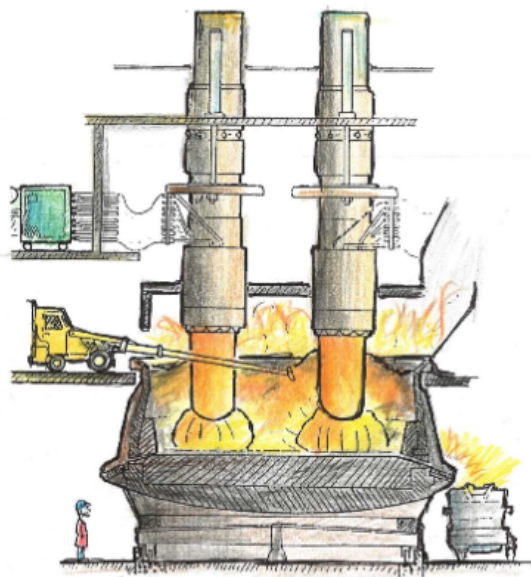


Figure 1.1: Drawing of a silicon furnace [5].

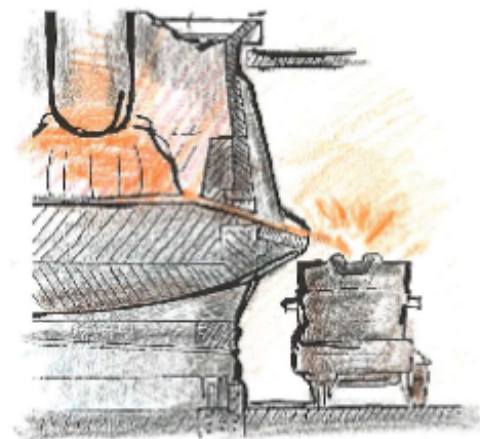


Figure 1.2: Drawing of the tapping process [5].

Sensors that can provide a means of non-intrusive measurement in this process is thermal imaging cameras and pyrometers. They both offer temperature measurement, but the thermal camera can be used in combinations with computer vision algorithms to extract information about tapping beam shape, slag detection and temperature at specific regions. Providing the process operators and metallurgists with as much information as possible about the process and the post tapping conditions, increases the final product quality.



Figure 1.3: IR camera installed at Elkem Thamshavn oven nr. 2 [6].



Figure 1.4: Thermal image from the tapping beam at Elkem Thamshavn oven nr. 2 [6].

As of the time of this project, an Infrared (IR) camera is installed at Elkem's plant in Thamshavn, Orkanger, providing a display of the tapping beam, ladle and surrounding area. The video feed is displayed on a separate monitor in the tapping control room, not directly connected to the operator's control and information system. Therefore, alerting the operators of unwanted and potentially dangerous conditions and logging information about the tapping beam temperature is highly sought-after.

Dangerous and unwanted conditions in the tapping process are listed as:

- Clogging of the tapping hole: Tapping beam flow ceases due to clogging of the furnace tapping hole.
- Inverted tapping beam: Tapping flow does not separate from the furnace spout; instead, it flows down and along with the spout, potentially hitting the ladle lining.
- Detect separation of tapping beam: The tapping beam is split into multiple smaller beams, increasing the surface area and lowering the overall temperature.

1.3 Project scope and objectives

This project aims to solve the challenge of using an IR thermal imaging camera for sensing parameters from an industrial process, specifically the tapping beam of molten ferrosilicon from the furnace into the ladle. Existing software for image processing, application development, and database communication is implemented as tools to help develop detection algorithms and display the parameters of interest. An IR camera is implemented as the sensor for non-intrusive measurement on the tapping beam.

Elkem has stated their expectations for this project, summarised as follows:

- Measure metal temperature in tapping beam.
- Measure the tapping beam profile.
- Give feedback on the shape of the tapping beam; is it a solid continuous beam or sparse and disrupted.
- Give feedback if the tappingbeam is no longer present, i.e. the tap-hole is clogged.

To help facilitate the above mentioned goals, further tasks are implemented:

- Build an intuitive cross-platform web-based Human Machine Interface (HMI) for interfacing the technology and presenting the operator with important values and video stream.

1.4 Limitations

Limitations for the work in this master's project. The main limiting factor in this project is the timeline, with a starting date of January 5th and a submission date set to the 28th of May, affecting the overall scope and possible workload. Throughout the project, simplifications of the process had to be made to develop a system that solves the objectives within the proposed timeline. For example, building a test stand of the tapping process that uses hot water as the medium was necessary as implementation throughout the project's development phase was impossible. Planning for a project of this magnitude and complexity also proved to be a challenge, as the author of this project had little experience with computer vision systems, process industry, IR camera and Python programming.

1.5 Source code repository

The application source code developed in this project is available as a GitLab repository. The Python code for the computer vision algorithms and the HMI is also included in the appendix C.1 and C.2.

<https://gitlab.com/gurgle96/elkemvision/>

1.6 State-of-the-art

Using an IR camera to sense parameters from an industrial environment is not a novel implementation. The British army was the first to develop a stand-alone camera system for detecting objects based on their heat (infrared radiation) [7]. This camera system was developed in 1929, and its sole purpose was to detect enemy aircraft. Since then, the IR camera development was mainly conducted through military R&D, resulting in systems for portable night vision and naval firefighting equipment. Today the IR technology is used in various industries, including; law enforcement, search and rescue, process industry and building inspection [7]. Regarding this thesis, implementations and research on IR thermal camera for detecting equipment-wear levels and process parameters are evaluated and put into context with this thesis scope and objectives.

Following the de-classification of IR camera technology in 1992 and the concurrent development of new detector technology, IR sensors and cameras became much more affordable and efficient. The IR detector's previous design and construction required the detector to be actively cooled, adding complexity and cost. At the end of the 1990s, these detectors were designed around Barium Strontium technology, which does not require cooling. Thus, significantly lowering the production complexity, cost and physical size [7]. Moving into the 21st century, where a higher focus has been placed on industrial efficiency, predictive maintenance and safety, the usage of IR cameras accelerated.

An industrial application of IR camera technology for predictive maintenance and fault detection is demonstrated in article [8]. In this article, a 3-phase electric motor, commonly used in industrial applications, is monitored with an IR camera to develop fault detection algorithms and techniques. The authors of this article evaluated several different signals for estimating the electric motor behaviour, such as mechanical vibration, stator current, acoustic signals, and thermal images. Closing in on the thermal image due to the availability of information and noise-free behaviour. To diagnose the electric motor, a series of neural network algorithms were developed and trained. The results of the research in this article was a system for detecting faults and give diagnostic feedback on a 3-phase electrical motor, categorising the motors into three separate categories; (1) healthy, (2) two broken rotor bars and (3) faulty squirrel-cage ring. This article also emphasises the use of neural networks for algorithm development, given that there is, or it is possible to create, data sets of reasonable size for training.

In the process industry, especially the metal production industry, thermal power is a common energy source and contains vital parameters about the raw materials, equipment and final product. In article [9], detecting slag in the tapping stream of steel from a Basic Oxygen Furnace (BOF) is investigated. Slag is a byproduct of the reduction process in the furnace; it floats on top of the molten metal and protects it from further oxidisation. When poured from the furnace into the ladle, slag is present in the stream and increases from 0 - 100 percent as the tapping process continues. Therefore, having an understanding of the amount of slag in the ladle is essential for further processing and alloying. In this article, the authors developed a system for monitoring the tapping beam and detecting slag based upon the difference in infrared radiation between slag and the desired metal product. A metal temperature probe mounted inside the BOF is also incorporated to calibrate the IR camera. Furthermore, the authors developed methods for calibrating the threshold temperature and tracking the tapping beam; these methods are described in the points below.

- Temperature threshold calibration: To separate the slag from the tapping beam, the temperature matrix from the IR camera and data from the internal temperature probe in the furnace is used. When tapping is initiated, and the flow of metal is slag-free, the IR camera temperature of the tapping beam is compared to the molten steel temperature from the probe inside the furnace, and the emissivity of steel is calculated with equation 1.1. The calibrated emissivity value for steel is used to give a precise representation of the tapping beam temperature, and while the beam is slag free the maximum IR camera temperature is recorded. This value is the threshold temperature between slag and molten metal in the tapping beam.

$$\epsilon = \left(\frac{T_{infrared}}{T_{probe}} \right)^4 \quad (1.1)$$

- Tracking of the tapping beam: The Region of Interest (ROI) where the tapping beam is located is found by horizontally iterating through the temperature columns, from left to right and from right to left. Finding the vertical edges of the tapping beam based upon the threshold temperature value. A square bounding box can then be defined around the tapping beam, with top and bottom height values manually defined.

With the research in the articles mentioned above, it is clear that using an IR camera for non-intrusive measurement of process parameters and extracting data not visible to the human eye is not a novel development. Thus, the existing research motivates this thesis, despite clear challenges and differences in this specific implementation.

In this project, the focus is not on closed-loop control of the ferrosilicon furnace, with feedback from the tapping beam. This is primarily due to the high degree of complexity in the ferrosilicon process. Despite this, the project is leaned towards extracting information about the tapping process that is of value to both on-site operators and the metallurgists for a safe and economic tapping operation and correct post-processing of the tapped metal. An IR camera developed by Optris GmbH is mounted at one of Elkem's ferrosilicon plants and monitors the tapping process. Today this video feed is only viewed by the on-site operators and not implemented in any algorithm.

Theory

2.1 Production of ferrosilicon

In this section, an overview of the metallurgical processes and equipment used in ferrosilicon production is described. The process of turning raw materials into ferrosilicon, basic construction of a Submerged Arc Furnace (SAF) and the arrangement of the Söderberg electrodes, are explained to better understand the complexity of the process.

2.1.1 Producing ferrosilicon

Ferrosilicon and other ferrous alloys are produced by carbothermic reduction of the added raw materials in a SAF. Mineral ores and carbon are added as charge material into the furnace, converted to the desired alloy through carbothermic reduction. The reduction process of charge material is highly endothermic, thus requiring a large amount of thermal energy. The thermal energy is converted from electrical energy by three self-baking Söderberg electrodes through Alternating Current (AC) arcing. Where heat is generated in the AC arcs that span between the electrode tip and the molten alloy bath. The electrodes are electrically arranged in a star connection, with the transformers supplying the stepped-down voltage arranged in a delta connection. Each electrode is connected to one phase.

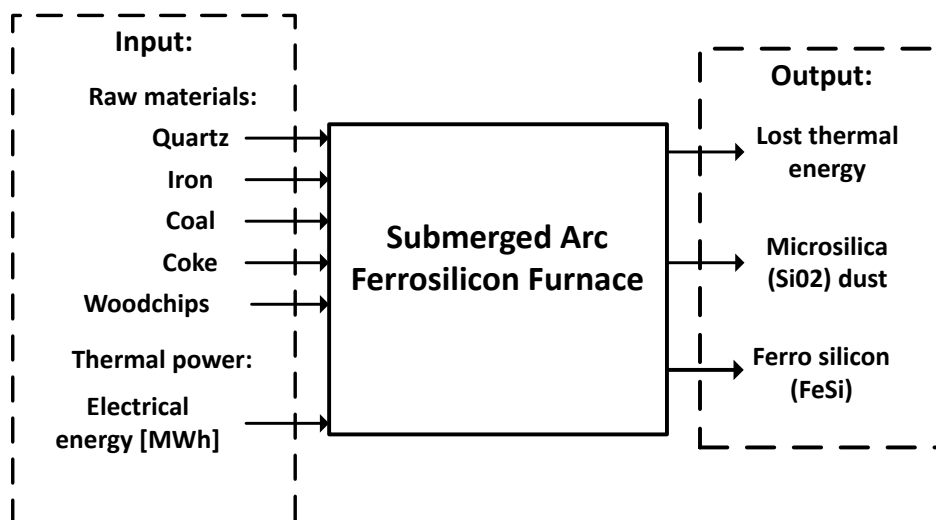


Figure 2.1: Process block of the Ferrosilicon process

Figure 2.2 describes the process of creating ferrosilicon from raw material to the tapping process. Starting with piles of raw material; quartz, iron, coal, coke and wood chips, loaded onto conveyor belts, refined and then stored in silos, ready to be discharged into the furnace. Inside the furnace, the three Söderberg electrodes creates electric arcs that generate the necessary thermal energy for the raw materials to reduce and combine into ferrosilicon.

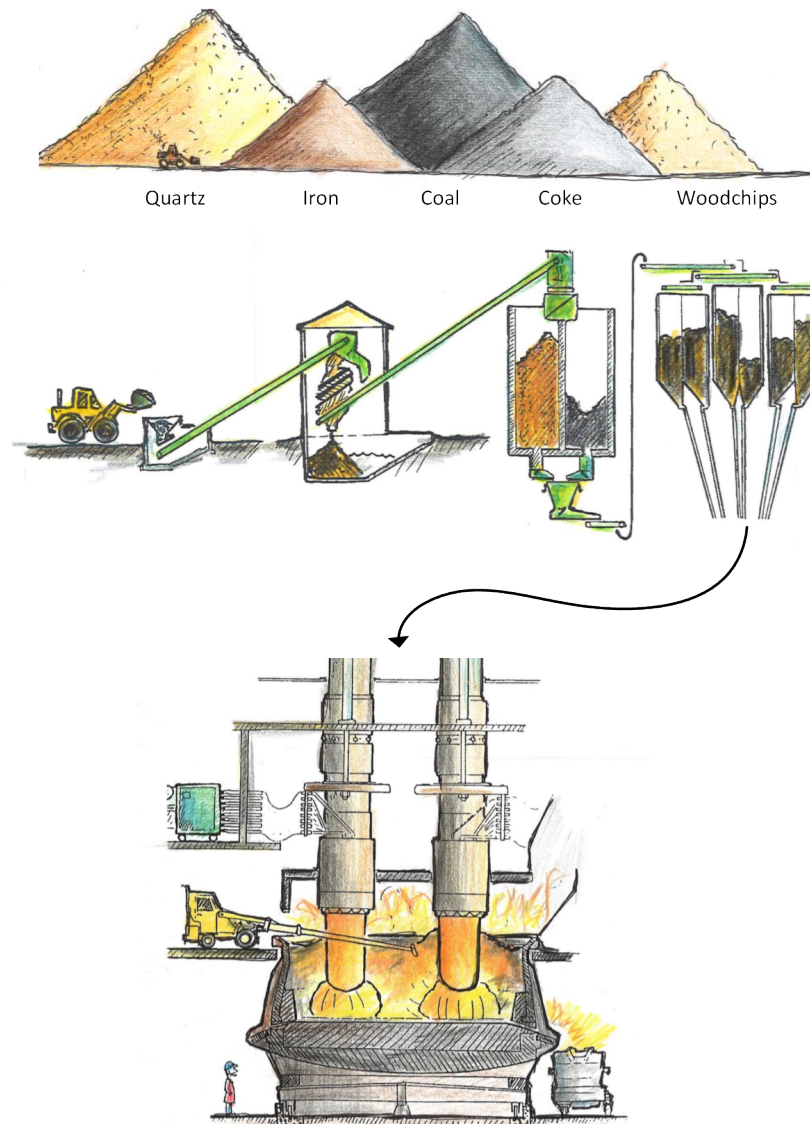


Figure 2.2: System overview of the ferrosilicon process [5].

2.1.2 Furnace construction

At the Elkem plant in Thamshavn, oven nr. 2 is designed and constructed as a typical SAF. The furnace is constructed as a cylindrical body, with an outer steel casing providing the structural rigidity and carbon blocks insulating the furnace to withstand the internal process temperatures. Tapping spouts that transfer molten silicon out from the furnace are positioned on the outside circumference of the furnace, towards the bottom. Around the furnace, there are tracks that move the ladle around with the furnace as it rotates. The furnace rotates around its centre axis to reduce the formation of cavities in the charge material, using the electrodes as stirring sticks. It takes several hours for the furnace to complete one full rotation, and the tapping process is done within approximately 2 hours. The tapping beam is still within the same angular quadrant from start to finish, continuously in line of sight for the tapping operators.

Transporting the molten metal away from the inside of the furnace is done by tapping into a ladle. A ladle is the containment vessel for the tapped ferrosilicon, constructed from many of the same materials as the inside of the furnace. The tasks of the ladle are to be positioned under the tapping spout, be filled up with molten ferrosilicon and contain this molten metal as it is transported over to the casting moulds. After casting, the molten metal cools down and hardens. When it reaches a specific temperature, it is removed from the moulds and crushed into finer particles. The tapping process is further explained in section 2.2.2.

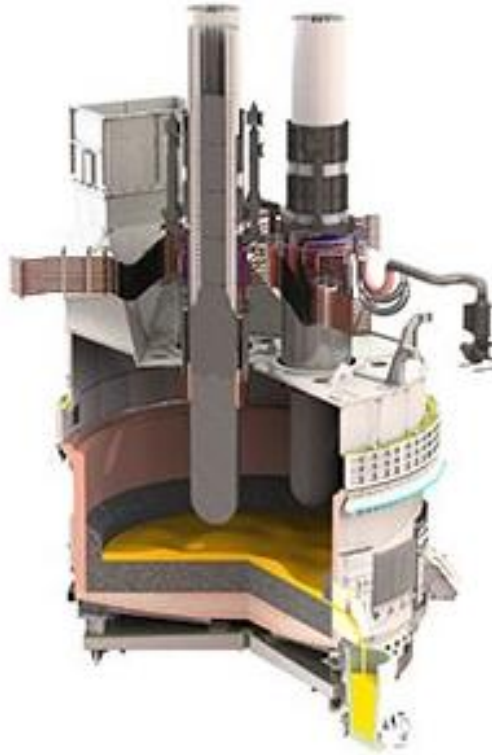


Figure 2.3: Furnace construction[10].

2.1.3 Electrical arrangement

Thermal energy is necessary for the carbothermic reduction process to take place; the most efficient way to produce this is to convert it from electrical energy. The electrical energy is converted to heat through AC arcing. Three Söderberg electrodes are positioned in a triangle, each connected to one phase of the system in a delta-star arrangement. The three electric arc spans from the tip of each electrode into the molten pool of ferrosilicon, directly heating the metal and surrounding charge. Some thermal energy is also generated in the upper parts of the electrode due to the electrical resistance, and the surrounding charge material absorbs this thermal energy. A simplified model of a typical electrical arrangement of the connected electrodes can be seen in figure 2.4 along with a detailed electrode cross-section in figure 2.5.

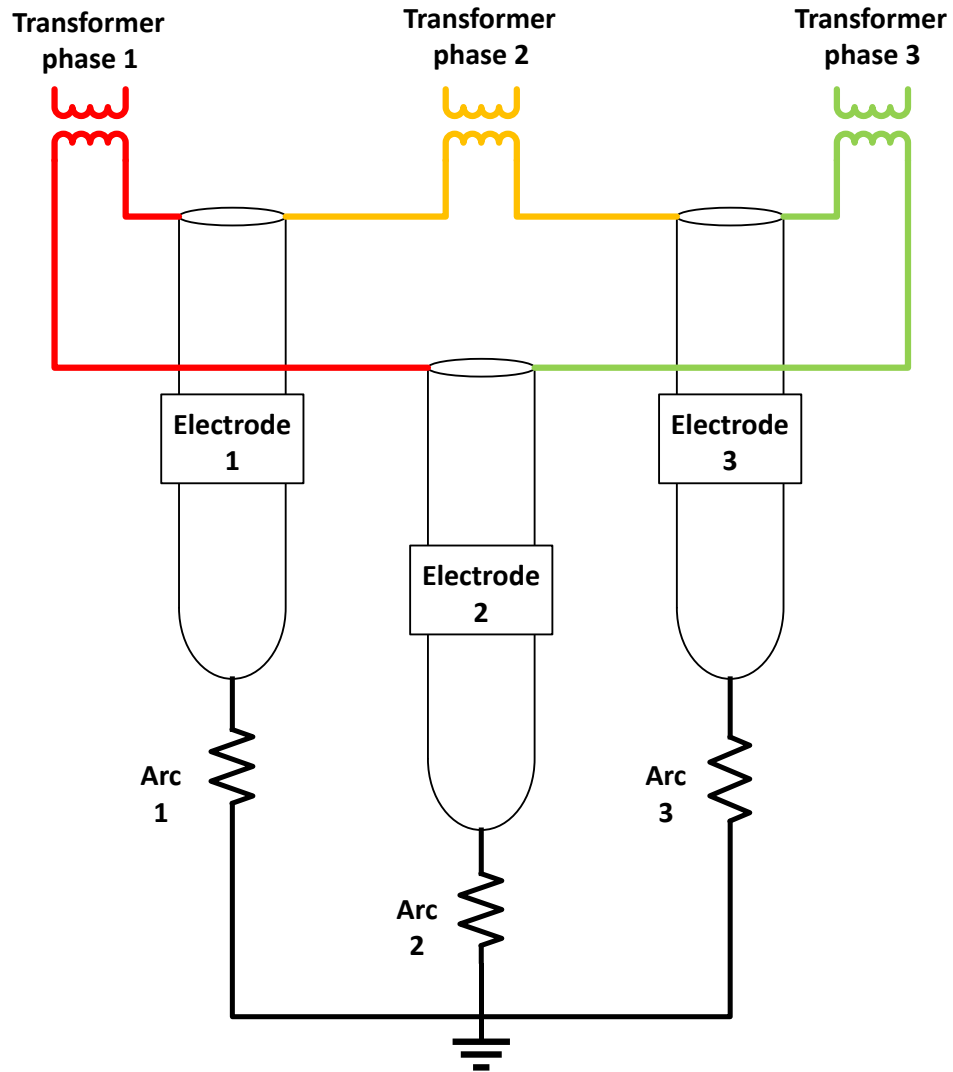


Figure 2.4: Electrical arrangement of electrodes.

The Söderberg electrode is composed of an outer steel casing, electrode paste, electrical slip-rings and height adjusting cylinders. The steel casing contains the paste and provides structural rigidity to the electrode. The electrode paste is a substance consisting of calcined anthracite, petroleum coke and pitch as a binder. Initially the paste is loaded into the electrode as hard briquettes, it is then liquefied as the temperature increases. Once the temperature reaches about 500°C , the paste is baked; transitioning from a soft viscous substance into the hard electrode tip that generates the AC arc [11]. During nominal operation, the phase voltage of the electrode is kept constant and the current flow in the electrode is regulated by the height between the electrode tip and ferrosilicon bath, explaining the need for the height adjusting cylinders [12].

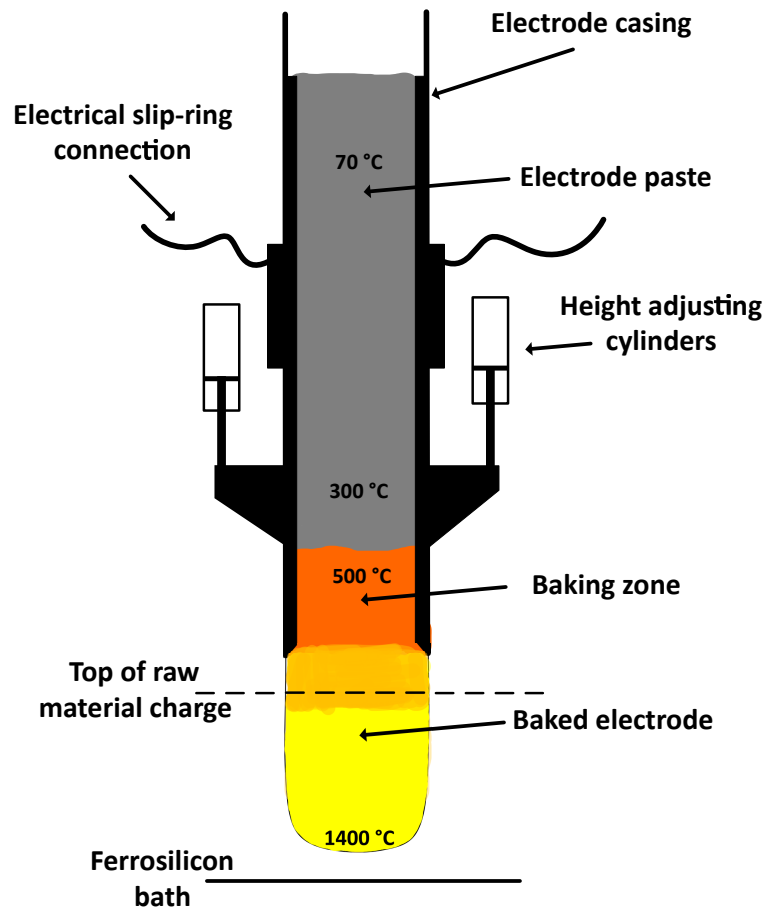


Figure 2.5: Section view of a Söderberg electrode

2.2 Tapping process

In this section, the theory and knowledge surrounding the process of tapping molten ferrosilicon from the furnace to ladle are explained. The working environment and challenges that the operators face in and around the tapping area and the discrete tasks that they complete, are presented.

2.2.1 Human operators

The process of creating ferrosilicon is a hybrid of automated systems and manually executed tasks. The integration and synchronisation of these systems are vital to sustain optimal performance of the furnace and to ensure the best possible product. The post-tap-hole operations that are done manually, can be summarised as follows:

- Temperature measurements of the tapped ferrosilicon.
- Material sampling.
- Monitoring the level of ferrosilicon in the ladle.
- Opening and closing of tap-hole.
- Cleaning and maintaining the tapping spout.
- Adding material to alloy the raw ferrosilicon.

The environment in the tapping area is described as a hazardous environment, due to high temperature radiation generated by the furnace and the risk of molten metal splashing during the tapping process. Figure 2.6 shows how close the operators are to the process. The equipment used to perform sampling and testing of the tapping beam is designed in such a way that the operators can stay within reasonable distance, an example are long reach lances and temperature probes used to condition and monitor the tapping beam during operation. The workers also wear protective clothing that reflects most of the radiant heat and can withstand minor splashing of slag/liquid metal.



Figure 2.6: Operators working in the tapping area at Elkem Salten [13].

2.2.2 Tapping timeline

The tapping process is initiated by manually drilling open a plug in the furnace, creating a direct flow-path for the molten metal into the tapping spout. Operators must continuously monitor the tapping beam and treat the spout and hole to prevent clogging and improper flow. Tapping of ferrosilicon into the ladle is done with certain interval's, as the internal level of ferrosilicon in the furnace must be brought back. One tapping process elapses over approximately 120 minutes and throughout this time a series of tasks are executed, as mentioned in section 2.2.1. Terminating the tapping process is done by inserting a plug made of clay, the plug rapidly solidifies due to the high temperature and blocks any more ferrosilicon to exit the tap-hole. Furthermore, the flow-chart in appendix B.1 describes the timeline for the tapping-process and the details surrounding each task.

2.3 Infrared thermal camera

In this section, the theory regarding the IR camera is presented. Explaining the basics of infrared radiation, where it is placed in the electromagnetic spectrum and how the wavelengths are classified as temperature regions. The detector element in an IR camera is also presented, explaining the design and working principle.

2.3.1 Infrared radiation

A body with a temperature above absolute zero ($-273[^\circ\text{C}]$) emits radiation in electromagnetic waves, scientifically called IR radiation. Figure 2.7 shows the spectrum of electromagnetic radiation and classifies the known sources of radiation. In the electromagnetic spectrum, the IR region is located to the right of the visible region, covering wavelengths from $0.7[\mu\text{m}]$ to $1[\text{mm}]$. Therefore, increasing the temperature of the emitting body yields a higher intensity of radiation, and IR waves with high energy are denoted by short wavelengths (close to $0.7[\mu\text{m}]$). However, IR is not visible to the human eye, requiring special sensors and cameras to be detected[14].

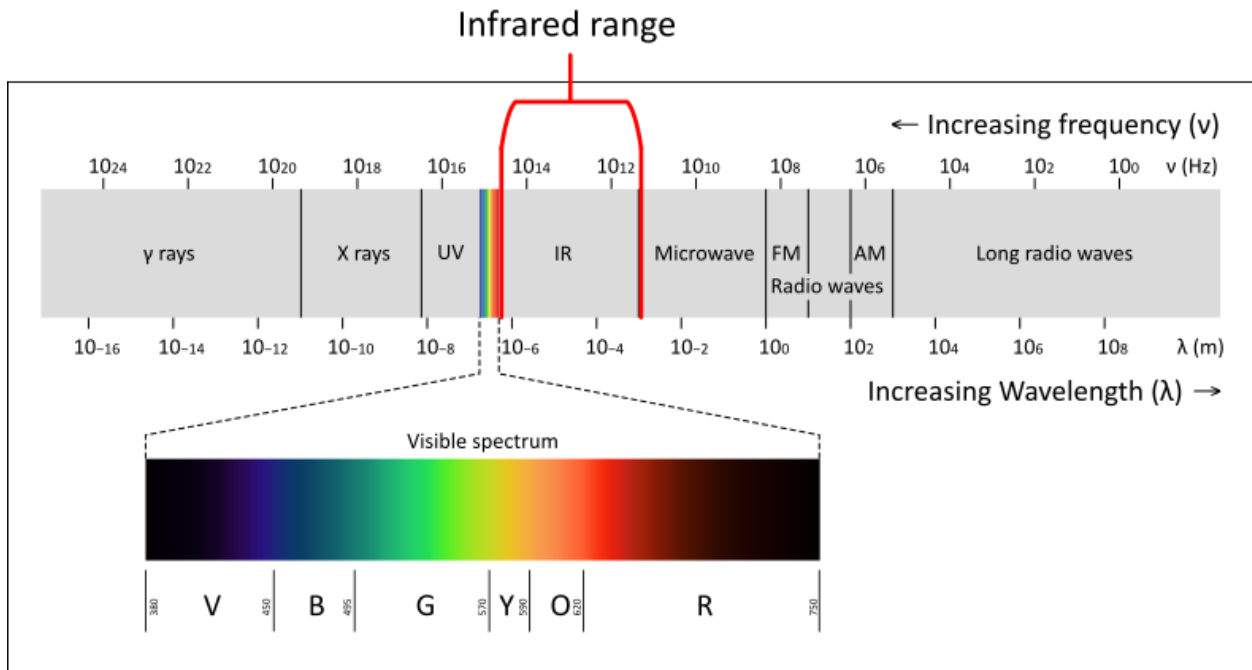


Figure 2.7: The electromagnetic spectrum [15].

The IR range can be divided into 5 categories [14]:

1. Near infrared: Wavelengths of $0.7[\mu\text{m}]$ to $1.4[\mu\text{m}]$, emitted from bodies with temperature between $3600[^\circ\text{C}]$ and $1800[^\circ\text{C}]$.
2. Short-wave infrared: Wavelengths of $1.4[\mu\text{m}]$ to $3[\mu\text{m}]$, emitted from bodies with temperature between $1800[^\circ\text{C}]$ and $700[^\circ\text{C}]$.
3. Median infrared: Wavelengths of $3[\mu\text{m}]$ to $8[\mu\text{m}]$, emitted from bodies with temperature between $700[^\circ\text{C}]$ and $90[^\circ\text{C}]$.
4. Long-waved infrared: Wavelengths of $8[\mu\text{m}]$ to $15[\mu\text{m}]$, emitted from bodies with temperature between $90[^\circ\text{C}]$ and $-80[^\circ\text{C}]$.
5. Far infrared: Wavelengths of $15[\mu\text{m}]$ to $1[\text{mm}]$, emitted from bodies with temperature between $-80[^\circ\text{C}]$ and $-270[^\circ\text{C}]$.

2.3.2 Infrared camera

To measure the IR radiation and temperature of a body and display this information as an image, a camera with a sensor that can detect the IR radiation is necessary. IR camera functions similarly to digital cameras. They have an optical lens, field-of-view angles, focal length, and a detector array that converts the focused beam of radiation into electrical signals. An IR camera's detector array consists of pixels, ranging in count from 20 000 to 1 million. A microbolometer is located in each pixel, and this is the detector element that changes its electrical properties when exposed to infrared radiation. Each microbolometer element is approximately $17[\mu m] \times 17[\mu m]$ to $35[\mu m] \times 35[\mu m]$ in size [16].

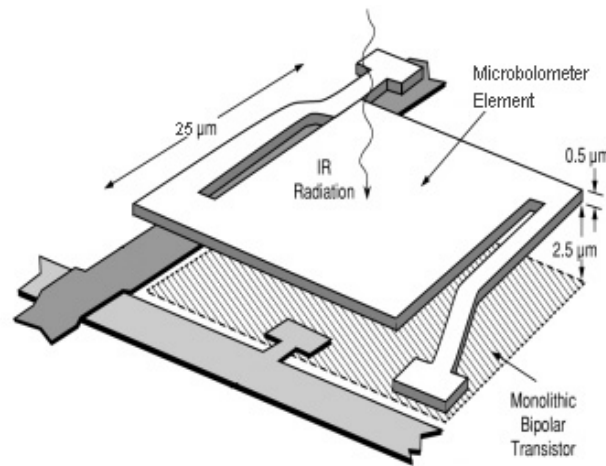


Figure 2.8: A typical microbolometer [17].

Figure 2.8 shows the composition of a typical microbolometer. When hit with IR radiation, the microbolometer element increases in temperature and thus, the electrical resistance of the element changes. Figure 2.9 further explains the key elements and their working principle. When the IR element is subjected to IR radiation, the absorbed radiation is converted to thermal energy as it impacts the absorbing element. The thermal energy is then transferred into the heat-sink through the support link, and a change in temperature over the support link is measured. From equation 2.1, the absorbed power from the radiation is calculated, given that the thermal conductance between the absorber and the heat-sink is G_t .

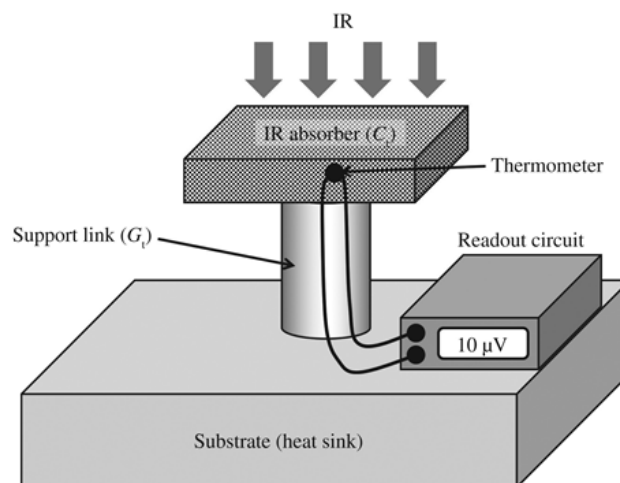


Figure 2.9: Working principle of a bolometer [18].

Equation 2.1 calculates the absorbed power in the bolometer circuit, based upon the change in temperature between the absorber element and the heat-sink. Where equation 2.2 uses the emissivity and fill-factor of the bolometer to calculate the actual amount of IR radiation on the absorber element, since some of the radiation is reflected of the pixel due to the physical properties of the microbolometer. Where the fill-factor (η) indicates the relationship between IR sensitive area to the total pixel area, and emissivity (ϵ) is the ability of the pixel to emit IR radiation. Figure 2.10, describes the readout circuit for an IR camera detector array.

$$P_{abs} = \Delta T G_t \quad (2.1)$$

$$P_{abs} = \eta \cdot \epsilon \cdot P_{in} \quad (2.2)$$

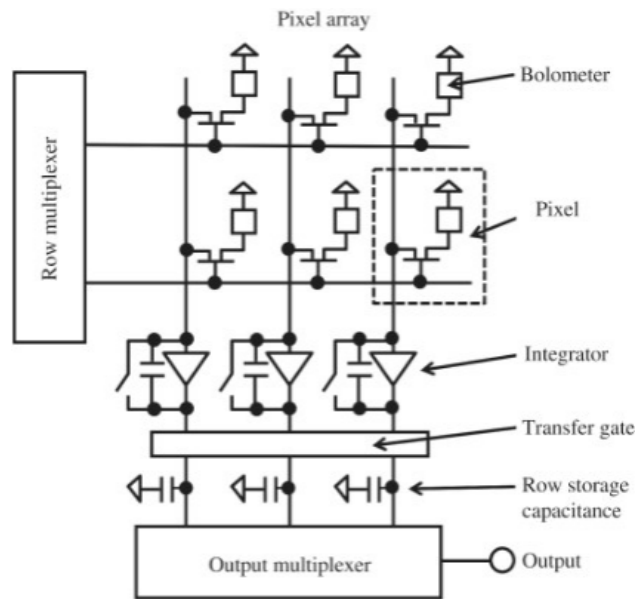


Figure 2.10: Readout circuit for a uncooled microbolometer array [18].

2.4 Software tools and packages

In this section, the theory regarding the programming language, software and other packages used to develop the source code and application are explained. Some examples of usage and implementation are also shown.

2.4.1 Python

Python is an efficient, easy to learn, high-level programming language constructed around the principles of Object-oriented programming (OOP). Compatible with an abundance of modules and packages from the open-source community. Python is suitable for rapid development of applications and combining other pieces of working software in either C, C++ or Python. These features make it an attractive programming language for developers and novices in programming, hence making it suitable as the code language in this project. Also, Python omits the compilation step, making the edit-test-debug process remarkably efficient [19].



Figure 2.11: Python logo [19].

2.4.2 Numerical Python

Numerical Python (NumPy) is a library package developed specifically for scientific computing in Python. It provides data types for multi-dimensional array objects and a vast assortment of routines for array operations. For example; linear algebra, discrete Fourier transforms, sorting and selecting, to mention a few. At the core of the NumPy library is the `ndarray` object; this object encapsulates n-dimensional arrays of homogeneous data types and performs many operations in compiled code for increased performance [20].

```
1 | # Python NumPy example
2 |
3 | import numpy as np
4 |
5 | a = np.array([1, 2, 3],[4, 5, 6],[7, 8, 9])
6 |
7 | b = np.array([1, 1, 1],[1, 1, 1],[1, 1, 1])
8 |
9 | c = a*b
10 |
11 | d = a+b
12 |
13 | e = np.append(a,b)
```


2.4.3 Numba compiler

In cases where Python and NumPy code does not achieve the appropriate computational frequency or uses too much processing power, optimizing the code by compiling it to C/C++ will give the code better performance. For Python and NumPy, Numba is an open-source Just-In-Time (JIT)-compiler, which translates Python code into faster machine code using the LLVM compiler infrastructure [21]. Figure 2.12 shows the general structure that Numba follows to JIT compile Python code, only a simple `@jit` decorator is required to compile a function. The code below shows two different implementations of Numba and JIT, one for a single function and one for an entire class, using the `@jitclass` decorator from `numba.experimental`. When compiling a function or class, it needs to be initiated with a set of data similar to the data it will be given when used after compilation.

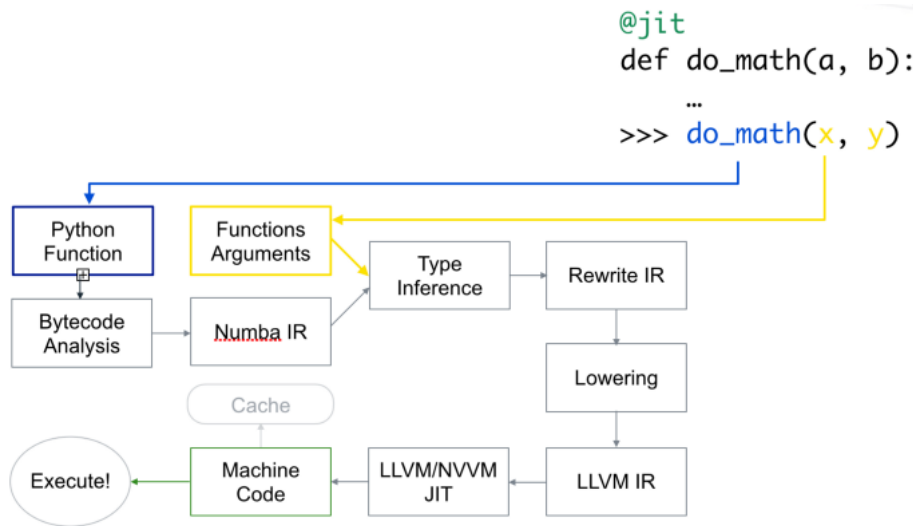


Figure 2.12: Process for compiling Python code with the JIT decorator [22].

```

1 from numba import jit
2 from numba.experimental import jitclass
3 import numba as nb
4
5 # JIT compiled function
6
7 @jit
8 def randomfunction(x):
9     # your loop or numerically intensive computations
10    return x
11
12 # JIT compiled class
13
14 # Specify the shared parameters within the class and their datatype
15 spec = [( 'self_parameter' ), nb.self_parameter_datatype]
16
17 @jitclass(spec)
18 class randomclass(object):
19     # functions to be JIT-compiled
  
```

A simple example shows the effect of JIT compilation on other wise computational heavy code.

```

1 | from numba import jit
2 | import numpy as np
3 | import time
4 |
5 | # Define dataset
6 | x = np.arange(100).reshape(10, 10)
7 |
8 | # This function will be compiled with JIT.
9 | @jit(nopython=True) # Set "nopython" mode for best performance,
   |     equivalent to @njit
10 | def go_fastJIT(a): # Function is compiled to machine code when called
   |     the first time
11 |     trace = 0.0
12 |     for i in range(a.shape[0]): # Numba likes loops
13 |         trace += np.tanh(a[i, i]) # Numba likes NumPy functions
14 |     return a + trace # Numba likes NumPy broadcasting
15 |
16 | # This function will not be compiled, it is only used for reference.
17 | def go_fast(a):
18 |     for i in range(a.shape[0]):
19 |         trace += np.tanh(a[i, i])
20 |     return a + trace
21 |
22 |
23 | # This step compiles the function to machine code
24 | go_fastJIT(x)
25 |
26 |
27 | # Measure the execution time of the JIT compiled function
28 | start_time = time.time()
29 | a = go_fastJIT(x)
30 | JIT_time = time.time() - start_time
31 |
32 |
33 | # Measure the execution time of the regular function
34 | start_time = time.time()
35 | b = go_fast(x)
36 | time = time.time() - start_time
37 |
38 | # Print the execution times to terminal
39 | print('JIT time = ',JIT_time)
40 | print('Regular time = ', time)

```

After running this Python script, the execution times for the JIT-compiled function and regular function is printed to terminal. For this example the times where; JIT time = 1.1682510375976562e-05 and Regular time = 0.0002472400665283203. This yields that the JIT compiled function is approximately 21 times faster.

2.4.4 OpenCV

Open Source Computer Vision Library (OpenCV) is a computer vision library that provides a broad range of image analysis and manipulation tools [23]. In this project, the Python implementation of OpenCV is used. An image is interpreted as a matrix, and each pixel in a grayscale image is represented by a value between 0 and 255. Grayscale images improve calculation speed and simplify the process since it only uses one value per pixel instead of three in RGB. In addition, this allows for mathematical manipulation of the image, for example, in a video stream, where each video frame is handled as a separate image and processed in real-time.



Figure 2.13: OpenCV logo[23].

2.4.5 GStreamer

GStreamer is a library for constructing video-feed and multimedia pipelines that can link together complex processes and create efficient workflows for media and other data types. In a specific case where two applications each run in their own separate thread, where one application is a source, and the other is a sink, GStreamer can develop a local streaming server that handles the communication between the two. For this project, GStreamer is used to manage the video-streaming between a computational application that runs the IR camera and computer vision tasks, and a second application that hosts the HMI [24].

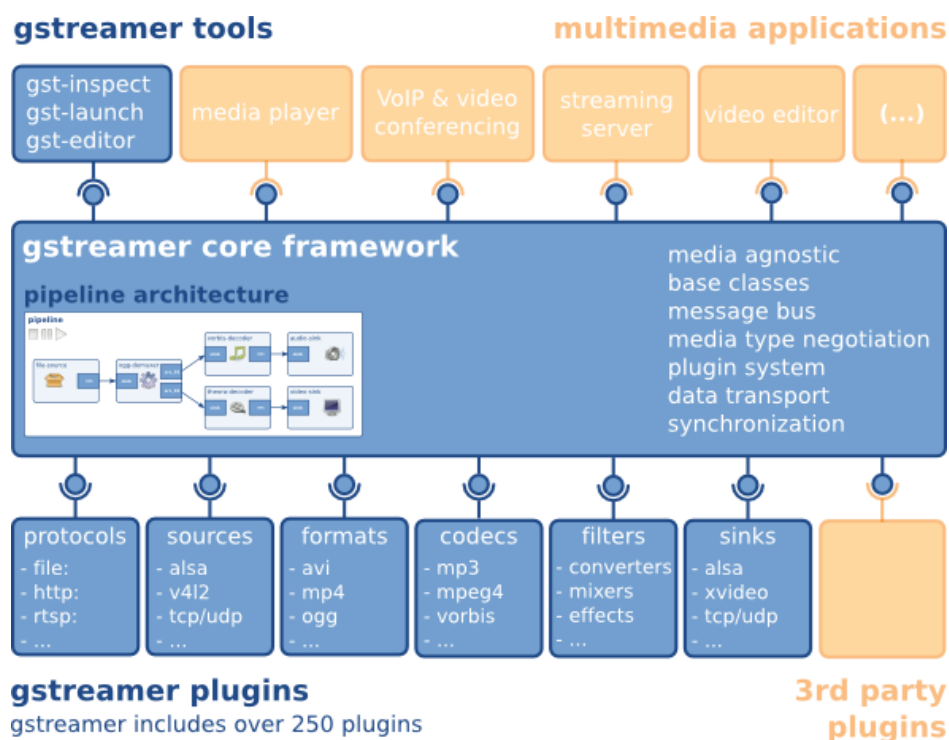


Figure 2.14: Gstreamer overview [24].

2.4.6 Flask application

Flask is a small and compact framework for developing web-hosted applications, varying in size and complexity. It is possible to create interfaces for hardware and display real-time information, host a blog or wiki. Flask is written in Python and makes it easy to give quite advanced Python applications a good looking interface. It is also possible to combine the framework with a database (SQLite), and front-end tool kit's such as *Bootstrap* [25]. For this project, it provides the framework for the HMI and creates the local server.

```
1 | from flask import Flask
2 | app = Flask(__name__)
3 |
4 | @app.route('/index')
5 | def hello_world():
6 |     return 'Hello, World!'
```

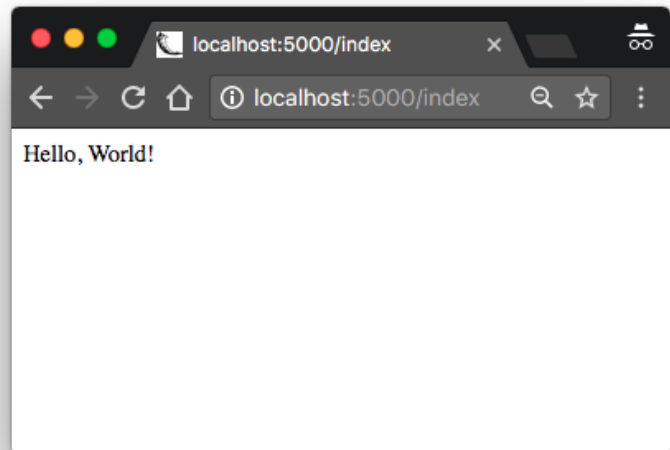


Figure 2.15: Flask "Hello world!" example.

2.4.7 GitLab

GitLab is a web-based hosting service generally used for version control of code. Version control allows for saving and logging changes made to a project. With version control, it is possible to track all the specific changes made, when they were made, and who made them. This makes GitLab widely used for various projects, as it provides the ability to track potential errors that might occur and find out when they were made. For projects involving multiple people, GitLab offers everyone in a group to synchronize their code, making sure all participants are updated with the latest version. Moreover, if a repository is made public, it enables users to view code that has been created and take inspiration [26].

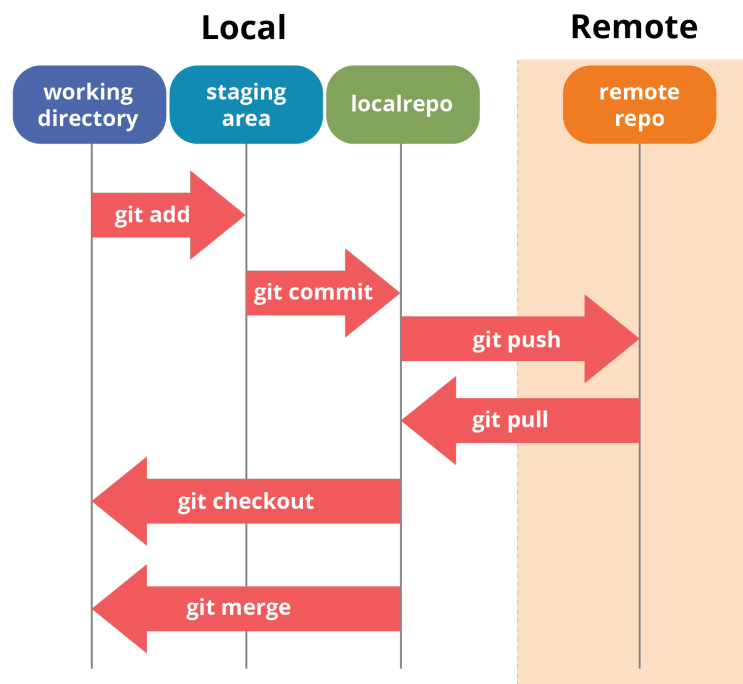


Figure 2.16: Git workflow [26].

2.5 Computer vision

In this section, the theory on computer vision and the algorithms developed in this project are explained. The mathematical principles behind the various functions and algorithms are explained, along with examples and figures to place the theory into context with research questions.

2.5.1 Locating features

To locate special features in an image, template matching is a popular option. It is quite simple to implement and requires minimal computational power when compared to regression with a neural network. For this thesis, it is chosen as the method for finding the position of the tapping beam. The theory behind this function is described in detail in the paragraphs below.

Template matching is the computational process where a template, typically a small image of a detail in a larger image, is used to find the position in the larger image that is most similar to the template. This function to locate specific regions is best implemented when the shape or form of the desired feature is kept more or less the same in the image stream supplied to the function. Within OpenCV there exists a function called: `cv.matchTemplate()`, that applies the common functions within template matching. Two-dimensional convolution is used to slide the template image across the larger image and compute the correlation between the template and the image patch. Within `cv.matchTemplate()`, it is also possible to choose between several different types of template matching operations. For this thesis, the function `cv.TM_CCoeff_NORMED` is used, the mathematical expression for this function is described by equation 2.3.

Equation 2.3, normalised correlation-coefficient technique:

$$R(x, y) = \frac{\sum_{x', y'} (T'(x', y') \cdot I'(x + x', y + y'))}{\sqrt{\sum_{x', y'} T'(x', y')^2 \cdot \sum_{x', y'} I'(x + x', y + y')^2}} \quad (2.3)$$

Equation 2.4, iterate through every pixel in the template and subtract the mean template value from it:

$$T'(x', y') = T(x', y') - 1/(w \cdot h) \cdot \sum_{x'', y''} T(x'', y'') \quad (2.4)$$

Equation 2.5, iterate through every pixel in the image patch and subtract the mean image patch value from it:

$$I'(x + x', y + y') = I(x + x', y + y') - 1/(w \cdot h) \cdot \sum_{x'', y''} I(x + x'', y + y'') \quad (2.5)$$

Where:

$T(x', y')$: Grayscale value of template pixels.

$I(x + x', y + y')$: Grayscale value of pixels in the image patch.

x, y : Local coordinates of pixels in the larger image.

x', y' : Local coordinates of pixels in the template.

x'', y'' : Are coordinates for iterating across the template $x'' \in [0, w - 1]$ and $y'' \in [0, h - 1]$.

w, h : The width and height of the template.

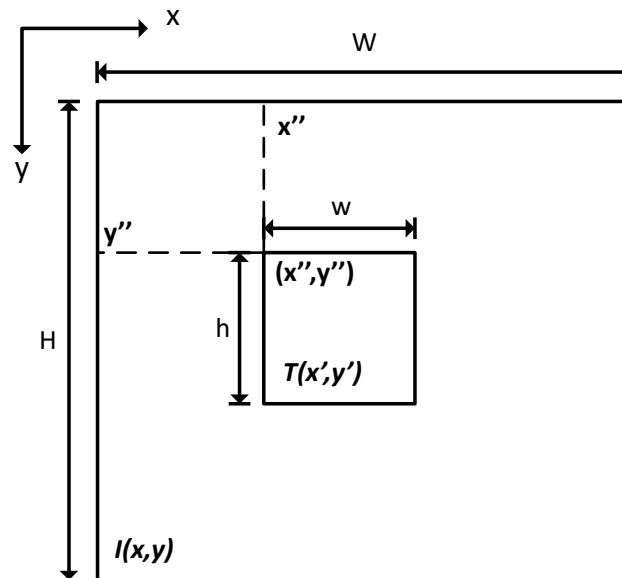


Figure 2.17: Coordinates used in template matching. $T(x', y')$ is the coordinates locally to the template and $I(x, y)$ is the coordinates locally to the larger image.

Equation 2.4 and 2.5, calculates the correlation between the template and the image as the filter is convoluted across the image. Only multiplying $T'(x', y')$ with $I'(x', y')$ would yield a value between $-\infty$, 0 and ∞ . Where $-\infty$ equals no correlation, 0 equals pixel values of zero, and ∞ equals a perfect match between the template and image. Since the function implemented is called `cv.TM_CCOEFF_NORMED`, the output value is normalised. Therefore, if $R(x, y)$ equals 1 we have a perfect match between image and template, 0 equals pixel values of zero and -1 equals no match. To select the image coordinates defined where the image and template match, a simple threshold is applied, and pixels with a higher value than the threshold are selected as the coordinates for the matching area.



Figure 2.18: Example picture for template matching.

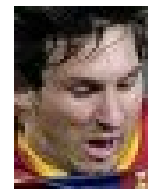


Figure 2.19: Template image extracted from figure 2.18.

An example of template matching is shown with figure 2.18 as the large picture and figure 2.19 as the extracted template. Using `cv.matchTemplate()` and `cv.TM_CCOEFF_NORMED`, the template correspondence to the image is calculated and shown in figure 2.20. The picture to the left is a grayscale image that describes the correlation between the image and template after using the `cv.TM_CCOEFF_NORMED`-method. Picture to the right is the detected face marked with a white boundary box. The bright spot visible in the upper part of the middle region in the left picture of figure 2.20, is where the correspondence is the highest and thus where the face is.

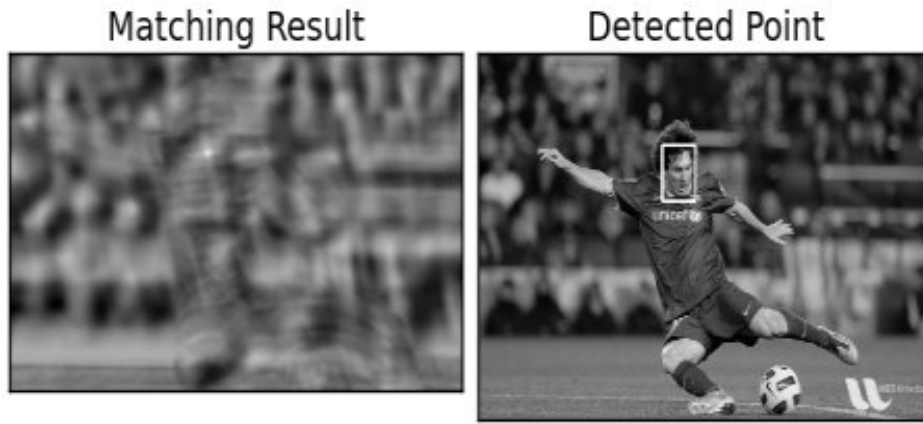


Figure 2.20: Applied template matching.

2.5.2 Detail enhancement with histogram equalisation

Enhancing the level of detail within an image can be done by increasing the contrast between bright and dark parts in the image, especially if the image is made up of a high concentration of similar pixels. The concentration of pixel values in an image is most commonly described with a histogram, a graph that shows the number of pixels of a specific value. Figure 2.21 shows the effects of equalisation on a histogram with such a narrow unimodal distribution, where the resulting histogram is transformed into a wide and flat distribution.

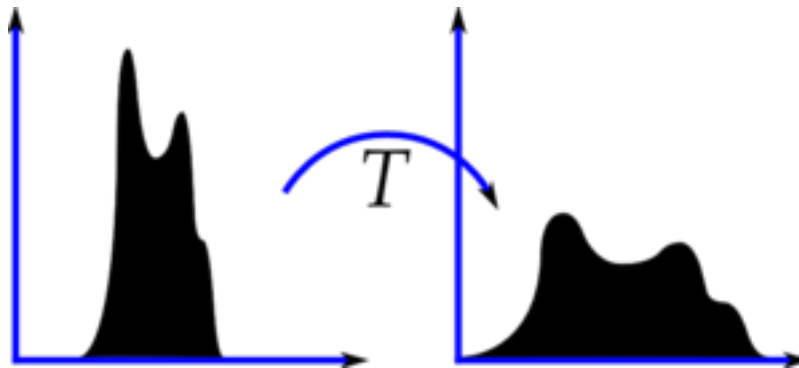


Figure 2.21: Effects of histogram equalisation [27].

$$H(j) = n_j, \quad 0 \leq j < 255 \quad (2.6)$$

Where:

n_j : Number of pixels with graylevel j .

Calculate the cumulative distribution and find the max and minimum values of the histogram. Note that the minimum value for the histogram is not to be 0:

$$cdf_x(i) = \sum_{j=0}^{255} H(j = i) \quad (2.7)$$

$$cdf_{max} = \max cdf_x \quad (2.8)$$

$$cdf_{min} = \min cdf_x \quad (2.9)$$

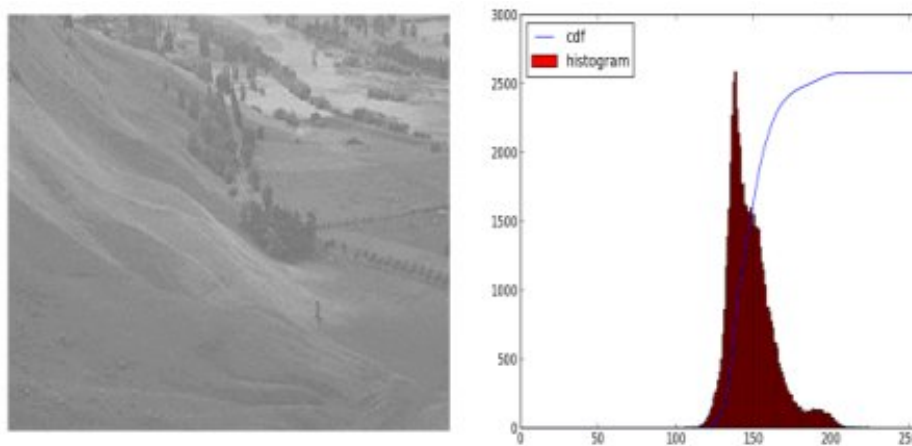


Figure 2.22: Normal histogram and the cumulative histogram [27].

To create an equalised image, it is necessary to transform the original image so that the cumulative distribution histogram of the new image would be linearised across the value range. See equation 2.10, where the cumulative distribution of the histogram is i , that is in the range of $[0, 255]$, multiplied with the constant K .

$$cdf_y(i) = iK \quad (2.10)$$

Finally, to create the new cumulative distribution histogram, equation 2.11 is applied.

$$cdf_y = \text{round} \left(\frac{cdf_x - cdf_{min}}{cdf_{max} - cdf_{min}} \cdot 255 \right) \quad (2.11)$$

The resulting transformation from the histogram equalisation can be seen in figure 2.23. The histogram distribution is now spread over the grayscale range, and the cumulative distribution follows closely to a linear profile. By comparing the image in figure 2.22 to the image in 2.23, the results from histogram equalisation is clearly visible by the enhanced level of detail.

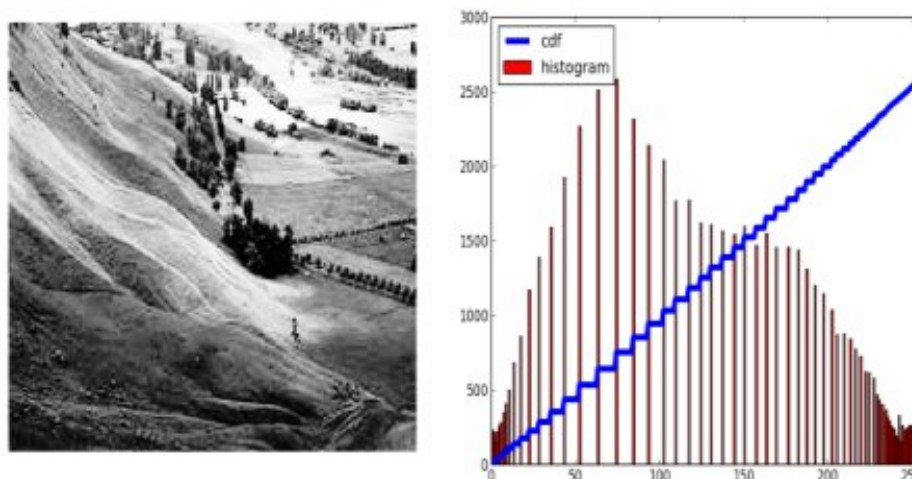


Figure 2.23: Histogram equalised image [28].

2.5.3 Model fitting and data filtering

Separating noisy data from robust signals is a common problem when working with all types of signals, and many approaches exist to separate noise from usable data. In this project, the signals are in the form of binary image arrays, basically a x-y plot of points. These points are either inliers or outliers, depending on their formation and what mathematical model that is to be fitted to the data. If the mathematical model is a linear system, $y(x) = ax + b$, a simple approach would be to use the least-squares algorithm. However, Least-squares uses all data points to establish the mathematical model, thus the noisy invalid data is biasing the result, see figure 2.25. A better and more robust approach is to use an iterative method called Random Sample Consensus (RANSAC).

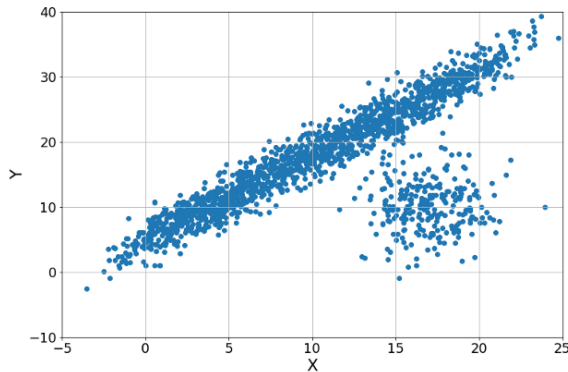


Figure 2.24: Data set containing both inliers and outliers [29].

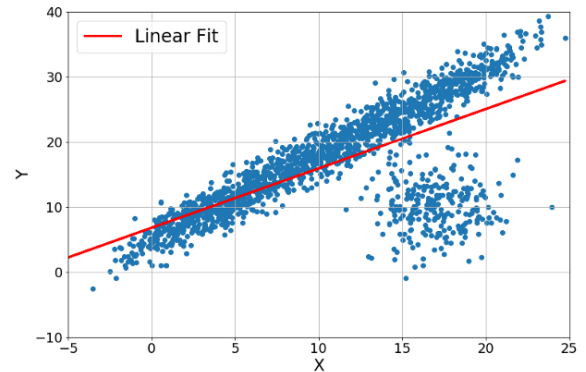


Figure 2.25: Least-squares linear fitting on the dataset [29].

RANSAC is an iterative method for fitting a mathematical model to a set of data and identify potential outliers. This method is classified as non-deterministic since the validity of the result is based upon a certain probability, thus increasing this probability by increasing the number of iterations of the algorithm. For every iteration, data points are randomly chosen and fitted into the mathematical model, a threshold is then applied, and every point in the dataset that is within this threshold from the experimental line is marked as a *inlier*. The distance from the point to the experimental line is calculated according to equation 2.12. The relationship between inliers and outliers determine if the iteration gave a valid result, RANSAC can work with up to 50 percent inliers.

$$distance = \frac{|ax_0 + by_0 + c|}{\sqrt{a^2 + b^2}} \quad (2.12)$$

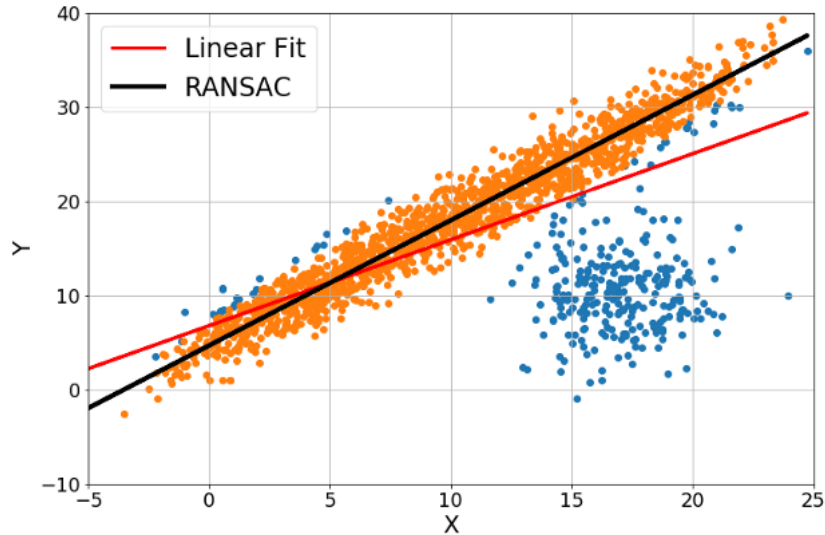


Figure 2.26: RANSAC compared to least-squares [29]. Note that the least-squares linear fitted line is biased by the blob of outliers.

RANSAC basics

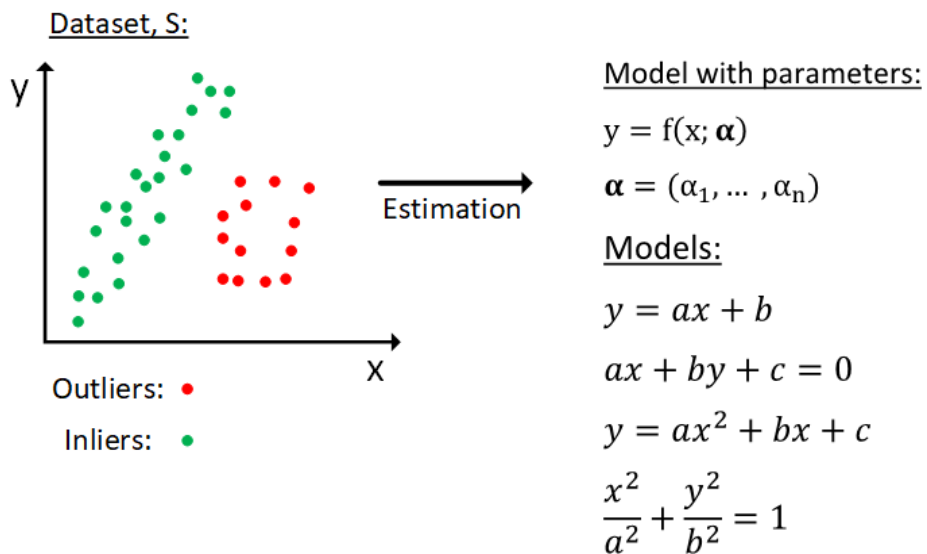


Figure 2.27: Illustration of the RANSAC principle. Where the data is presented in the \mathbb{R}^2 -domain.

Figure 2.27 illustrates the process of fitting a mathematical model to a set of data embedded with outlier noise. Note that the data described here is designated for a linear $y = ax + b$ model. The iteration process and selection of inliers is the same for every mathematical model; they are only separated by the complexity of establishing model parameters from the subset of random points.

Algorithm 1 describes how a RANSAC algorithm is implemented with pseudo-code.

Algorithm 1: RANSAC psuedocode

```

numIteration = 0;
bestNoInliers = 0;
bestModelParams = None;
while numIteration < maxIteration do
    Select random points in dataset;
    Calculate model parameters from random points;
    Find the inliers based upon the model parameters and the inlier threshold;
    Count the detected inliers;
    if number of detected inliers > bestNoInliers then
        Update bestModelParams;
        Update bestNoInliers;
    else
        Continue sampling random points from dataset;
    end
end
  
```

2.5.4 Edge detection

An edge is defined as a sudden change in image brightness, i.e. going from black to white in a binary image or the opposite. These changes in brightness are classified as discontinuities. The ability to detect edges in an image is an important feature in many computer vision algorithms, and in this project used to count the number of edges in a horizontal vector of the detected tapping beam. Usually, edge detection is computed across an entire image, finding edges in both the vertical and horizontal axis of the image. However, it is also possible and highly common to only detect edges in one direction. Thus only finding vertical or horizontal edges.

By extracting a horizontal 1D - vector from a binary image, it is possible to see if there are such discontinuities in the data when moving from left to right. Figure 2.28 shows an example of this data vector in both image format and signal format. In this example, the edges are clearly defined, and the discontinuities are strong. Convolution is applied to generate a signal that describes the position of the edges.

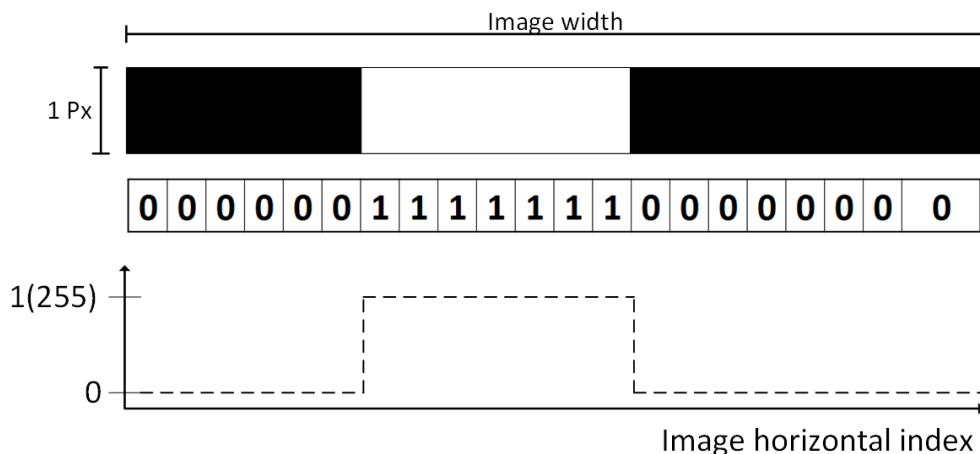


Figure 2.28: Sampled horizontal 1D-vector of an image

Convolution is the principle of combining two signals to form a third. This third signal is a representation of how the two influences each other. In edge detection, convolution is used on data similar to figure 2.28 in combination with a specified filter. The design of this filter controls the output from the convolution and must be chosen in regards to what type of data that is wanted [30]. An example of a filter for one-dimensional data is the Gaussian filter, which has a Gaussian normal distribution shape and can be used to detect discontinuities in data. The convolution is applied by sliding the filter across the data vector, computing the convoluted value for every step. Figure 2.29 is an example of using a Gaussian-filter, the edge can be located by looking for the peak in $\frac{\delta}{\delta x}(h * f)$.

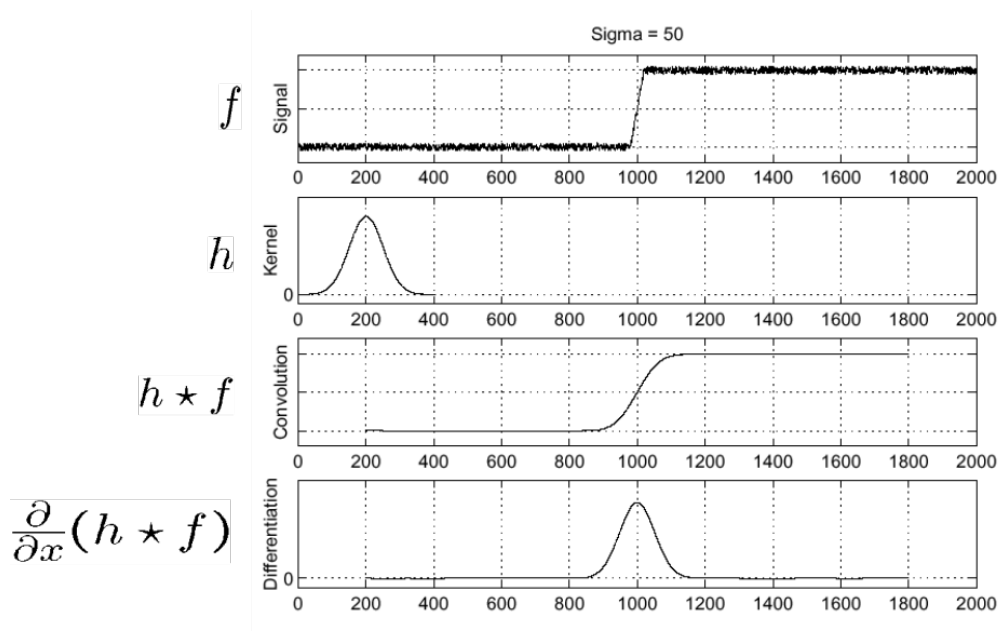


Figure 2.29: One dimensional convolution of a Gaussian filter and its partial derivative.

A simplification of the convolution process in figure 2.29 is to take the partial derivative of the filter before the convolution takes place, see equation 2.13. This is equivalent to taking the partial derivative after convolution with a Gaussian filter.

$$\frac{\delta}{\delta x}(h * f) = \left(\frac{\delta}{\delta x}h\right) * f \quad (2.13)$$

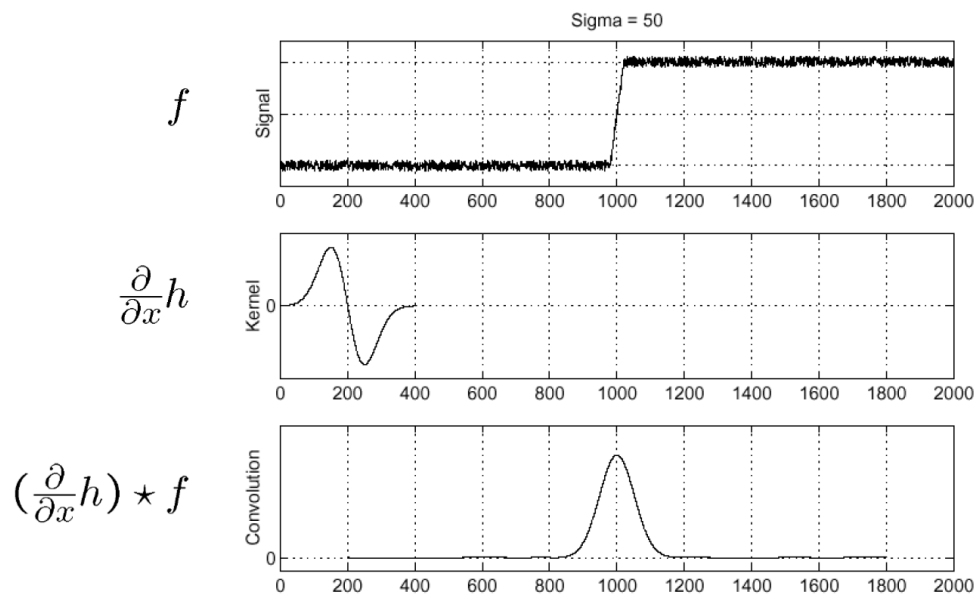


Figure 2.30: Convolution with a Gaussian partial derivative filter [31].

2.6 Project management and development

Planning for, and keeping track of a project of this size and complexity, implies that project management tools must be incorporated and used. Such tools are used to keep track of milestones, expose internal dependencies and manage weekly tasks. This section describes the different methods and approaches used in managing and developing the timeline and tasks for this project. Common for both timeline and task planning is the focus on using a strategy of Plan, Execute and Reflect (PER) and agile methods.

2.6.1 Gantt chart

Development of the project timeline is done using a Gantt chart. Gantt displays the different tasks and milestones in the project visually as horizontal bars, with start and finish dates indicating the length of these bars and with clearly marked dependencies for each task. One of the main benefits of a Gantt chart is the holistic overview it applies, making it easy to monitor the status of a project and quickly develop a overview of the tasks at hand. For this project, TeamGantt is used to keep track of milestones and task timelines. TeamGantt is an online project management tool that is based upon the Gantt structure, offering a clean and straightforward user interface and all the tools needed to structure milestones, tasks and sub-tasks [32].

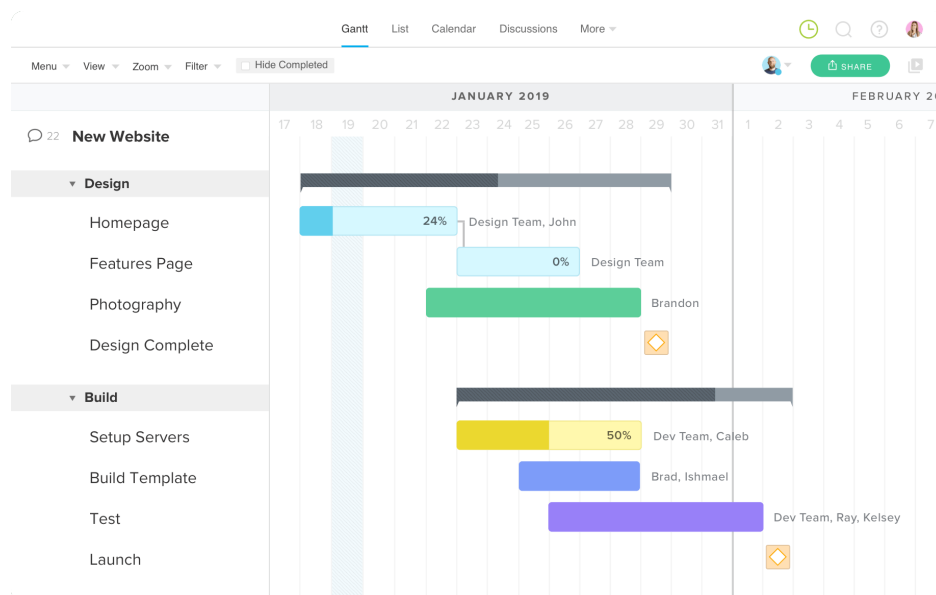


Figure 2.31: TeamGantt example [32].

2.6.2 Task management

As TeamGantt applies a holistic overview of the project and puts it into perspective with a timeline, it does not keep a detailed description of the tasks that must be executed to reach the specific milestones. Therefore, a task scheduler is necessary. Trello is another web-based project management tool, though different from TeamGantt in that it does not incorporate a timeline; instead using a Kanban-style board for keeping track of tasks [33]. For this project, Trello is used as the framework for detailed task scheduling and revised daily with both new and updates on ongoing tasks [34]. An agile approach is held towards the structuring and development of different Trello-boards, where it is adapted to fit new developments on the scope of the project [35]. PER strategy also helps new tasks and future planning learn from old tasks, increasing the effectiveness of the project management.

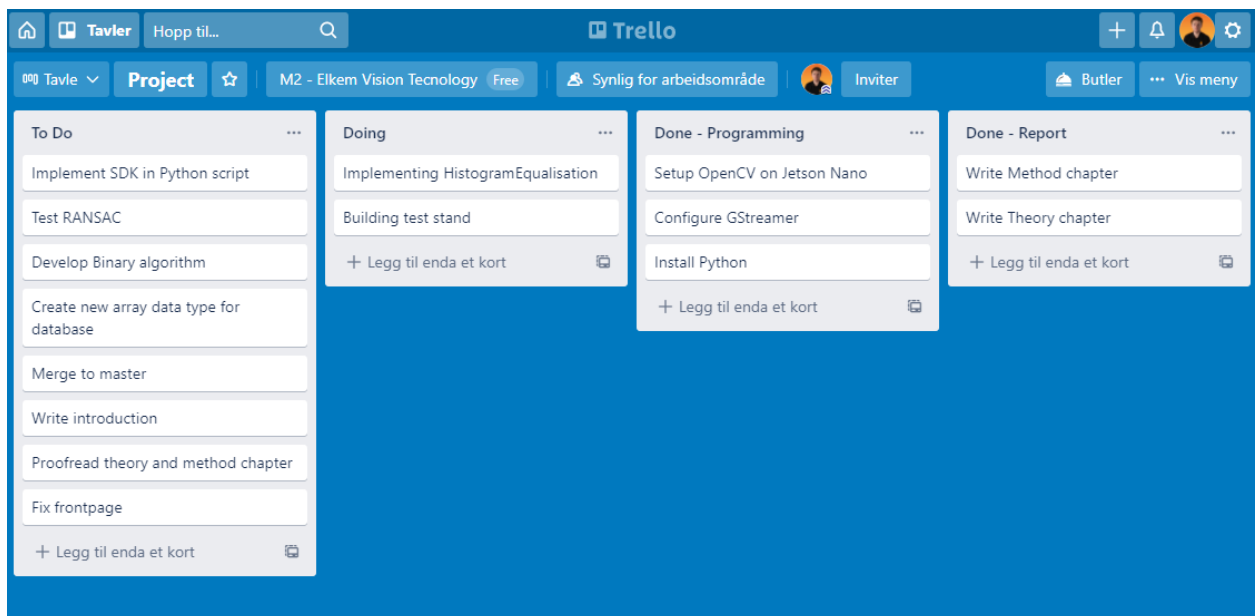


Figure 2.32: Trello example

Method

This chapter presents the method's used throughout this project to develop the final system design, hardware integration and software. An effort has been made to explain the application structure, computer vision processes and data communication as clearly as possible with either code examples or describing figures.

3.1 Implementation and use of thermal infrared camera

3.1.1 Optris PI400i thermal camera

For the development and testing in this project, an Optris Pi 400i thermal camera was borrowed from Elkem. The Optris PI 400i is a compact high-performance thermographic camera developed by Optris GmbH, with both Universal Serial Bus (USB) 2.0 and Industrial Process Interface (PIF) connectivity. Making it a popular choice for integration into Programmable Logic Circuit (PLC) systems and other types of industrial monitoring. Also worth noting that the temperature range specified in table 3.1 for this camera makes it ideal for local testing since the temperature of the test specimen can be below any dangerous levels for humans to interact with.

For the duration of this project, this camera will be implemented into the software loop, supplying the computer vision algorithms with raw data from an experimental test setup. Also worth noting that this camera has the same interface, both software and hardware, as the IR camera installed at Elkem's plant in Thamshavn, Orkanger, overlooking the tapping process at oven nr. 2. See section 1.2 and figure 1.3 for more details on the camera installation.



Figure 3.1: Optris PI 400i thermal camera with standard O29 lens [36].

Optris PI 400i specifications

Temperature range	-20°C to 900°C
Spectral range	8 to 14 [μm]
Resolution	382x288 @ 27/80 [Hz]
Connectivity	USB 2.0 & PIF
Software	PIX Connect & IRImager SDK
Detector	Uncooled focal panel array (UFPA)
Optics	29° x 22°, F = 0.9
Focal length	13 [mm]
Thermal sensitivity	40 [mK]

Table 3.1: Optris PI 400i general specifications [36].

3.1.2 Hardware integration

Connectivity between the IR camera and the processing computer is simply done with the USB connection supplied with the camera. The provided PIF cable is not used in this project, as the system architecture does not include any form of PLC systems. Figure 3.2 shows the input terminals on the camera body and figure 3.3 shows how the camera is connected to a computer, running either Ubuntu or Windows 10.

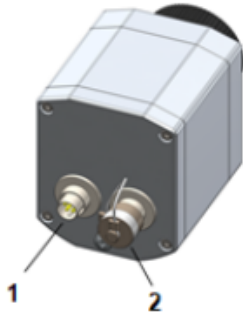


Figure 3.2: Optris PI 400i thermal camera, USB and PIF input terminals [36].

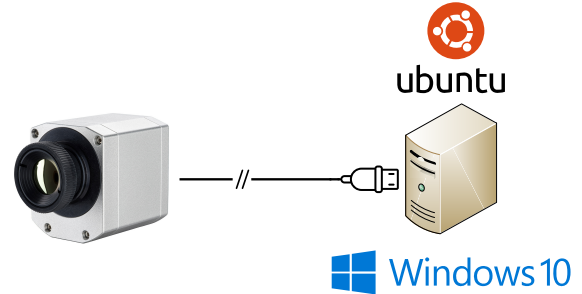


Figure 3.3: Optris PI 400i thermal camera connected to a computer running either Linux Ubuntu or Windows 10.

The applications developed in this project is implemented on a NVIDIA Jetson Nano single-board computer running Ubuntu 18.04. It is chosen due to its affordability, good GPU and CPU performance and the potential to train neural networks. The specification on the Jetson Nano is listed in table 3.2.

Jetson Nano specs:	
GPU	128-core Maxwell
CPU	Quad-core ARM A57 @ 1.43 GHz
Memory	4 GB 64-bit LPDDR4 25.6 GB/s
Storage	64 GB microSD
Connectivity	Gigabit Ethernet, M.2 Key E
USB	4x USB 3.0, USB 2.0 Micro-B

Table 3.2: NVIDIA Jetson Nano specifications [37].

3.1.3 Software integration

Supplied with the IR camera are two different software packages, dependent on the type of implementation. There is the *Optris PIX Connect* software, a real-time IR analysis program with several built-in functions to monitor and log temperature data. The software is fully capable of monitoring an industrial process, but prototyping detection algorithms and implementation on single-board computers such as the NVIDIA Jetson Nano is not possible. *PIX Connect* is only compatible with Windows 7, 8 and 10. As cross-platform compatibility between Windows and Linux-based operating systems is desired, it is not used as the interface for the camera data.

Integrating the IR camera data-feed in real-time with algorithms from open-source libraries such as OpenCV and NumPy, requires the use of the Software Development Kit (SDK) developed by Evocortex for the Optris PI-series cameras [38]. The SDK supplied is called *IRImagerDirectSDK* and can output thermal image and temperature data for both C/C++ and Python programming languages. Implementation of the SDK is possible with two different Application Programming Interface (API)'s, *Expert API* and *Easy API*, dependent on the desired level of control over the camera functions, see table 3.3 for comparison. Since the *Easy API* has support for the Python language, it is used in developing the computer vision application.

Comparing Easy API and Expert API		Easy API	Expert API
Programming style		Simple function calls	Object oriented
Programming language	C/C++, Matlab, Python & Labview		C++
Thermal image		Yes	Yes
Palette image		Yes	Yes
Change palette color		Yes	Yes
Change Palette Scale		Yes	Yes
Change Palette Temperature Range		Yes	Yes
Set Focus Motor Position		Yes	Yes
High Precision Mode (PI450)		Yes	Yes
Extended Temperatur Range		Yes	Yes
RAW Data Recording for PIX-Connect		No	Yes
Access to visible frame (PI230)		No	Yes
Multiple Cameras		Yes	Yes
PIF I/O Support		No	Yes
Detect Connection Loss		No	Yes
Flagcontrol during Runtime		Yes	Yes
Create Optris Tiff Files		No	Yes
Temperature referencing with external probe (BR 20AR)		No	Yes

Table 3.3: Optris SDK API comparison [38].

IR Imager Direct-SDK on Windows OS

For the SDK to be implemented into the program, it is saved as a Dynamic-link Library (DLL) file inside of the application folder structure. Figure 3.4 shows the general structure of the application. The SDK DLL file is then called into the application file `elkemvision/src/IRCamera.py` by the function `ctypes.CDLL("PATH_TO_DLL")` from the `ctypes` foreign function library in Python [39]. This method is specific to Windows operating system, section 3.1.3 describes the process for systems running Ubuntu.

IR Imager Direct-SDK on Ubuntu OS

The SDK is also compatible with the Linux-based operating software Ubuntu and supports the *amd64*, *I386*, *arm64*, *armhf*, *armel* and *atom* architectures. For this project, the IR camera is integrated with a NVIDIA Jetson Nano single-board computer with *arm64* and Ubuntu 18.04 operating system. Installation of the SDK is done using the Debian package (dpkg) manager and is dependent on *cmake*. A basic installation guide is available at the Evocortex *IRImagerDirectSDK* documentation website [40]. Implementing the SDK in Python for a Linux-based operating system is mostly similar to the method described in section 3.1.3, but does not require the path to the DLL-files. The path is found using `ctypes` and the function `ctypes.util.find_library("name")`, where `"name"` must be the library name without any prefix, suffix or version nr.. Then the library is loaded with `ct.cdll.LoadLibrary("path")`, where `"path"` is the path to the library.

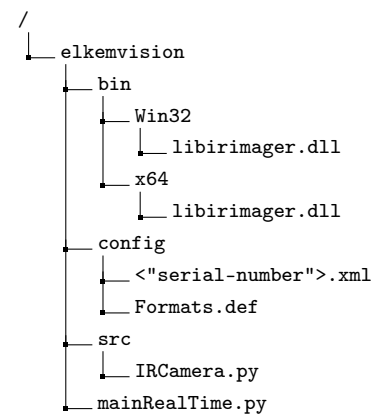


Figure 3.4: General application structure for cross-platform compatibility.

Receiving data from the IR camera

Initialising the connected IR camera and reading thermal data is done in the file `IRCamera.py`, which contains the class `IRCamera()`. This class contains all elements that are connected to the IR Imager Direct-SDK. During initialisation, the class will detect if the host's operating system is either Windows or Linux and then load the appropriate .DLL-file. Shared variables across the class are initiated with `self`-parameters. All functions within this class are described in the paragraphs below. The complete code for this class is available in the appendix C.1.2.

`IRCamera()` Class constructor; takes in the global path where the program is executed. And prints the camera serial number, thermal image size and temperature array size to the terminal.

`IRCamera.status()` Status function; when called it prints the status of the camera and library to the terminal.

`IRCamera.getThermal()` Get thermal data; when called it returns the thermal image and temperature array as `np.array` datatype.

`IRCamera.calibrate()` Calibrate the thermal image. Takes in a distorted thermal image, using the camera matrix and distortion coefficients it applies `cv.initUndistortRectifyMap()` and returns a undistorted image. Given that the correct camera matrix and distortion coefficients are used.

3.2 Computer vision algorithms

This section will cover the development, structure and implementation of the computer vision algorithms developed in this project. Code generated in this project is written using Microsoft Visual Studio Code, a well-supported and straightforward source code editor that makes developing code more efficient. The general structure of the application code is described in figure 3.5. Regarding re-usability, the code is developed to be as versatile as possible, meaning that all the necessary parameters are initialised during instantiating of the classes.

3.2.1 Tappingbeam detection

Finding the position of the tapping beam in the IR camera image is done using the theory described in section 2.5.1. The source code for detecting the tapping beam is located in the file `elkemvision/src/FeatureTracking.py`, where the program is structured as a class, with initialised `self`-variables and functions. Each function is built as a wrapper for their respective OpenCV functions. This is done, so integration with other algorithms is as simple as possible. The usage of these functions is described in the paragraphs below and the code is available in appendix C.1.3.

`FeatureTracking("path_to_template")` Class constructor; takes in the path to the template and initialises it as a `self`-variable.

`TemplateMatching(thermal_image)` Template matching function; takes in a blue, green and red (BGR) image from `IRCamera.getThermal()` and calculates the correlation between the image and template. This function uses the OpenCV-function `cv.matchTemplate(image, template, method)` where; `image` is the input grayscale image, `template` is the image template and `method` is the chosen correlation method. The matching function returns an array containing the correlation parameters, this array contains values in the range of -1 to 1 , section 2.5.1 describes these values. The best matched position of the template is found with a threshold value of 0.8 , using `np.where(condition[, x, y])` to find indexes for values higher than the threshold. If the match is successful, the function returns a tuple containing the template-position, width and height of the template and a black image with the tappingbeam region. An example input image, template and output image are shown in figure 3.6, 3.7 and 3.8.

`BoundingBox(image, location, angle)` Draw bounding-box function; takes in an image, location tuple and angle tuple. The purpose of this function is to overlay a bounding box on a preferred image of the tapping beam, only meant as a tool for visual representation. The `location` data field contains the top left corner coordinate as well as the height and width of the template, and the angle data includes the absolute angle of the trapping beam measured from the image x-axis.

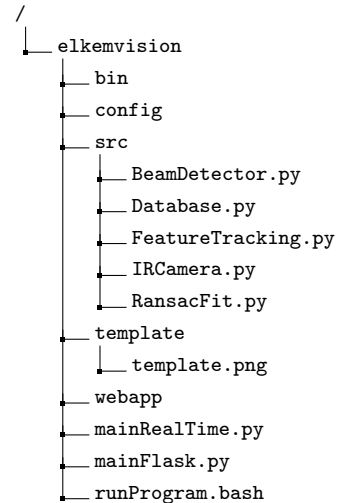


Figure 3.5: Application layout.



Figure 3.6: Grayscale input image for the template matching.

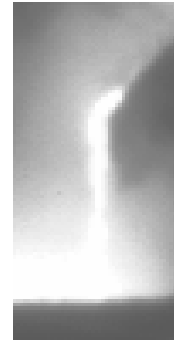


Figure 3.7: Template for the input image.

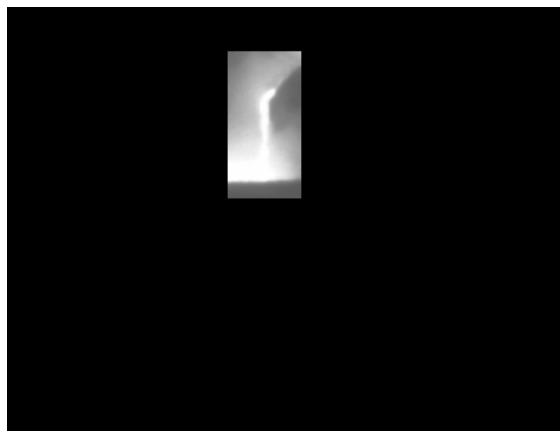


Figure 3.8: Resulting example image from `TemplateMatching()`.

3.2.2 Detail enhancement and binarization

Template matching and segmentation, as described in section 3.2.1 eliminates most of the disturbances in the image. However, some are still present, and as visible in figure 3.8 where most of the picture is now black, i.e. a grayscale value equal to zero. The tapping beam is visible in the middle of the image, surrounded by smoke and other bright disturbing objects. To increase the contrast in the image and better define a separation between the desired features in the foreground and the background, a histogram equalisation as described in section 2.5.2 is performed. The code for these functions are available in appendix C.1.4.

Equalising the histogram

`HistogramEqual(image)` The function for histogram equalisation, it is located in the class `BeamDetector()`, in the file `BeamDetector.py`. Input for this function is a template-matched and segmented image, as represented by figure 3.8. First, the histogram for the image is created using NumPy function `np.histogram(image, bins, range)` where; `image` is the input, `bins` is the number of different values the histogram should represent and `range` defines the upper and lower range for the `bins`. Then, a cumulative histogram is created with the NumPy method `numpy.ndarray.cumsum()`. Following equation 2.11, the minimum value of the histogram can not be 0, this is solved by applying a masked array. The NumPy masked array module is used to filter out and delete certain values within an array. In this instance the function `np.ma.masked_equal(x, value)` is used, where `x` is the input array to be filtered and `value` is the value to filter out.

After filtering of the cumulative array, the minimum and maximum value is calculated and the histogram is iterated through equation 2.11. The returned equalised histogram array has some indices where the value is equal to NaN, function `np.ma.filled(x,value)` solves this by filling in the empty array positions with the value 0. Using the histogram as a look-up table, the input image is transformed accordingly with `image_equalised = cdf_m[image]`. An example output image is available in figure 3.9.



Figure 3.9: Histogram equalised image.

Creating a binary image

After equalising the image histogram, the desired features in the image is now more prominent and thus easier to separate from the background. This algorithm is based upon the idea that the tapping beam always exists in the brightest parts of the image and within some margin below the maximum intensity value. A gain is applied to adjust the margin for which pixel intensities should be considered a part of the tapping beam. This is only adjusted if the binary representation is not valid, where the binary image displays an improper tapping beam. The algorithm is located in the class `BeamDetector()`.

$$i_{thresh} = np.round\left(i_{max} - \frac{i_{mean}}{i_{max}} * thresh_{gain}\right) \quad (3.1)$$

`BinaryImage(image)` The function for creating a binary image. Input for this function is the histogram equalised image, represented in figure 3.9. The max and mean values, i_{max} and i_{mean} are calculated using the `np.amax` and `np.mean` functions. They are then applied into equation 3.1 and the threshold for binarization of the image is calculated. Indices for the foreground objects in the binary image are found using `np.where(condition[, x, y])`, this function returns the indices of the array where the condition is satisfied. With `indices = np.where(image >= i_thresh)`, the tapping beam is separated out from the background objects. `indices` is a tuple containing the indexes in x- and y-direction, a black image (`image_binary`) is then indexed and the respective positions have their value set to 255. Figure 3.10 displays the binary image that is returned from function `BinaryImage(image)`.

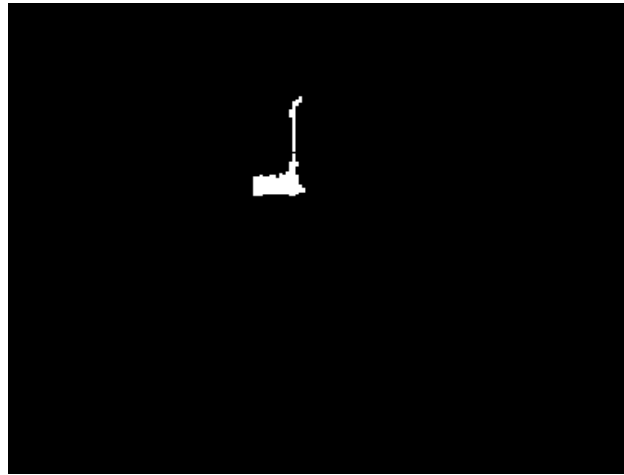


Figure 3.10: Binary image.

3.2.3 Data-filtering and model-fitting

The algorithms in section 3.2.1 and 3.2.2 removes much of the disturbances and unwanted features in the image. However, the image displayed in figure 3.10 still contains unwanted features that are not a part of the actual liquid metal tapping beam. And by looking at the raw thermal image in figure 3.6, it is fairly easy for a human to visually separate the tapping beam from the high-temperature smoke that the previous algorithms also detected. Given that the beam of liquid metal is mostly following a 2D linear model, pouring downwards into the ladle after leaving the tapping spout. The task of isolating the tapping beam is then adapted into finding the parameters for a 2D linear model ($y = ax + b$), that gives the desired number of inliers. To solve this, a RANSAC algorithm as described in section 2.5.3, is implemented into the Python application. If successful, this algorithm will find the best parameters of the model it is assigned, based upon the dataset it is given. The algorithm is structured in the class `RansacFit(threshold)` and located in file `elkemvision/src/RansacFit.py`. During the initialisation of the class, the inlier threshold is also defined. The source code for this class is available in appendix C.1.5.

`FindInliers()` The main function of the class. Designed as a wrapper for the `fit_ransac` function. Takes in a binary image of the tapping beam with outliers and returns the best inliers, model parameters of the fitted line and an image with the inliers showing. First, the input image is analysed, and the indexes that have a value of 255 are chosen as data points with `np.where(image == 255)`. These data points are then given to the function `fit_ransac`, that finds the best-fitted inliers and model. The resulting model parameters and inliers are then used to calculate the absolute angle of the tapping beam using the image coordinate system. Using model parameters in variable `bestModel` and the lowest and highest index value for the inliers (`np.min(bestInliers[:,0])` and `np.max(bestInliers[:,0])`), the data points for the two-dimensional line is calculated. The angle is calculated by taking the coordinates for the two end-points of the line data points, calculating the delta distance in x and y and using the function `np.arctan2(deltaY,deltaX)`.

`fit_ransac()` The function that contains the core RANSAC algorithm. Takes in a data set of inliers and outliers, the maximum number of iterations, number of samples for the model parameters, a threshold to classify data points as inliers and a minimum number of inliers to find. First, the RANSAC parameters are initialised and then iterated through the number of iterations.

`evaluate_model()` Function for evaluating the chosen model parameters. Input for this function is the dataset of inliers and outliers, model parameters from randomly selected points and the inlier distance threshold. The distance from the experimental line to every point in the data set is calculated according to equation 2.12. The inlier indexes are found by filtering out the distances that are larger than the desired threshold.

`fit_lsq()` The function that fits a two-dimensional line model to the randomly selected data points. Takes in coordinates of the randomly sampled data points and returns the model parameters. Calculating the model parameters for a two-dimensional line using least-squares method, `np.linalg.lstsq()`.

3.2.4 Temperature calculation

Along with a thermal image, the IR camera function also outputs a temperature matrix. Combining the temperature matrix with the filtered image of the tapping beam from the RANSAC algorithm, it is possible to find the maximum, average and minimum temperature of the liquid metal tapping beam and display this as a parameter in the HMI. Function `TempCalculation()` in the `BeamDetector()` class, incorporates NumPy function `np.where()` to find the pixel coordinates of the tappingbeam and transfers these points over to the temperature array. Then, `np.max()`, `np.mean()` and `np.min()` calculates the max, mean and minimum temperature in the beam. The code for this function is listed in appendix C.1.4.

3.2.5 Tapping beam algorithms

To give the process operators the desired feedback on the status of the tapping beam, an algorithm that can retrieve the desired data must be developed. Typically the beam is pouring directly downwards as a consistent stream of liquid metal, but with the introduction of slag and potentially degrading flow properties of the tapping spout, the tapping beam will at times divide itself into two to three smaller, more sparse and disrupted beams. The effect from this is an increased surface area of the liquid metal exposed to cool air and a lower temperature of the tapped metal in the ladle. If a split tapping beam occurs, it is possible to intervene and normalise the flow by treating the tap-hole or cleaning out the tapping spout.

The continuity and uniformity of a tapping beam can be represented by the average number of edges in a series of horizontal vectors over the height of the tapping beam. If the average of detected edges in the tapping beam is 2 per horizontal vector analysed, then the beam is classified as highly uniform and continuous. Figure 3.11 displays how the tapping beam is divided into horizontal vectors of 1 by $(width - 1)$ -dimension. The value 0 indicates the black colour, and value 1 indicates white, note that this value is 255 in a real image. An edge is denoted by the image values going from low to high or from high to low. Detecting the edges in each horizontal vector is done according to the theory described in 2.5.4.

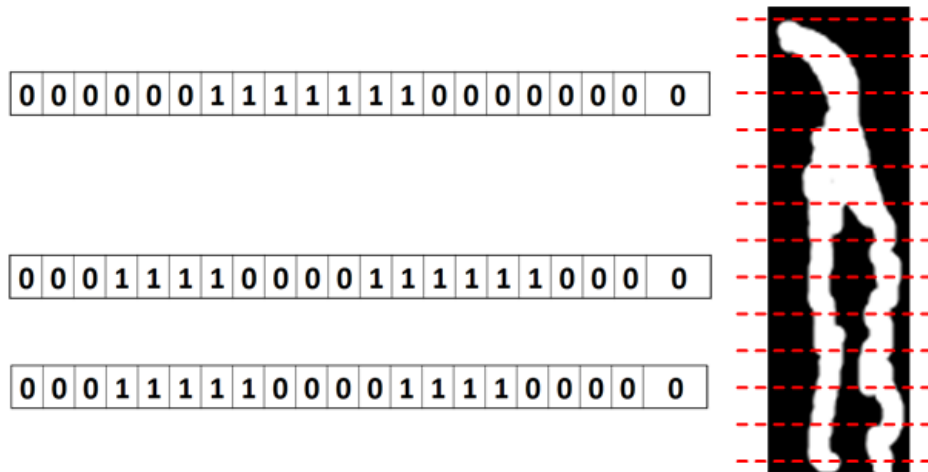


Figure 3.11: Horizontal sampling of the tappingbeam to detect shape.

The algorithm for counting the edges in the tappingbeam is located under `elkemvision/src/BeamDetector.py`, structured in function `BeamShape()` in the class `BeamDetector()` and available in appendix C.1.4

`BeamShape()` Function for classifying the shape of the beam. Takes in a binary image of the tapping beam and a tuple containing coordinates for where the template matched, and the width and height of the template. With this information, the function can crop the binary image down to the size of the template and only focus on the tapping beam ROI. It is also possible to adjust the vertical start and stop position of the horizontal sampling by adjusting the values of `height_top` and `height_bottom`, note that `height_bottom` must be a negative value. After adjusting the vertical span for the sampling, a vector containing the specific increments are created with `np.arange(height_top, (height + height_bottom), 10)`, this vector is used to index the sampling of horizontal vectors for every 10 pixels. Iterating through the index vector, a row of pixel values is sampled from the image and convoluted with a derivative-Gaussian filter. The immediate results from the convolution is a data vector as shown by the *Convoluted vector* in figure 3.12. For a rising edge, the convolution generates a normal-distribution-like curve with a positive maximum point, and for a falling edge, it generates a curve with a negative maximum point. To solve this, and only have to look for peak-values in the detected edge-curves, the absolute value of the signal is computed.

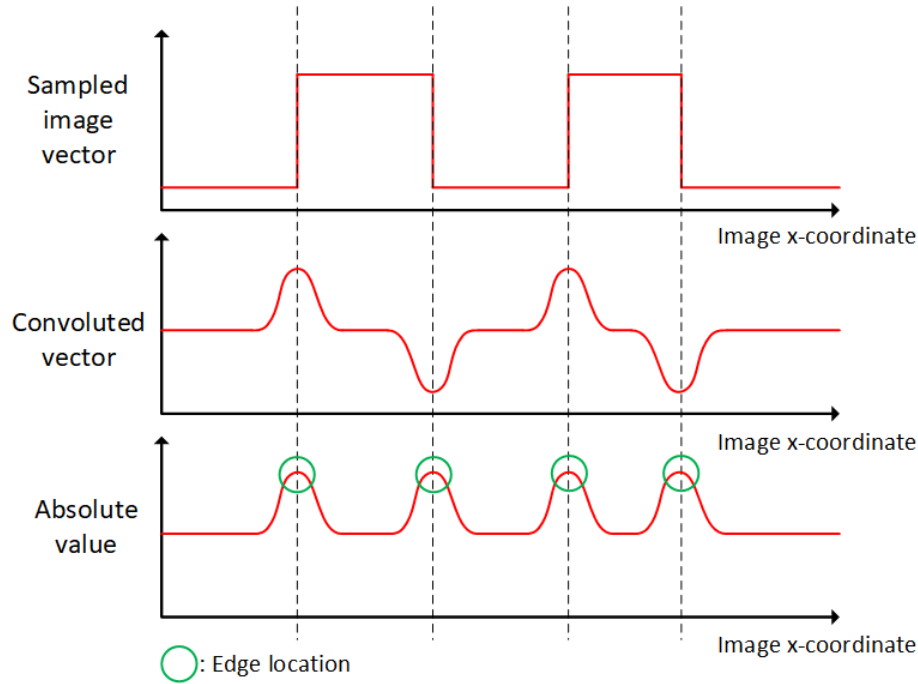


Figure 3.12: Convolution with a derivative-Gaussian filter and absolute value on the result.

Peak values in the data vector, *Absolute value*, are found by differentiating the dataset with respect to x , computing the sign of the differentiated data and then differentiating the sign data. It can be viewed in figure 3.13, that the edge is located at a transient point equal to -2 . In a real situation, these transient values will possibly go towards negative infinity. The edges are therefore found by looking for where the graph; *Derivative of sign-data*, is of value smaller than 0. Note that this process of differentiating the sign-data will shift all the indexes one pixel to the left; therefore, the peak positions are added with a value of 1.

```

1 | # Isolate row of image data
2 | row = image_isolated[i,:]
3 |
4 | # Convolve the extracted image data with a Gaussian derivative filter
5 | row_convolve = np.convolve([1,0,-1], row)
6 |
7 | # Find peaks in dataset
8 | row_convolve_peak = (np.diff(np.sign(np.diff(np.abs(row_convolve)))) <
9 |     0).nonzero()[0] + 1
10 | # Count number of edges in row
11 | edges = len(row_convolve_peak)

```

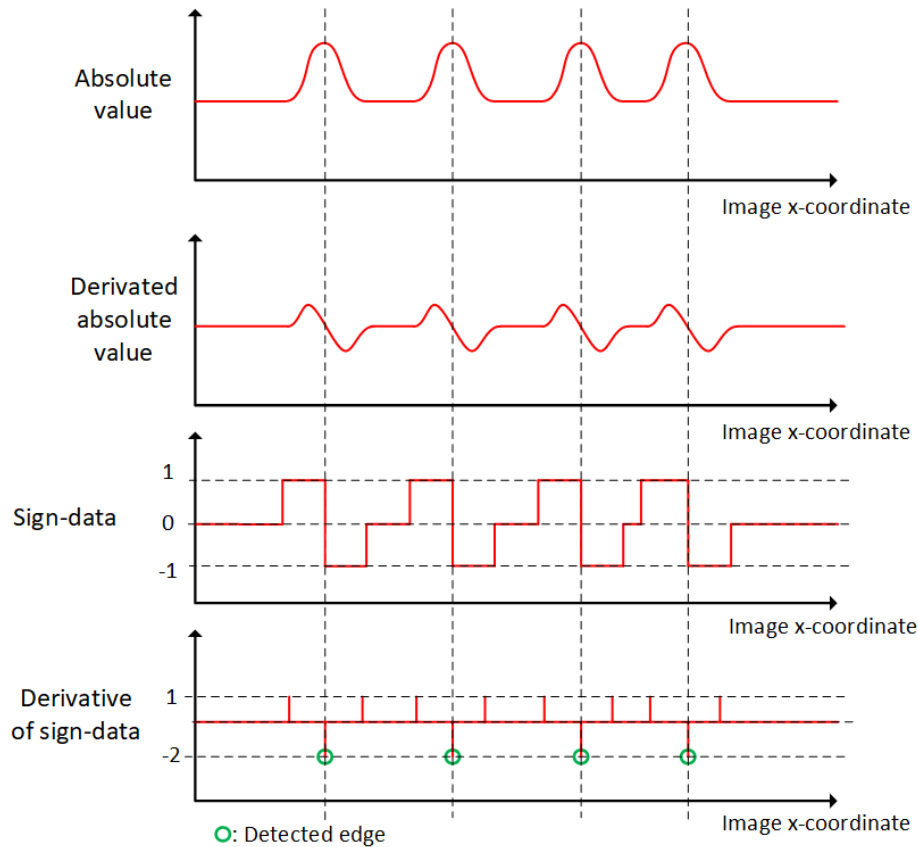


Figure 3.13: Edge detection algorithm example.

After the iteration process mentioned above, the average number of detected edges in each row is computed and used as a parameter for the shape of the beam. If the average lies in between 1 and 3, the shape is classified as optimal; if the average value is larger than 3 it is classified as sparse and discontinuous and finally if it is less than 1 a warning label is presented. An average value of detected edges less than 1 indicates that something is wrong with the input image or the algorithm itself.

3.2.6 Application structure and data flow

Figure 3.5 provides an overview on the application structure, in regards to where the files are located and the hierarchy that exists and figure 3.15 explains how the application is incorporated with the tapping operators. Every function is dependent on certain data and variables generated by the previously executed function. The Python script `mainRealTime.py` serves as the main file for launching the IR camera application, importing the necessary packages, creating instances of the classes and executing the functions inside of a while-loop. And the Python script `mainFlask.py`, launches the web-based HMI. A flowchart that presents the dependency and execution order for each function in `mainRealTime.py` is available in appendix B.4.

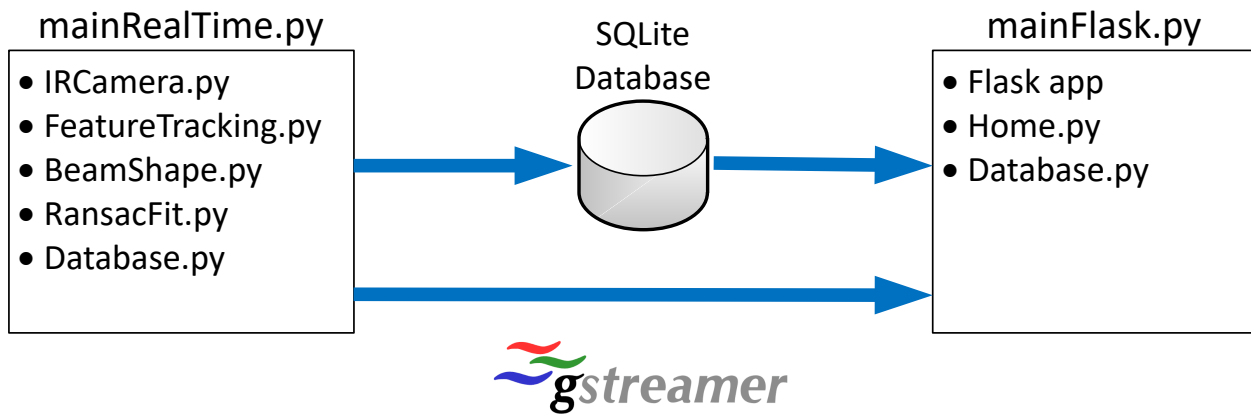


Figure 3.14: Application structure and data flow.

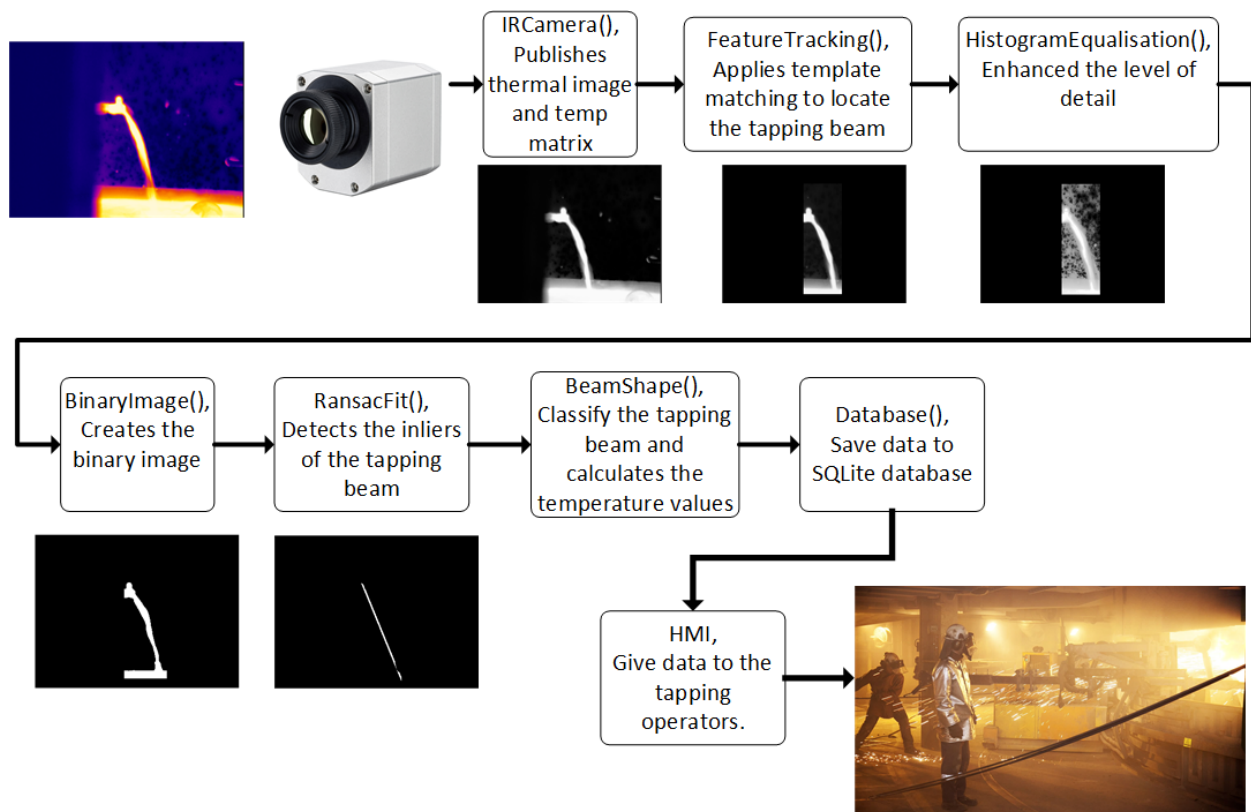


Figure 3.15: Application sequence and data flow.

3.3 Database and Human Machine Interface

As mentioned in this projects scope and objectives in section 1.3, an interface between the human operators and the IR camera application is to be developed. This application aims to provide the operators with detailed real-time information about the ongoing tapping process and data-logging for metallurgists. The source of information is provided by the applications developed in section 3.2, where specific data are stored in a database at a given frequency and a video stream is transported with a pipeline-based multimedia framework.

3.3.1 SQLite database

SQLite is chosen as the framework for data storage since it easily incorporates a Python application and allows for the customisation of tables and data types. File `Database.py` contains the functionality of the database and is implemented into both the `mainRealTime.py` and `mainFlask.py`, launch file for the IR camera application and web-based HMI. The functionality is structured in the class `Database()` with functions for connecting the database file, writing and reading of data. Functionality is described in the paragraphs below and the code is available in appendix C.1.6.

`Database("path_to_database")` The initialisation of the class. Takes in the global path for the `.db`-file, and stores it as a `.self`-variable. After execution, a connection to the database is established, and if the file does not exist, a new one is created with the specified tables. After executing, the function prints to the terminal; `==== Created connection to database! =====` if successful, and the opposite if the connection fails.

`create_connection()` Establishes a connection to the the database. Takes input from the class `.self`-variables. `conn = sqlite3.connect()` is then used to establish connection to the database, given input parameters; `self.dbPath`, `check_same_thread=False`, `detect_types=sqlite3.PARSE_DECLTYPES`. Where `self.dbPath` is the path to the database file, `check_same_thread=False` enables multi-thread operation and `detect_types=sqlite3.PARSE_DECLTYPES` makes the SQLite module parse the declared type for each column of data it returns [41].

`create_table()` Creates the desired tables. Takes input from `.self`-variables and the variable for the declared table structure. First the function establishes a cursors to the active database connection with `c = self.conn.cursor()`, and then executes the `create_table` command. This function is only used during the initialisation of the class. The structuring and creation of data tables are shown below.

```

1 | # Create temperature data table
2 | sql_temperature_table = """ CREATE TABLE IF NOT EXISTS temperature (
3 |     id                integer PRIMARY KEY,
4 |     tempMax           float          NOT NULL,
5 |     tempMean          float          NOT NULL,
6 |     tempMin           float          NOT NULL,
7 |     timestamp         text           NOT NULL); """
8 |
9 | # create a database connection
10 | self.conn = self.create_connection()
11 |
12 | # create tables
13 | if self.conn is not None:
14 |     # create temperature table
15 |     self.create_table(sql_temperature_table)

```

`update_temperature()` **and** `update_imagedata()` Functions for updating the database with new data. Takes in input from `.self`-variables and the data it is to update the database with. A cursor to the database is established and the specific data is written to the database with `cur.execute(sql, data)` and `self.conn.commit()`. Where `data` denotes the variables that is to be stored in the database and `sql` specifies the data table. This function is integrated into `mainRealTime.py` and is executed for every 5th iteration in the `while`-loop.

```
1 | # Define data to be updated
2 | sql = ''' INSERT INTO temperature(tempMax, tempMean, tempMin, timestamp)
3 |         VALUES(?,?,?,?) '''
4 | # Create connection cursor
5 | cur = self.conn.cursor()
6 |
7 | # Udata data
8 | cur.execute(sql, data)
9 |
10 | # Commit the data into the database
11 | self.conn.commit()
```

`select_data()` The function that reads from the database and returns the values as a list of tuples. Takes input from the class `.self`-variables and returns a specified number of rows from the tables, only publishing the newest data. A cursor to the active database is established and the specified number of rows are extracted from the table, the command `cur.fetchall()` returns the row as a list of tuples [41]. This function is integrated into `home.py`, the Python-view for the home page of the web-based HMI.

3.3.2 Flask web interface

A HMI between the tapping operators and the IR camera application is developed using the Flask framework, providing the operators with a live feed of the detected tapping beam, status indicators and a temperature trend graph. Where the SQLite database and GStreamer pipeline are used to connect the HMI application to the IR camera application, sharing temperature data, image data and video feed asynchronously between the two.

Figure 3.16 displays the application structure, divided into sub-folders containing either CSS, JavaScript, Python or HTML files.

Position, size and configuration of the different elements in the HMI are defined in the HTML templates, with the help of Bootstrap CSS and JavaScript templates. Bootstrap makes it possible to structure the website into columns and rows that dynamically adapts and changes its size, making it compatible with all types of browsers and units (PC, tablet, smartphone).

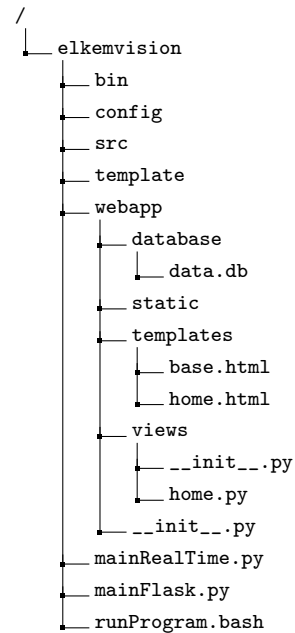


Figure 3.16: Application layout.

`mainFlask.py` The main python script for the HMI, imports the application instance from `webapp/___init___py`. Thus, launching this python program initialises the HMI and starts the Flask web-server, on the condition that the file `mainRealTime.py` have been launched and is running. This is because the GStreamer pipeline must exist for the HMI to successfully launch. The code is available in appendix C.2.1.

`webapp/___init___py` Initialises the Flask application instance. Imports `webapp/views/___init___py`, which in return imports `views/home.py`.

`home.py` The main python function for the HMI application. This file serves as the connection layer between the database, GStreamer and the HTML templates, where data is extracted from the database and video feed is read from the GStreamer pipeline using a series of functions. Every function returns data to the HTML-templates via separate URL's that are routed into the application with `@application.route("URL")`. The routing function either returns a rendered HTML-template or a response to any variables in the template, for instance; displaying a video stream, updating temperature chart data and status labels. Which status label that is presented on the HMI is decided by if-else statements in `home.py`. For the beam angle; two angle intervals are used to categorise the tapping beam, and which interval the tapping beam angle lies within decides the label. The same principle applies for the beam angle; where the label is decided by an if-else statement using the beam existence and beam status parameter. The various labels used to signal the state of the tapping beam are listed below in figures 3.17 to 3.21. The source code for this Python script is available in appendix C.2.2 and the HTML-templates are listed in appendix C.2.3 and C.2.4.

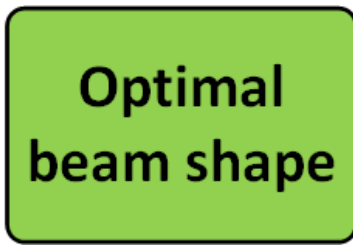


Figure 3.17: HMI label for optimal tapping beam profile.

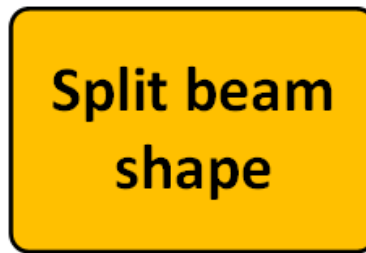


Figure 3.18: HMI label for split tapping beam.



Figure 3.19: HMI label for stopped tapping beam.

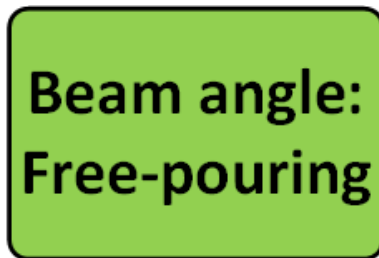


Figure 3.20: HMI label for free pouring tapping beam.

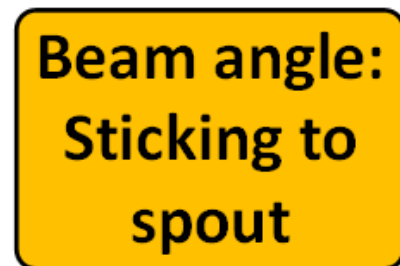


Figure 3.21: HMI label for inverted tapping beam.

3.4 Tapping beam test stand

Initial development of the algorithms presented in the previous sections was done using images from the IR camera installed at Elkem's plant in Thamshavn. These images provided a good base for development and local testing of the `HistogramEqual()`, `BinaryImage()` and `FindInliers()` functions. But for development and real-time testing of the IR application a simple test-stand that could to some extent replicate the actual tapping beam was necessary.

A simple test-stand was built using a 12[V] pump and warm water. The benefits of this setup were the simplicity and low-risk usage; there were no temperatures that could be of potential harm, and testing only required warm water from the sink. Figures 3.22, 3.23 and 3.24, show the configuration of the test stand as well as the resulting thermal image.



Figure 3.22: Top view of the test stand.



Figure 3.23: Camera view of the test stand.

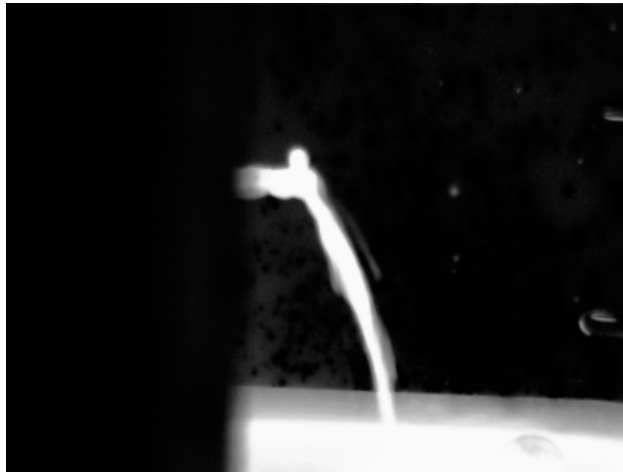


Figure 3.24: Grayscale thermal image from the test stand.

Results

4.1 Computer vision algorithms

In this section, the results from the different computer vision functions and algorithms are presented. All of the data presented here have been generated from testing with the experimental tapping beam test-stand shown in section 3.4 and synthetically developed images for the tapping beam shape classification.

4.1.1 Overall results

The IR camera application yielded in a functional program that takes in the thermal image and temperature matrix from the Optris IR camera, processes it through the computer vision algorithms and returns a set of data about the tapping beam that is sufficient to solve the scope and objectives set for this project, referring to section 1.3.

Final testing of the algorithms has been done on the NVIDIA Jetson Nano single-board computer, running the Linux based operating system, Ubuntu 18.04, connected to the Optris IR camera via USB. While running the application, it was clear that the processing power of the Jetson Nano would be a limiting factor. As a result, the time between launching the file `mainRealTime.py` and the algorithms had compiled were recorded to 56[s]. But it must be taken into consideration that the JIT compiling of `RansacFit()` takes on average 50[s]. The table in figure 4.1 shows the average CPU and memory load as well as the processing time for each frame.

Jetson Nano performance	
CPU load [1 core]	80 [%]
Memory usage	7.5 [%]
<code>mainRealTime.py</code> computing time	0.6 [s]

Table 4.1: Average load and performance while running `mainRealTime.py` on the Jetson Nano.

4.1.2 Template matching

The template matching algorithm `TemplateMatching()` localises the specified template feature, returning the top-left corner position in the image as well as the width and height of the segmented image region. Using the OpenCV method `cv.TM_CCOEFF_NORMED` to calculate the correlation between the input image and template has proven to be a valid method for detection and localisation of specified features. Real-time implementation of the algorithm with the IR camera and experimental tapping beam have provided the results shown in figure 4.1 and 4.2.

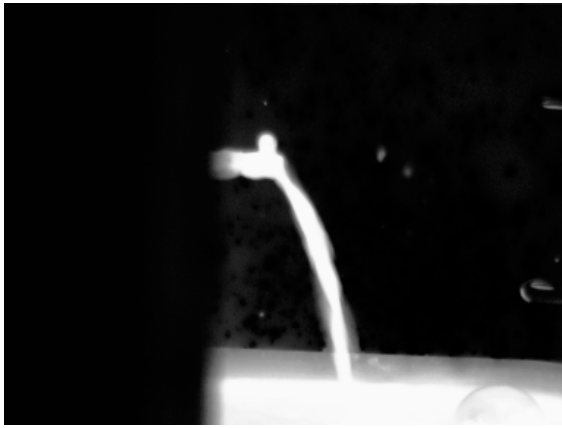


Figure 4.1: Input thermal image to the template matching.

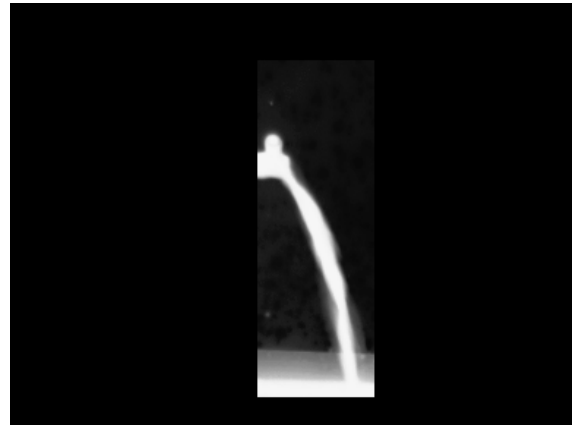


Figure 4.2: Isolated tapping beam image returned from template matching.

4.1.3 Histogram equalisation and detail enhancement

Increasing the level of detail within the tapping beam using histogram equalisation proved to be a successful method. In the early stages of development, detail enhancement on a grayscale thermal image directly from the IR camera resulted in only a minor change in detail level and did not provide the necessary separation between the tapping beam and background disturbances. A solution to this was to isolate the tapping beam ROI on beforehand, using the function `TemplateMatching()`. Histogram equalisation on the isolated image in figure 4.2 resulted in the image shown in figure 4.3.

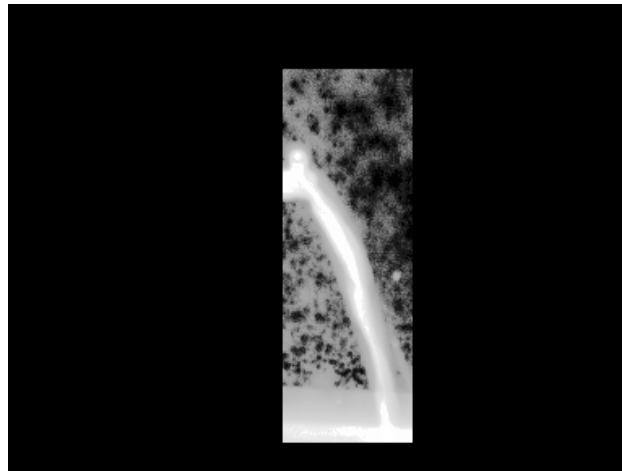


Figure 4.3: Histogram equalised image.

To substantiate the resulting image in figure 4.3, the histogram before and after equalisation can be examined. In figure 4.4, the histogram is denoted by a large collection of pixels close to 255, as well as close to grayscale value 0. This correlates to the unequalised image in figure 4.2, as most of the image pixels are black (i.e grayscale value close to 0) and the pixels within the detected template are mostly bright (i.e grayscale value close to 255). There are also some intermittent pixels with value between 50 and 200 in the unequalised histogram. Then, by looking at the equalised histogram in figure 4.5, it can be seen that the pixel values are now localised around 0 and in the range of 175 to 230. Effectively increasing the level of detail in the tapping beam.

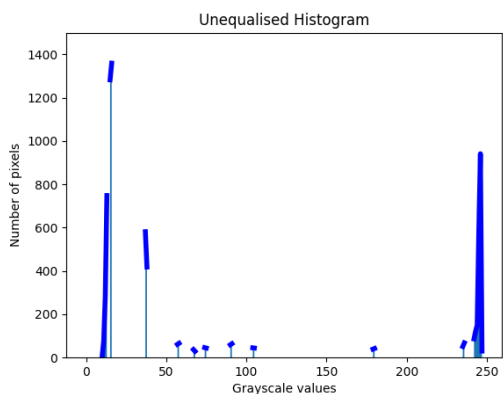


Figure 4.4: Unequalised histogram of figure 4.2.

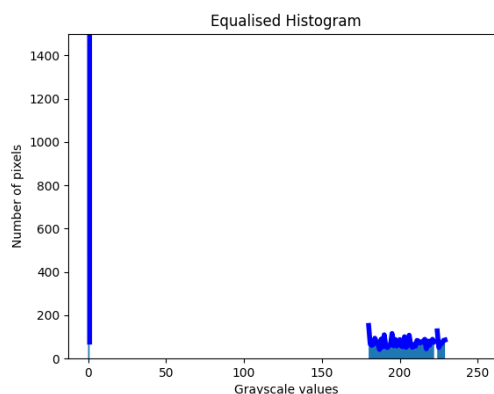


Figure 4.5: Histogram of the equalised image in figure 4.3.

By studying the cumulative distribution of the histogram after the equalisation, it can be verified that the cumulative histogram of the equalised image in figure 4.7 follows closely to a linear profile.

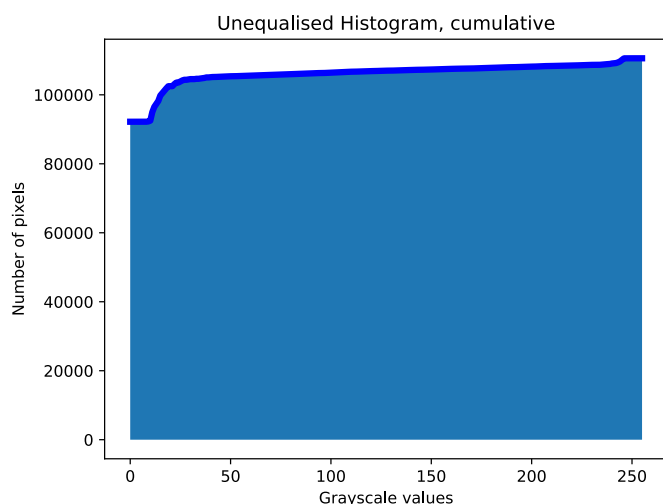


Figure 4.6: Unequalised cumulative histogram of figure 4.2.

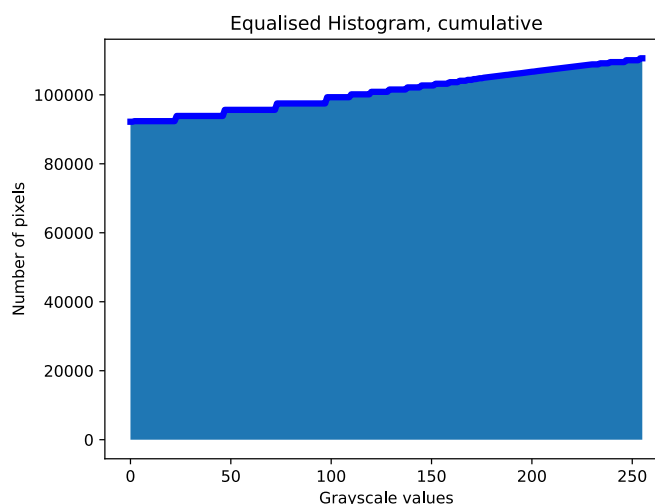


Figure 4.7: Cumulative histogram of the equalised image in figure 4.3.

4.1.4 Binary image

After equalisation, the binary image is created with function `BinaryImage()`. For this binarization, the threshold-gain variable is set to 255 as it gave the best representation of the tapping beam. Comparing the binary image to the thermal image in figure 4.1, shows that the binary representation of the tapping beam is valid.

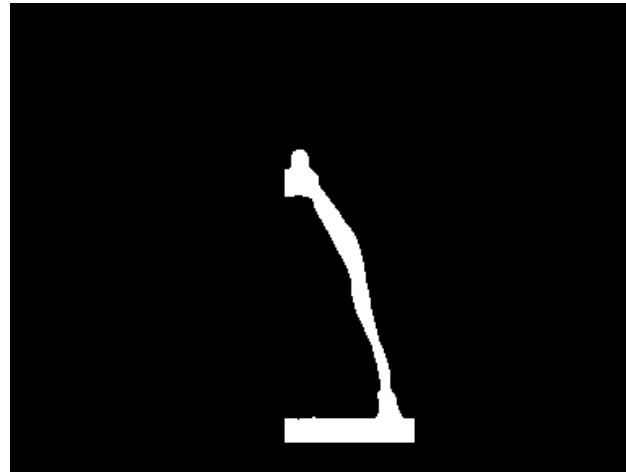


Figure 4.8: Resulting binary image

4.1.5 Inlier detection with RANSAC

The RANSAC algorithm manages to isolate the inliers of the tapping beam, with the image in figure 4.8 as the input dataset. For the results listed here, the parameters for the RANSAC algorithm is set to:

Number of iterations = 1000

Number of samples for model parameters = 4

Minimum number of inliers = 50

Inlier distance threshold = 3

Resulting in a filtered image containing the inliers of the tapping beam in figure 4.2 and the model parameters for the fitted line in table 4.3. Note that the values are based upon the image coordinate system, where the origin is located in the top left corner, and the y axis is pointing downwards.

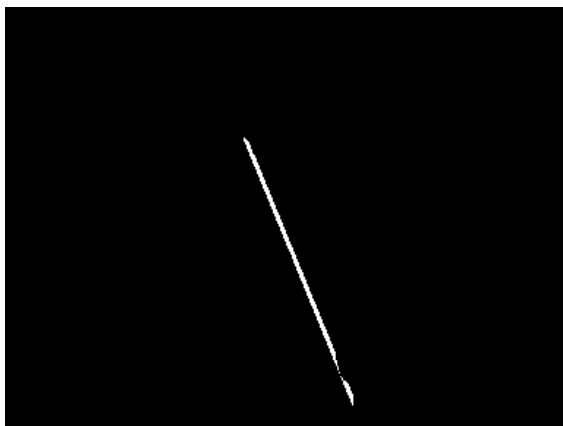


Table 4.2: Detected inliers from binary image in figure 4.8.

Model parameters, $Y(x) = Ax + B$	
Inclination, A	2.437
Y-axis crossing, B	-309.843

Table 4.3: Optimised parameters for the RANSAC linear model.

Just-In-Time compilation

The use of Numba to JIT compile the RANSAC function have resulted in a significant decrease in computing time, removing on average 0.861[s] from the execution time when compared to regular Python and NumPy.

Making the JIT compiled version approximately 3 times faster when used in real-time with the tapping beam test stand. To further prove the value of Numba and JIT compiling of Python code, a test was conducted. The RANSAC algorithm was timed with its regular NumPy functions and with the JIT compiled functions while increasing the number of iterations in the RANSAC function from 500 to 15000. The results from this test is shown in figure 4.9.

Average execution time:	
With JIT	0.389 [s]
Without JIT	1.25 [s]

Table 4.4: Average execution time of the RANSAC-function, with and without JIT-compiling.

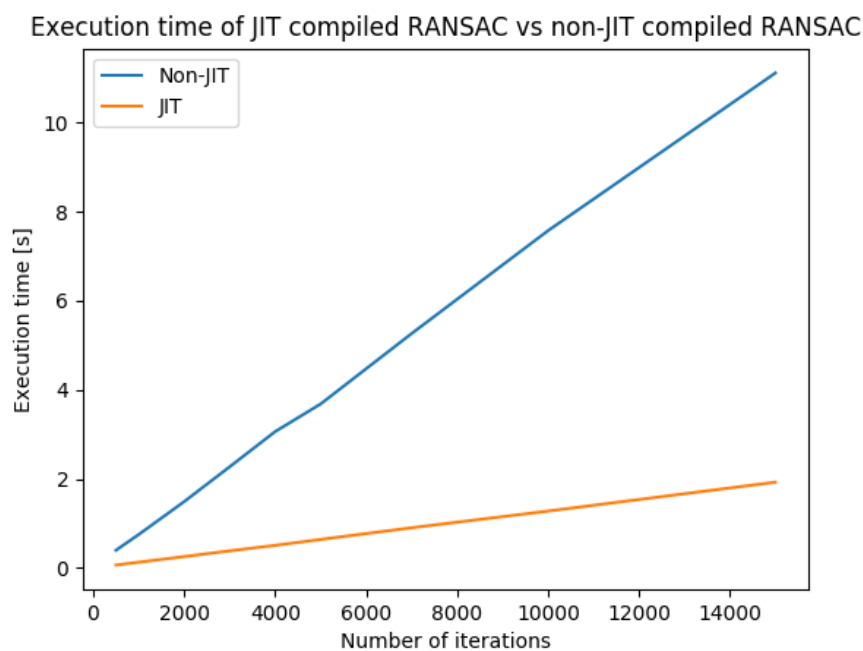


Figure 4.9: Effects of JIT-compilation with increasing computational load.

4.1.6 Beam shape classification

The edge detection algorithm used to classify the tapping beam as either continuous or split is tested using a synthetically developed image; based upon images of a split tapping beam from the plant in Thamshavn. This is mostly due to limitations of the tapping beam test-stand in combination with the available images from the physical tapping beam. The challenges with the split tapping beam are further explained in the discussion. Figure 4.10 shows the characteristics of a split tapping beam, and figure 4.11 shows the synthetic image. In total, 5 images were created to test the edge detection performance, one of them is shown in the figure below, and the rest are attached in the appendix B.2.3.

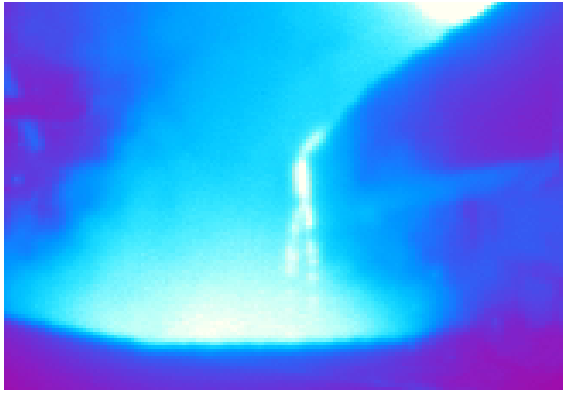


Figure 4.10: Observation of a split tapping beam at the plant in Thamshavn.



Figure 4.11: Synthetically created image of a divided tapping beam.

Table 4.5 lists the number of detected edges in figure 4.11, where the horizontal image vectors are sampled for every 20 pixels vertically. Note that the y-coordinate column is based upon the template coordinate system. The average number of detected edges in this specific image is 3, categorising it as a *split tapping beam*.

Detected edges:	
Y-coordinate	Number of edges
0	0
20	3
40	2
60	2
80	4
100	4
120	4
140	4
160	4

Table 4.5: Number of detected edges

4.2 Human Machine Interface and database

This section presents the results from the web-based HMI and data communication to the computer vision application `mainRealTime.py`.

4.2.1 Overall results

Development of the HMI application `mainFlask.py`, has resulted in a minimalist interface for the computer vision application, providing the users with the information that the computer vision algorithms produce. The information is displayed in real-time through video-streaming routes and parsing of *JSON* data from the `home.py` view-script to the HTML template. Structuring the front-end layout with *Bootstrap* made it easy to define columns and position of these elements, allowing the HMI to responsively fit the layout to the specific browser window size. An image of the HMI home screen is attached in appendix B.5. Figure 4.12 and 4.13 shows the video stream from the IR camera and the tapping beam status labels.

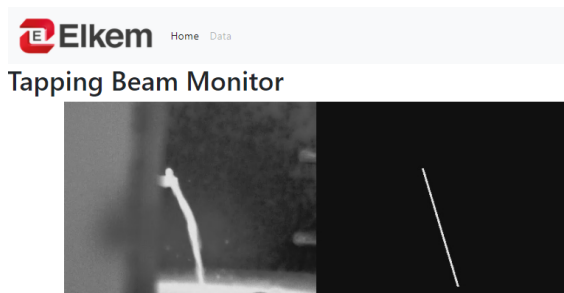


Figure 4.12: HMI video stream.

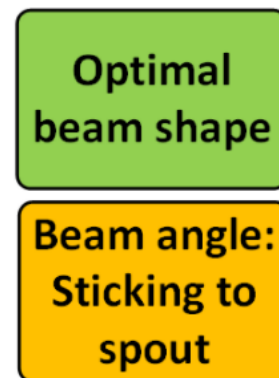


Figure 4.13: HMI status labels.

4.2.2 SQLite database

The SQLite database provided a simple framework for sharing data between applications running in separate threads and a stable platform for logging data over an extended time. A sample of the logged temperature and image data is available in appendix B.4.2 and B.4.2. Both the `mainRealTime.py` and `mainFlask.py` runs in their own separate thread while data is transferred in real-time, using the multi-thread capabilities of SQLite.

4.2.3 Temperature data

Displaying the temperature data with a line chart from the JavaScript package *Chart.js*, resulted in a responsive graph with automatic updating of temperature values and the option to select and deselect specific data.

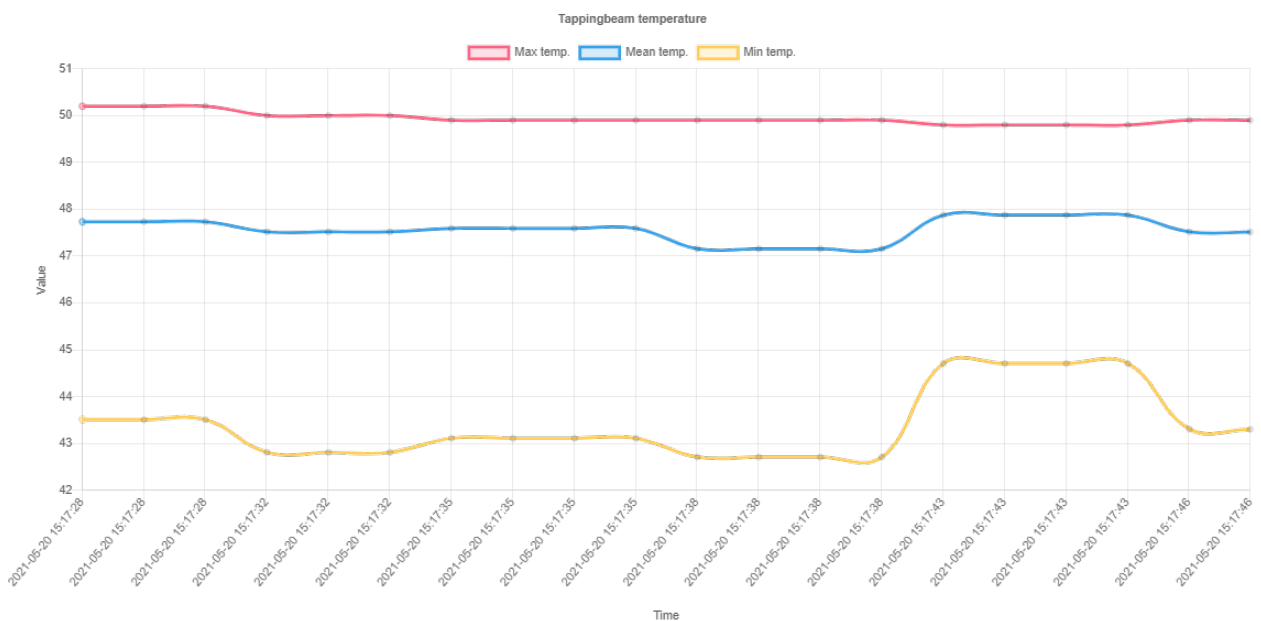


Figure 4.14: HMI temperature graph made with Chart.js

Discussion and further work

The purpose of this chapter is to discuss the presented results, observations made throughout the project and the application framework as a whole. Possible solutions and improvements are also presented as further work under each section.

5.1 Position of IR camera at Elkem Thamshavn

In the early stages of development, video and image data from the physical tapping beam at Elkem's plant in Thamshavn, Orkanger, were used to develop the first iterations of the feature tracking, histogram equalisation and binary image algorithms. Data was accessed via a remote login using a Virtual Private Network (VPN) connection, this made it possible to directly interact with the IR camera software and capture image data of the tapping process. But despite the ease of accessibility, the quality and level of detail in the images did not suffice to be used for any further development with RANSAC and beam shape classification. The most significant challenge with the IR images from Thamshavn was the poor resolution of the tapping beam in the image, as a result of the long distance between the tapping area and the IR camera. The low resolution made it difficult to extract detailed information about the tapping beam, nonetheless develop functional algorithms. This was also the primary motivation for building the tapping beam test stand, as it provided a simple platform for the development, testing and verification of the algorithms.

Further work: Fit the IR camera with a telephoto lens that can make the tapping beam ROI cover more of the image area, i.e. increasing the number of pixels in the width and height of the tapping beam. Or simply dismantle the camera from its wall-mount and position it close to the tapping beam before recording sets of image data. For instance, it could now be possible to develop algorithms for slag detection and estimation of the tapping beam's mass flow rate.

5.2 Detection of tapping beam

During testing of the template matching algorithm developed in this project to localise and isolate the tapping beam, it became clear that the OpenCV function `cv.matchTemplate()` had some limitations in regards to the robustness of the template matching. These limitations were visible once testing with the tapping beam test stand started.

In the development phase, images from the IR camera at the plant in Thamshavn were used to validate if the OpenCV-function would be adequate to find the position of the tapping beam. A series of video frames from the IR camera at Thamshavn was then tested in the OpenCV template matching function, returning the position of the tapping beam for every frame. Thus, indicating that it would be a valid method for finding the location of the tapping beam. However, testing with the tapping beam test-stand proved otherwise, as the OpenCV template matching function was susceptible to small changes in the shape of the test beam that occurred when varying the pump voltage to simulate the different beam shapes. Resulting in losing the position of the tapping beam. Seeing as this is a potential issue for the overall functionality of the IR camera application, it would be of interest to revise the method for localisation.

Further work: By gathering an image dataset from the tapping beam, it is possible to create training data for a neural network that can localise the position of the tapping beam. This method is called regression, and it can find the image coordinates of features defined in the training dataset. As an example, the NVIDIA Deep Learning Institute offers an introductory level course on AI on the Jetson Nano, where one of the sections in the course is to train a neural network for regression [42]. In this course, the basics of *deep learning* and neural networks are explained, and the pre-trained ResNet-18 network is trained with data gathered through a connected USB web camera. The computational load necessary to train and use the network is handled by the NVIDIA 128-core Maxwell GPU of the Jetson Nano. A motivating factor for this solution is that the use of neural networks and *deep learning* in the process industry is already in development through projects like SINTEF's COGNITWIN [43].

5.3 Application structure

The suggested application structure presented in this thesis is perhaps not the most optimal in regards to computational load and in keeping a high frame rate video stream from the IR camera to the HMI. As it is presented in section 3.2.6, the IR camera is initiated in `mainRealTime.py` together with all of the other computer vision functions. There the thermal image frames are only written to the GStreamer pipeline once every iteration of the while-loop in `mainRealTime.py`, resulting in a low frame-rate stream of the original thermal image in the HMI. Which is not optimal for the operators working in the tapping area.

Further work: Since the execution time of RANSAC and the tapping beam detection algorithm's does not suffice for a video feed of 30 [FPS], a solution is to restructure the application, so the IR camera is initiated by the HMI-application and streams images to `mainRealTime.py` via GStreamer. This would yield slower feedback on parameters such as tapping beam existence and temperature but an increased frame rate of the original thermal image in the HMI. This suggestion would also require two GStreamer pipelines to be established.

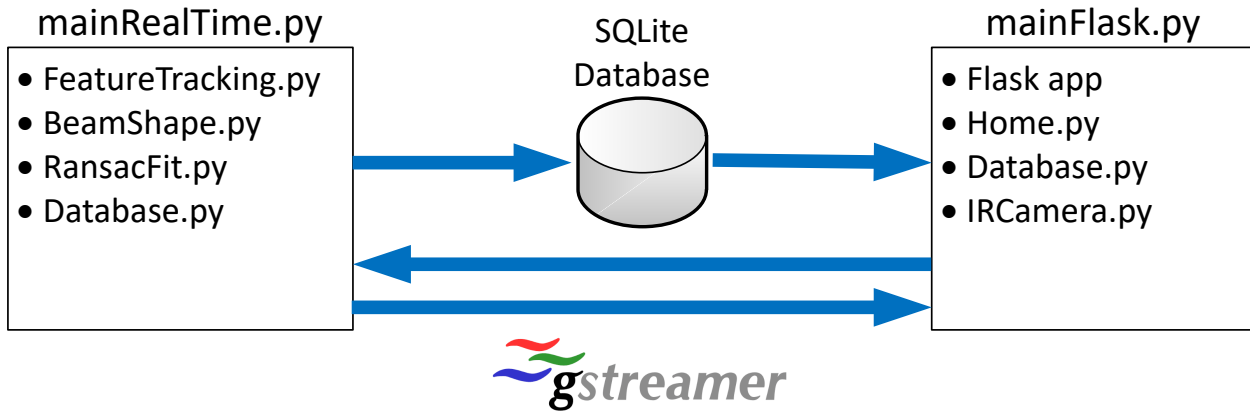


Figure 5.1: Suggested application structure

5.4 Jetson Nano performance

Throughout testing and developing the computer vision algorithms in this project, the Jetson Nano single-board computer has been used as the main platform. The reason for choosing the Nano was the possibility of using the GPU to perform training and processing of neural network algorithms that could perform classification and regression on images. As the application presented in section 3 is structured, only the CPU of the Nano is used for computing, making it equivalent to a Raspberry Pi 4. Even though Numba and JIT-compiling increases the performance quite significantly, it lacks support for the complete OpenCV library and some NumPy functions. With this in mind, it is a possibility that utilising the GPU for parallel computing of the OpenCV and NumPy functions would significantly boost the applications real-time performance. An example on the benefits of using OpenCV with GPU acceleration is shown in article [44].

Furhter work: For accelerating the performance NumPy functions, the open-source CuPy library offers GPU optimising using NVIDIA CUDA cores. Where as OpenCV already has a CUDA toolkit available. For it to be installed, the flag `WITH_CUDA=ON` must have been set in the initial build of OpenCV using CMake. Then combining these functions with the suggested application structure discussed in the previous section 5.3.

Conclusion

The research and methods developed in this project aimed to solve the challenge of analysing a complex industrial process with a high level of uncertainties and disturbances, while providing the operators with real-time feedback on the specific conditions of the process. A application that uses an industrial IR camera to extract information about the ferrosilicon tapping beam was developed. Requirements for the application is that the tapping beam must be the most considerable feature in the image, i.e. represented by as many pixels as possible, and a template image of the specific tapping beam must be captured. The computer vision algorithms can then be launched, and data on the tapping beam gets saved to the database. After validation of the image and temperature data, the tapping beam HMI can be launched. With the HMI running, live feed of the tapping beam thermal image and detected inliers, status labels, and temperature graph is available as a locally hosted website.

Throughout this project, several different subjects have been investigated, evaluated and tested. These include; feature localisation, image detail enhancement, binary image thresholding, inlier detection with RANSAC and edge detection to determine beam shape.

- **Feature localisation:** Finding the position of the tapping beam and isolating the specific ROI was solved using a function within OpenCV. And as presented in the discussion at section 5.2, this method proved to be a suitable solution when testing with low resolution image data sets from the physical tapping beam at the plant in Thamshavn, but proved otherwise when testing with the tapping beam test stand. Arguably, it could have been the test stand that gave the template matching such poor performance. Still, when taking into account the uncertainties and process disturbances such as smoke and human operators blocking the camera line-of-sight, it can be concluded that more research and testing is necessary to develop a robust algorithm specific to tapping beam detection.
- **Detail enhancement:** Increasing the level of detail in the image of the isolated tapping beam was necessary to create a robust definition between the background and foreground objects. Histogram equalisation, where the cumulative distribution of the equalised image follows a linear model, has proved to be a good algorithm for increasing detail and contrast. This algorithm is necessary when dealing with images from the physical ferrosilicon tapping beam at the plant in Thamshavn, as the beam is surrounded by high-temperature smoke. It can be concluded that detail enhancement helps to better represent the tapping beam, but needs to be validated with images where the actual tapping beam is the most significant feature.

- **Binary image thresholding:** Transforming the equalised image into a binary representation consisting only of pixel values 0 and 255 was necessary for the inlier detection with RANSAC and the edge detection algorithm for the beam shape classification. This was done by calculating an intensity value for thresholding with the max and mean image intensities and an adjustable gain parameter. The gain parameter made it possible to manipulate the thresholding value to give a better binary representation of the tapping beam. The algorithm worked as intended and has yielded credible results.
- **Inlier detection:** The inlier detection algorithm was developed on the assumption that the tapping beam mostly follows a vertical line, which gave the reason for using a RANSAC algorithm. This was also confirmed with the image data set from the tapping beam at the plant in Thamshavn. The resulting algorithm iterates through the input dataset and finds the tapping inliers with the specified distance threshold and a minimum number of inliers. With the detected inliers, the tapping beam angle is calculated and saved to the database. Using RANSAC to filter out the tapping beam profile and finding the inliers for a 2D line proved to be a successful implementation. But it needs to be tested on a physical ferrosilicon tapping beam.
- **Beam shape classification:** Classification of the tapping beam by sampling horizontal image vectors of the isolated tapping beam and counting the number of edges in each vector gave good results. But further testing is necessary, as the images for testing this algorithm are produced synthetically.

To summarise, the research conducted in this project, along with the methods and software developed, has answered the project scope and questions of research presented in section 1.3. A method for measuring the temperature, algorithms for detecting and extracting information about the tapping beam and an HMI for visualisation of the data has been developed. Despite the challenges met and the simplifications that were done to achieve results within the given time frame. A system that enhances the level of information about the tapping beam in real-time for the process operators and logs data for the metallurgists were developed. The application can also serve as a platform for gathering image and temperature data for developing more advanced algorithms, with the COGNITWIN project as an example.

Bibliography

- [1] K. Sogner, Creative Power, En. Elkem, Oslo 2014: Messel Forlag AS, ISBN: 9788276311242.
- [2] Elkem ASA. (2021). “About Elkem,” [Online]. Available: <https://www.elkem.com/about-elkem/> (visited on 03/15/2021).
- [3] —, (2021). “Sustainability,” [Online]. Available: <https://www.elkem.com/sustainability/> (visited on 03/13/2021).
- [4] Global Silicones Council. (2016). “Socio-economic evaluation of the global silicones industry,” [Online]. Available: <https://sehsc.americanchemistry.com/Socio-Economic-Evaluation-of-the-Global-Silicones-Industry-Final-Report.pdf> (visited on 01/20/2021).
- [5] T. Hannesson. (2016). “The si process,” [Online]. Available: <https://www.elkem.com/globalassets/iceland/si-process.pdf> (visited on 05/20/2021).
- [6] Elkem ASA, General information about the plant in thamshavn, 2021.
- [7] A. Szajewska, “Development of the thermal imaging camera (tic) technology,” *Procedia Engineering*, vol. 172, pp. 1067–1072, 2017, *Modern Building Materials, Structures and Techniques*, ISSN: 1877-7058. DOI: <https://doi.org/10.1016/j.proeng.2017.02.164>. [Online]. Available: <https://www.sciencedirect.com/science/article/pii/S1877705817306707>.
- [8] A. Glowacz and Z. Glowacz, “Diagnosis of the three-phase induction motor using thermal imaging,” *Infrared Physics and Technology*, vol. 81, pp. 7–16, 2017, ISSN: 1350-4495. DOI: <https://doi.org/10.1016/j.infrared.2016.12.003>. [Online]. Available: <https://www.sciencedirect.com/science/article/pii/S1350449516306259>.
- [9] Z. Zhang, L. Bin, and Y. Jiang, “Slag detection system based on infrared temperature measurement,” *Optik*, vol. 125, no. 3, pp. 1412–1416, 2014, ISSN: 0030-4026. DOI: <https://doi.org/10.1016/j.ijleo.2013.08.016>. [Online]. Available: <https://www.sciencedirect.com/science/article/pii/S0030402613011790>.
- [10] Environmental-Expert. (2021). “Elkem carbon - model elsep - elkem søderberg electrode paste,” [Online]. Available: <https://www.environmental-expert.com/products/elkem-carbon-model-elsep-elkem-soderberg-electrode-paste-516916> (visited on 05/18/2021).
- [11] M. Miranda-Martínez, J. R. Campello-García, and D. Castaño-Laviana, “Development of soderberg carbon electrodes bonded with a carbon nanofibre reinforced coal-tar pitch,” *Refractories world forum*, vol. 11, no. 1, pp. 63–67, 2018. [Online]. Available: https://www.refractories-worldforum.com/paper?article_id=100689.

- [12] A. S. Hauksdóttir, A. Gestsson, and A. Vésteinsson, “Current control of a three-phase submerged arc ferrosilicon furnace,” *Control Engineering Practice*, vol. 10, no. 4, pp. 457–463, 2002, *Mechatronics*, ISSN: 0967-0661. DOI: [https://doi.org/10.1016/S0967-0661\(01\)00104-6](https://doi.org/10.1016/S0967-0661(01)00104-6). [Online]. Available: <https://www.sciencedirect.com/science/article/pii/S0967066101001046>.
- [13] Teknisk Ukeblad, Per-Ivar Nikolaisen, Slik kuttet elkem utslipp tilsvarende 150.000 dieserbiler på rekordtid, [Online; accessed April 28, 2021], 2014. [Online]. Available: https://img.gfx.no/1702/1702551/_MG_0431_6212.jpg.
- [14] Store Norske leksikon. (2021). “Infrarød stråling,” [Online]. Available: https://snl.no/infrar%C3%B8d_str%C3%A5ling (visited on 04/29/2021).
- [15] Wikipedia Commons, *Em spectrum*, [Online; accessed April 30, 2021], 2021. [Online]. Available: https://commons.wikimedia.org/wiki/File:EM_spectrum.svg.
- [16] Optris GmbH. (2021). “What web cams and ir cameras have in common,” [Online]. Available: <https://www.optris.global/how-thermal-imaging-cameras-and-thermography-work> (visited on 01/22/2021).
- [17] Optotherm, Inc., *Microbolometers*, [Online; accessed April 30, 2021], 2018. [Online]. Available: <https://www.optotherm.com/microbolometers.htm>.
- [18] M. Kimata, “Uncooled infrared focal plane arrays,” *IEEJ Transactions on Electrical and Electronic Engineering*, vol. 13, no. 1, pp. 4–12, 2018. DOI: <https://doi.org/10.1002/tee.22563>. [Online]. Available: <https://onlinelibrary.wiley.com/doi/abs/10.1002/tee.22563>.
- [19] Python Software Foundation, *What is python? executive summary*. [Online]. Available: <https://www.python.org/doc/essays/blurb/> (visited on 05/08/2021).
- [20] The SciPy community, *What is numpy?* [Online]. Available: <https://numpy.org/doc/stable/user/whatisnumpy.html> (visited on 05/08/2021).
- [21] LLVM Project, *The llvm compiler infrastructure*. [Online]. Available: <https://llvm.org/> (visited on 05/08/2021).
- [22] Towards data science: Puneet Grover, *What is numpy?* [Online]. Available: https://miro.medium.com/max/700/0*bJ6XIUE05phjWZgz (visited on 05/08/2021).
- [23] OpenCV team. (2021). “About - OpenCV,” [Online]. Available: <https://opencv.org/about/> (visited on 05/25/2021).
- [24] GStreamer Team, *What is gstreamer?* [Online]. Available: <https://gstreamer.freedesktop.org/documentation/application-development/introduction/gstreamer.html?gi-language=c> (visited on 05/08/2021).
- [25] Pallets Projects, *Flask: Foreword*. [Online]. Available: <https://flask.palletsprojects.com/en/1.1.x/foreword/> (visited on 05/08/2021).
- [26] Simplilearn - Online Certification Training Course Provider. (2021). “What is gitlab and how to use it,” [Online]. Available: <https://www.simplilearn.com/tutorials/git-tutorial/what-is-gitlab> (visited on 05/10/2021).
- [27] OpenCV-Python Tutorials. (2020). “Opencv-python tutorials: Histogram equalisation,” [Online]. Available: [https://opencv-python-tutroals.readthedocs.io/en/latest/py_tutorials/py_imgproc/py_template_matching/py_template_matching.html] (visited on 05/03/2021).
- [28] —, (2020). “Opencv-python tutorials: Template matching,” [Online]. Available: [https://opencv-python-tutroals.readthedocs.io/en/latest/py_tutorials/py_imgproc/py_template_matching/py_template_matching.html] (visited on 05/03/2021).

- [29] A. Manzur. (2019). “Got outliers? ransac them!” [Online]. Available: <https://medium.com/@angel.manzur/got-outliers-ransac-them-f12b6b5f606e> (visited on 05/04/2021).
- [30] MathWorld—A Wolfram Web Resource: Weisstein, Eric W. (2021). “Convolution,” [Online]. Available: <https://mathworld.wolfram.com/Convolution.html> (visited on 05/14/2021).
- [31] M. Ottestad, “Lectures in instrumentation: Edge Detection Concepts in 1-D,” Lecture notes from MAS506 Instrumentation at the University of Agder, 2021.
- [32] TeamGantt. (2021). “TeamGantt,” [Online]. Available: <https://www.teamgantt.com/> (visited on 05/18/2021).
- [33] Atlassian. (2021). “What is kanban?” [Online]. Available: <https://www.atlassian.com/agile/kanban> (visited on 05/18/2021).
- [34] —, (2021). “Trello,” [Online]. Available: <https://trello.com/> (visited on 05/18/2021).
- [35] —, (2021). “What is Agile?” [Online]. Available: <https://www.atlassian.com/agile> (visited on 05/18/2021).
- [36] Optris GmbH, Infrared camera optris pi 400i. [Online]. Available: <https://www.optris.global/thermal-imager-optris-pi-400i-pi-450i> (visited on 05/06/2021).
- [37] NVIDIA Corporation. (2021). “Jetson Nano Developer Kit,” [Online]. Available: <https://developer.nvidia.com/embedded/jetson-nano-developer-kit> (visited on 05/23/2021).
- [38] Evocortex, Irimagerdirectsdk. [Online]. Available: <https://evocortex.org/products/irimagerdirect-sdk/> (visited on 05/06/2021).
- [39] Python Software Foundation, Ctypes — a foreign function library for python. [Online]. Available: <https://docs.python.org/3/library/ctypes.html> (visited on 05/06/2021).
- [40] Evocortex, Irimagerdirectsdk, linux installation. [Online]. Available: <http://documentation.evocortex.com/libirimager2/html/Installation.html> (visited on 05/06/2021).
- [41] Python Software Foundation. (2021). “Db-api 2.0 interface for sqlite databases,” [Online]. Available: <https://docs.python.org/3/library/sqlite3.html> (visited on 05/16/2021).
- [42] NVIDIA Corporation: Deep Learning Institute. (). “Getting started with ai on jetson nano,” [Online]. Available: <https://courses.nvidia.com/courses/course-v1:DLI+S-RX-02+V2/about> (visited on 05/21/2021).
- [43] SINTEF. (2021). “Cognitwin - cognitive plants through proactive self-learning hybrid digital twins,” [Online]. Available: <https://www.sintef.no/projectweb/cognitwin/> (visited on 05/21/2021).
- [44] K. Pulli, A. Baksheev, K. Korniyakov, and V. Eruhimov, “Realtime computer vision with opencv: Mobile computer-vision technology will soon become as ubiquitous as touch interfaces.,” Queue, vol. 10, no. 4, pp. 40–56, Apr. 2012, ISSN: 1542-7730. DOI: 10.1145/2181796.2206309. [Online]. Available: <https://doi.org/10.1145/2181796.2206309>.

Appendix **A**

Administrative

A.1 Project description



Tapping beam recognition



and measurement using infrared camera

Master's thesis 2021

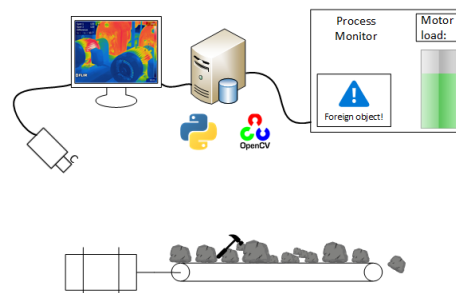
Short Introduction

Elkem is one of the world's leading companies in the environmentally responsible manufacture of metals and materials. Elkem is a fully-integrated producer with operations throughout the silicon value chain from quartz to silicon and downstream silicone specialities as well as speciality ferrosilicon alloys and carbon materials.

This project concerns the production-process and safety at Elkem's production plant. Elkem has a high focus on health, environment, and safety in their production as well as ensuring excellent product quality. The use of modern technology and smart sensing for detecting levels of wear on equipment, process parameters and potential hazardous situations is a key motivator for this project.

Keywords

- Computer science
 - Python algorithms
 - Web-based HMI
 - IR-camera interface
- Image processing
 - OpenCV
 - RANSAC
 - Feature detection



Project Description

The scope of this project is to develop solutions for monitoring process variables, analyzing equipment levels based on thermal radiation, using camera-vision technology and image processing tools such as OpenCV in an industrial environment. A system that can detect abnormalities in production, potential hazardous situations and alert the process operators of these situations. The tapping process of molten ferrosilicon is mostly a manual process, where human operators perform various tasks to ensure safe and efficient tapping of ferro silicon from furnace to ladle. Key points for this project are to enhance the visual representation of the tapping beam and give these operators direct feedback on how the tapping beam is behaving, more specifically:

- Measure temperature of the tapping beam.
- Measure the tapping beam profile.
- Give feedback on the shape of the tapping beam, is it a solid continuous beam or sparse and disrupted.
- Give feedback if the tappingbeam is no longer present, i.e. the tap-hole is clogged.

Contact information:

Full name	E-mail address	Phone number
Ali Hussain	ali.hussain@elkem.no	
Jørgen Nilsen	Jorgen16@uia.no	92299206

A.2 Gantt chart

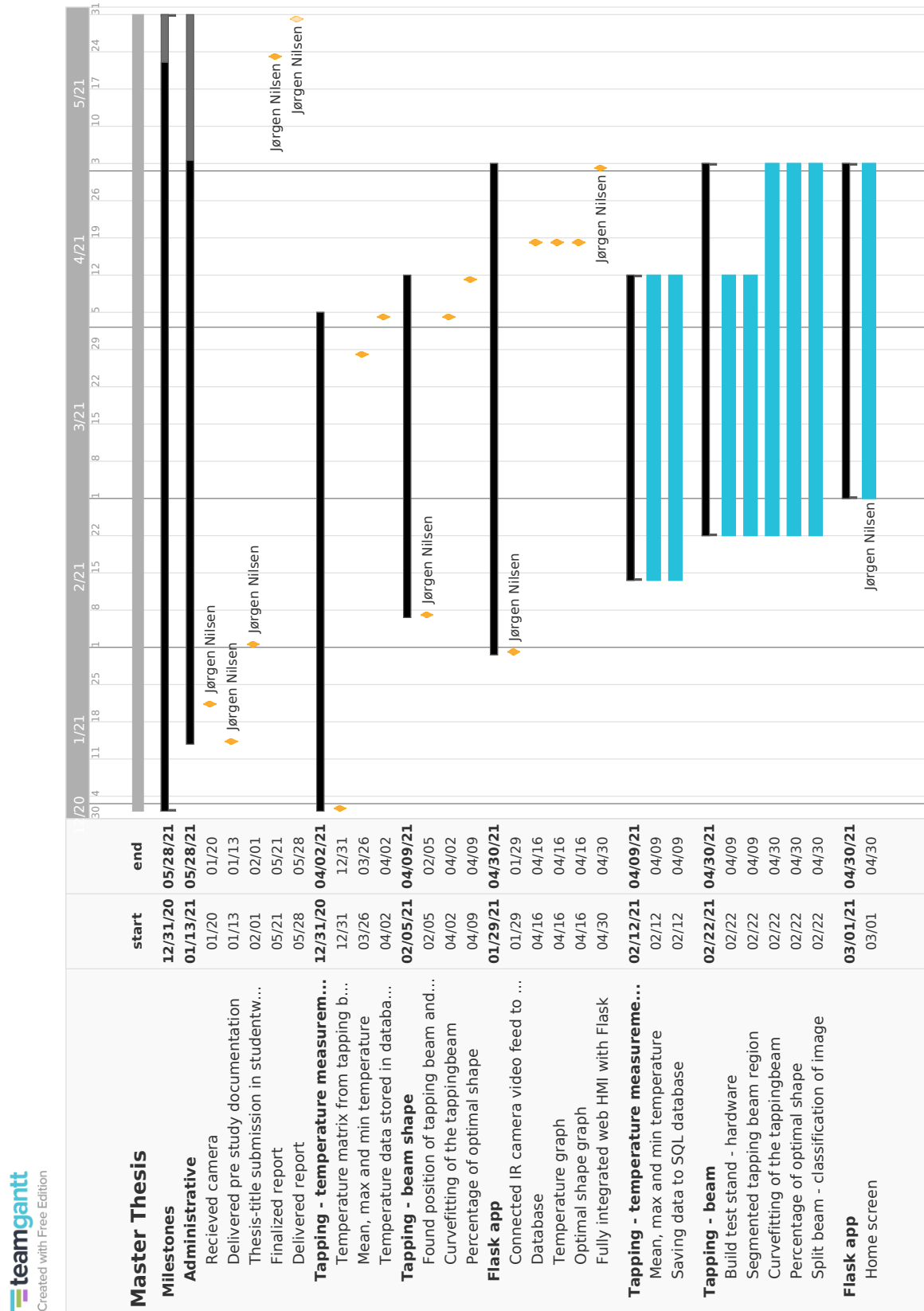


Figure A.2: Gantt chart, page 1.



Figure A.3: Gantt chart, page 2.

Appendix **B**

System

B.1 System charts

B.1.1 Tapping process timeline

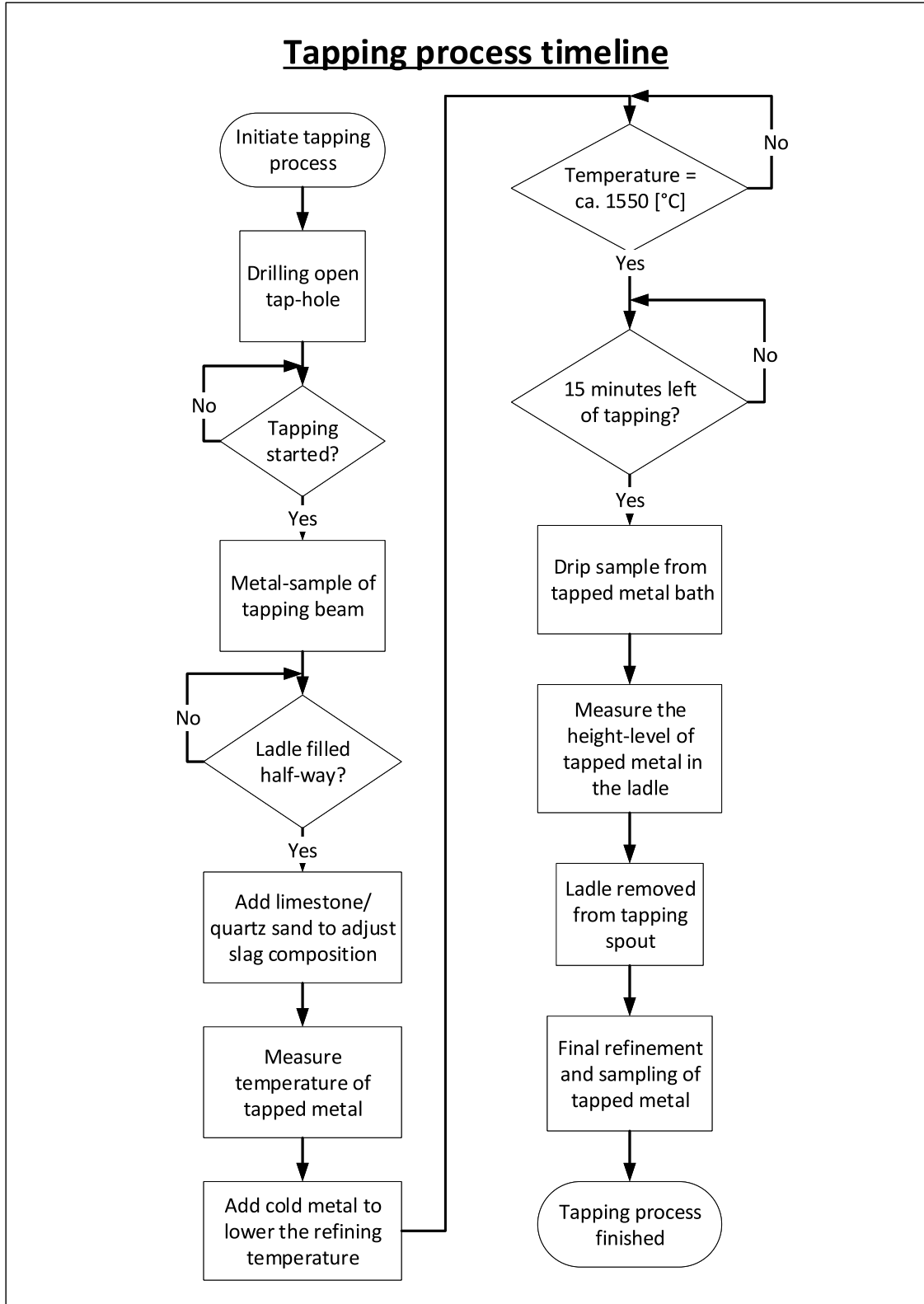


Figure B.1: Tapping process manual operations timeline.

B.2 Datasheets

B.2.1 Optris PI 400i

optris PI 400i
TECHNICAL DATA



Compact high resolution infrared camera






Features:

- Smallest camera in its class (46 x 56 x 68 – 77 mm)
- Interchangeable lenses and industrial accessories
- Framerate 80Hz
- License-free analysis software and full SDK included

Technical specifications	
Optical resolution	382 x 288 pixels
Detector	FPA, uncooled (17 µm x 17 µm)
Spectral range	8 – 14 µm
Temperature ranges	-20 ... 100 °C, 0 ... 250 °C, (20) 150 ... 900 °C ¹⁾ , optional temperature range: 200 ... 1500 °C
Frame rate	80 Hz / switchable to 27 Hz
Optics (FOV)	18° x 14° / f = 20 mm or 29° x 22° / f = 12.7 mm or 53° x 38° / f = 7.7 mm or 80° x 54° / f = 5.7 mm
Thermal sensitivity (NETD)	75 mK with 29° x 22° FOV / F = 0.9 75 mK with 53° x 38° FOV / F = 0.9 75 mK with 80° x 54° FOV / F = 0.9 0.1 K with 18° x 14° FOV / F = 1.1
System Accuracy	±2 °C or ±2 %, whichever is greater
PC interfaces	USB 2.0 / optional USB to GigE (PoE) interface
Standard process interface (PIF)	0–10 V input, digital input (max. 24 V), 0–10 V output
Industrial process interface (PIF) (optional)	2x 0–10 V input, digital input (max. 24 V), 3x 0/4–20 mA outputs, 3x relays (0–30 V/ 400 mA), fail-safe relay
Cable length (USB)	1 m (standard), 5 m, 10 m, 20 m 5 m and 10 m also as high temperature USB cable (180 or 250 °C)
Ambient temperature	0 ... 50 °C
Storage temperature	-40 ... 70 °C
Relative humidity	20 – 80 %, non condensing
Enclosure (size / protection)	46 x 56 x 68 – 77 mm (depending on lens + focus position) / IP 67 (NEMA 4)
Weight	237 - 251 g (depending on lens)
Shock / Vibration ²⁾	IEC 60068-2-27 (25G and 50G) / IEC 60068-2-6 (sinus shaped), IEC 60068-2-64 (broadband noise)
Tripod mount	¼ – 20 UNC
Power supply	via USB
Scope of supply (standard)	<ul style="list-style-type: none"> • USB camera, incl. 1 lens • USB cable (1 m) • Table tripod • PIF cable, incl. terminal block (1 m) • Software package optris PIX Connect • Test certificate • Aluminum case



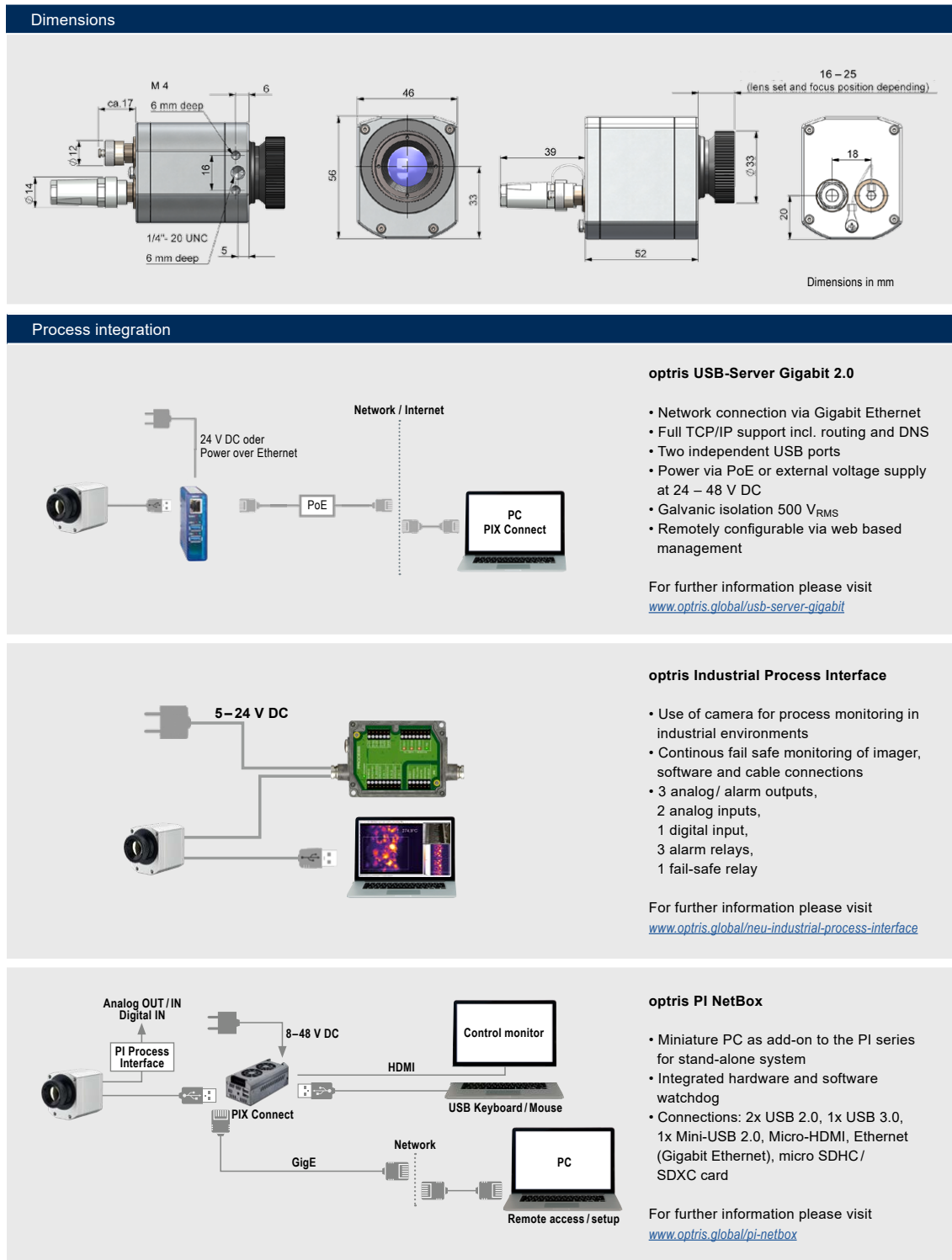
For further information as well as the product configurator, please visit www.optris.global/thermal-imager-optris-pi-400i-pi-450i

¹⁾ Accuracy for the (20°C) 150 °C ... 900 °C range effective starting at 150 °C
²⁾ For further information see operator's manual.

Optris GmbH · Ferdinand-Buisson-Str. 14 · 13127 Berlin · Germany
 Phone: +49 30 500 197-0 · Fax: +49 30 500 197-10 · Email: info@optris.global · www.optris.global

Figure B.2: Optris PI 400i datasheet, page 1.

optris PI 400i



Specifications are subject to change without further notice · PI 400i-DS-EN2019-12-A

Figure B.3: Optris PI 400i datasheet, page 2.

B.2.2 IR Camera application flowchart

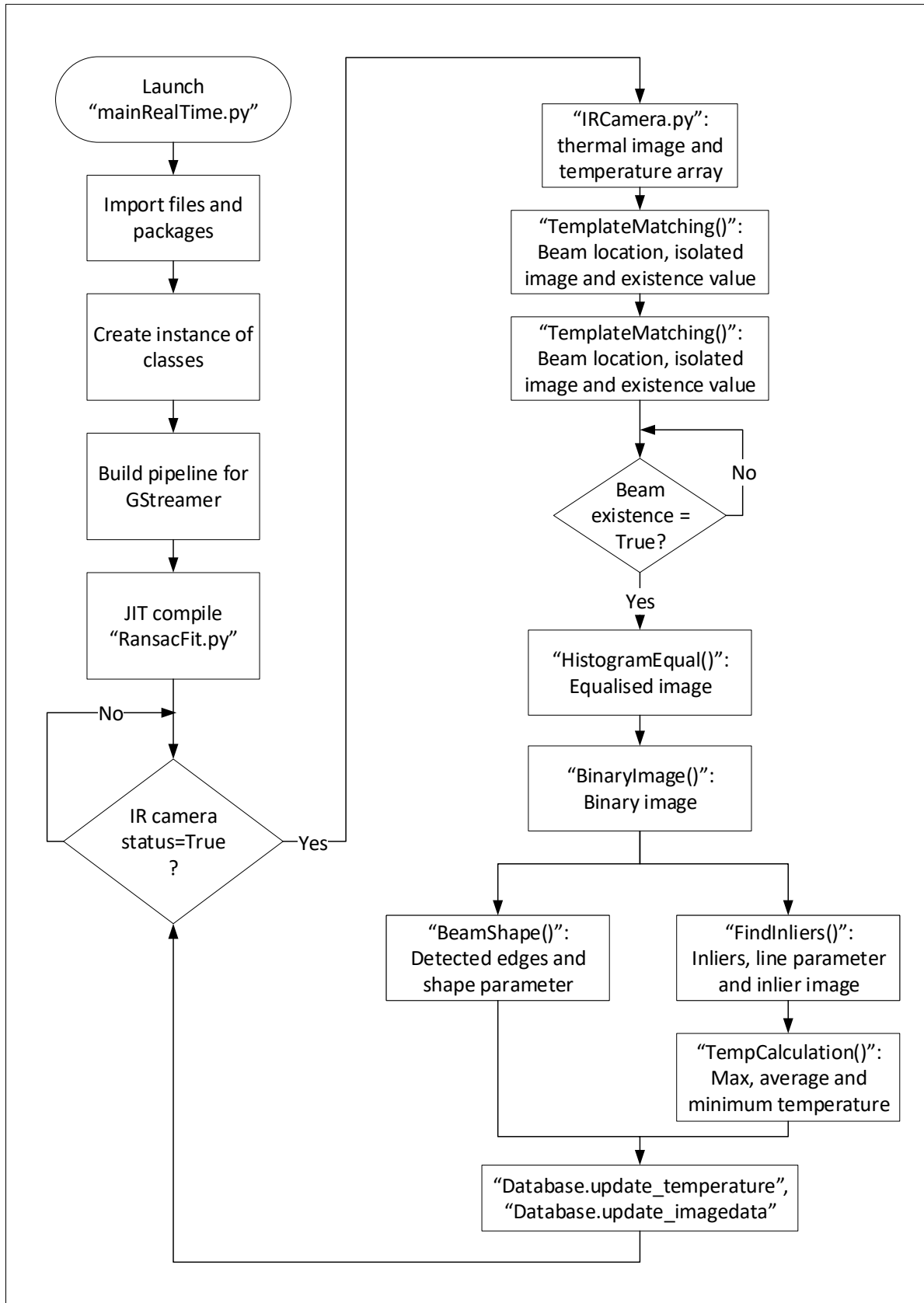


Figure B.4: Camera application process flowchart

B.2.3 Synthetically developed images



Table B.1: Synthetically developed image number 2.

Detected edges:	
Y-coordinate	Number of edges
0	0
20	3
40	2
60	2
80	4
100	4
120	4
140	7
160	4

Table B.2: Number of detected edges in image number 2.



Table B.3: Synthetically developed image number 3.

Detected edges:	
Y-coordinate	Number of edges
0	0
20	3
40	2
60	2
80	2
100	2
120	2
140	3
160	2

Table B.4: Number of detected edges in image number 3.



Table B.5: Synthetically developed image number 4.

Detected edges:	
Y-coordinate	Number of edges
0	0
20	3
40	2
60	4
80	4
100	6
120	4
140	2
160	2

Table B.6: Number of detected edges in image number 4.

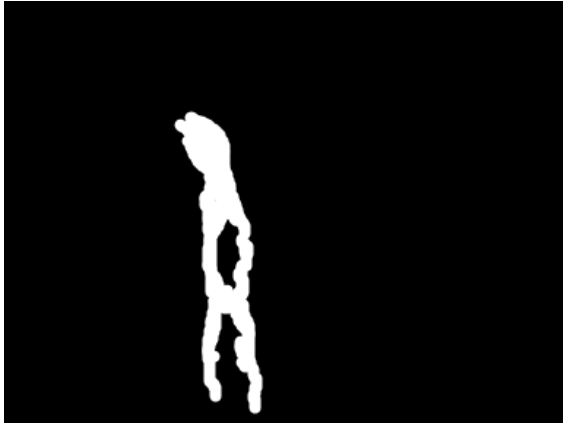


Table B.7: Synthetically developed image number 5.

Detected edges:	
Y-coordinate	Number of edges
0	0
20	3
40	2
60	2
80	4
100	4
120	4
140	2
160	4

Table B.8: Number of detected edges in image number 5.

B.3 Human Machine Interface

B.3.1 Flask web-HMI homepage

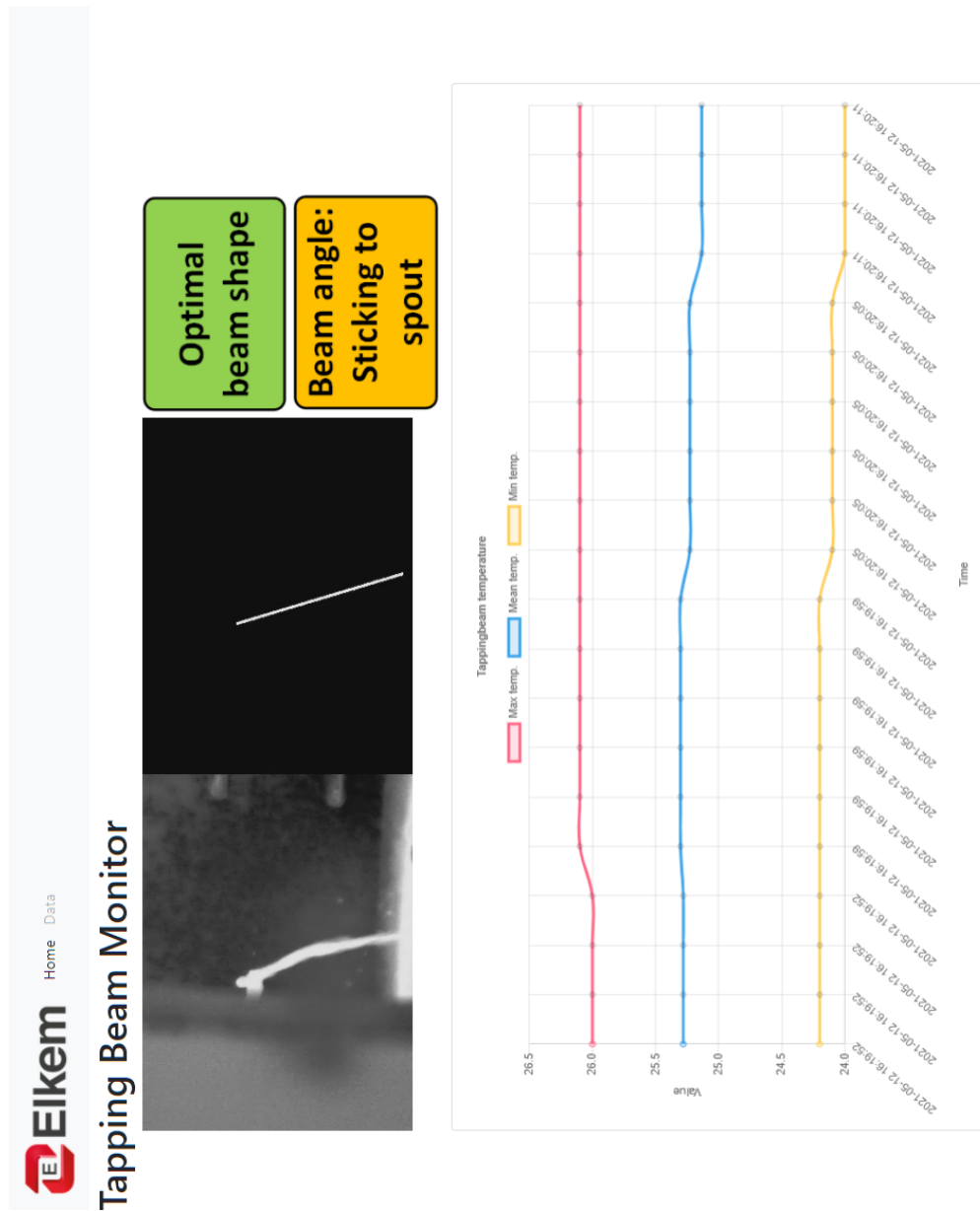


Figure B.5: HMI homepage

B.4 Database file

B.4.1 Temperature table

id	tempMax	tempMean	tempMin	timestamp
1	29.2	28.1597765363128	26.3	2021-05-13 11:06:33
2	29.2	28.3669619422572	26.7	2021-05-13 11:06:36
3	29.2	28.2631596306069	26.5	2021-05-13 11:06:40
4	29.2	28.3225806451613	26.7	2021-05-13 11:06:43
5	29.2	28.2537211569711	26.5	2021-05-13 11:06:46
6	29.2	28.3802344513188	26.8	2021-05-13 11:06:49
7	29.1	28.3627263747119	27.0	2021-05-13 11:06:52
8	29.1	28.0893904448105	26.3	2021-05-13 11:06:55
9	29.0	27.9879572677242	26.3	2021-05-13 11:06:58
10	29.0	28.0710611979167	26.2	2021-05-13 11:07:01
11	28.9	28.0672745034191	26.4	2021-05-13 11:07:04
12	28.9	27.9145087833442	26.1	2021-05-13 11:07:07
13	28.9	27.7831585845347	25.9	2021-05-13 11:07:10
14	29.0	28.2003293807642	26.7	2021-05-13 11:07:13
15	29.0	28.0917709019091	26.5	2021-05-13 11:07:16
16	28.9	27.9019785922802	26.1	2021-05-13 11:07:19
17	28.9	27.8538734667527	26.1	2021-05-13 11:07:22
18	28.9	27.8508303484207	26.0	2021-05-13 11:07:25
19	29.0	27.8365782664942	26.2	2021-05-13 11:07:28
20	28.9	27.8111111111111	25.9	2021-05-13 11:07:31
21	28.9	27.7957746478873	26.1	2021-05-13 11:07:34
22	28.9	27.9865416255347	26.3	2021-05-13 11:07:37
23	28.9	28.00393240169	26.4	2021-05-13 11:07:40
24	28.8	27.7106796116505	26.1	2021-05-13 11:07:43
25	28.9	27.8856863384415	26.2	2021-05-13 11:07:47
26	28.8	27.9283431180691	26.2	2021-05-13 11:07:50
27	28.8	27.9695197647827	26.4	2021-05-13 11:07:53
28	28.8	27.9125367286974	26.2	2021-05-13 11:07:56
29	28.8	27.8934378060725	26.2	2021-05-13 11:07:59
30	28.8	27.6779242174629	26.0	2021-05-13 11:08:02
31	28.9	28.0454098360656	26.5	2021-05-13 11:08:06
32	28.7	27.7583496412264	26.0	2021-05-13 11:08:09
33	28.8	27.9427035830619	26.4	2021-05-13 11:08:12
34	28.8	27.952274225445	26.4	2021-05-13 11:08:15
35	28.9	27.9328348504551	26.2	2021-05-13 11:08:18
36	28.8	27.8921971922951	26.4	2021-05-13 11:08:21
37	28.8	27.9887269193392	26.6	2021-05-13 11:08:25
38	28.7	27.7643840104849	26.2	2021-05-13 11:08:28
39	28.7	27.5547728768927	25.9	2021-05-13 11:08:31
40	28.7	27.8295601552393	26.1	2021-05-13 11:08:35
41	28.6	27.7725991478204	26.0	2021-05-13 11:08:38
42	28.6	27.6518458020255	25.9	2021-05-13 11:08:41

1

Figure B.6: Database temperature data.

B.4.2 Image data table

id	inliers	lineXY	lineAngle	beamExistence	beamShape	beamStatus	timeStamp
1			76.0067993793224	1.0		1.0	2021-05-13 11:06:33
2			71.9671344730085	1.0		1.0	2021-05-13 11:06:36
3			71.8167468131493	1.0		1.0	2021-05-13 11:06:40
4			71.0226258870393	1.0		1.0	2021-05-13 11:06:43
5			75.2744579200138	1.0		1.0	2021-05-13 11:06:46
6			70.3452964709037	1.0		1.0	2021-05-13 11:06:49
7			68.7160600011367	1.0		1.0	2021-05-13 11:06:52
8			68.9512513769319	1.0		1.0	2021-05-13 11:06:55
9			68.7815871026929	1.0		1.0	2021-05-13 11:06:58
10			71.5055951837049	1.0		1.0	2021-05-13 11:07:01
11			70.1846329140177	1.0		1.0	2021-05-13 11:07:04
12			71.5133601927014	1.0		1.0	2021-05-13 11:07:07
13			74.739982686605	1.0		1.0	2021-05-13 11:07:10
14			71.5444106617952	1.0		1.0	2021-05-13 11:07:13
15			65.4598519892283	1.0		1.0	2021-05-13 11:07:16
16			71.7246490359247	1.0		1.0	2021-05-13 11:07:19
17			71.6910680842454	1.0		1.0	2021-05-13 11:07:22
18			73.344532172439	1.0		1.0	2021-05-13 11:07:25
19			76.1737314452193	1.0		1.0	2021-05-13 11:07:28
20			73.6284450028599	1.0		1.0	2021-05-13 11:07:31
21			76.716413751595	1.0		1.0	2021-05-13 11:07:34
22			70.3509330907169	1.0		1.0	2021-05-13 11:07:37
23			70.0427251924203	1.0		1.0	2021-05-13 11:07:40
24			71.6054572208119	1.0		1.0	2021-05-13 11:07:43
25			69.794884117159	1.0		1.0	2021-05-13 11:07:47
26			72.4746637142078	1.0		1.0	2021-05-13 11:07:50
27			69.5349342450218	1.0		1.0	2021-05-13 11:07:53
28			69.5080966069459	1.0		1.0	2021-05-13 11:07:56
29			71.6934431930889	1.0		1.0	2021-05-13 11:07:59
30			72.2649874894791	1.0		1.0	2021-05-13 11:08:02
31			71.8895310356115	1.0		1.0	2021-05-13 11:08:06
32			74.3621197671694	1.0		1.0	2021-05-13 11:08:09
33			70.5369703732876	1.0		1.0	2021-05-13 11:08:12
34			71.5504609610671	1.0		1.0	2021-05-13 11:08:15
35			71.7215966331984	1.0		1.0	2021-05-13 11:08:18
36			71.5156923165169	1.0		1.0	2021-05-13 11:08:21
37			71.1415638538675	1.0		1.0	2021-05-13 11:08:25
38			71.5911302738264	1.0		1.0	2021-05-13 11:08:28
39			71.5799023378427	1.0		1.0	2021-05-13 11:08:31
40			71.9998494817049	1.0		1.0	2021-05-13 11:08:35
41			70.5096953533994	1.0		1.0	2021-05-13 11:08:38

1

Figure B.7: Database image data.

Code

C.1 Computer vision algorithms

C.1.1 mainRealTime.py

```
1 from src import IRCamera, BeamDetector, FeatureTracking, Database,
   RansacFit
2 from datetime import datetime
3 from time import sleep, time
4 import numpy as np
5 import cv2
6 import os
7
8 path = os.path.dirname(os.path.abspath(__file__))
9
10 # Template root folder
11 template_root = 'template/frame2904.png'
12
13 # Initialize variables
14 thresh_gain = 500 # binary image threshold gain, tune this value
   between 0 and 255 for better binary representation of tapping beam
15 heigth_top = 0 # top heigth of the beam shape edge detection algorithm
16 heigth_bottom = 0 # bottom heigth of the beam shape edge detection
   algorithm
17 thresh_inlier = 3 # inlier distance threshold for the RANSAC algorithm
18 iterations = 1000 # number of iterations in the RANSAC algorithm
19 samples = 4 # number of samples per iteration to fit the RANSAC model
20 inliers = 50 # minimum number of inliers for the RANSAC model
21
22
23 # Create instance of classes
24 beamDetector = BeamDetector.BeamDetector(thresh_gain, heigth_top,
   heigth_bottom)
25
26 featureTracking = FeatureTracking.FeatureTracking(template_root)
```



```

27
28 ransacFit = RansacFit.RansacFit(thresh_inlier, iterations, samples,
    inliers)
29
30 irCamera = IRCamera.IRCamera(path)
31
32 path_db = os.path.join(path, 'webapp/database/data.db' )
33 database = Database.Database(path_db)
34
35
36 # Frame dimensions
37 framerate = 10
38 frame_width = 384
39 frame_height = 288
40
41 # Create videowriter as a SHM source, two images side-by-side
42 out = cv2.VideoWriter("appsrv ! video/x-raw, format=BGR ! queue !
    videoconvert ! video/x-raw, format=BGRx ! nvvidconv ! omxh264enc !
    video/x-h264, stream-format=byte-stream ! h264parse ! rtpH264pay pt
    =96 config-interval=1 ! udpsink host=0.0.0.0 port=5000", 0,
    framerate, (frame_width*2, frame_height))
43
44 # Initiate loop parameters
45 i = 0
46 k = 0
47 beam_existence_old = 1
48 beam_existence_old_old = 1
49
50 if __name__ == '__main__':
51
52     # Compile RansacFit.py with JIT
53     ransacFit.InitJIT((frame_height, frame_width))
54
55     # Check camera status
56     status = irCamera.status()
57
58     while status is True:
59
60         # Add sleep time to the program - used to lower the CPU usage
61         sleep(0.2 - time() % 0.2)
62
63         # Get thermal image and array from IR camera
64         image_thermal, array_temp = irCamera.getThermal()
65
66
67         # Find the tapping beam region and check for existence of the
            tappingbeam

```

```

68     loc, image_tapping, beam_existence = featureTracking.
        TemplateMatching(image_thermal)
69
70     # Calculate the average of the beam existence parameter, used to
        filter out transient values
71     beam_average_existence = np.mean([beam_existence,
        beam_existence_old, beam_existence_old_old])
72
73     if beam_average_existence == 1:
74
75         # Equalize the histogram of the image
76         image_eq = beamDetector.HistogramEqual(image_tapping)
77
78         # Create a binary image
79         image_binary = beamDetector.BinaryImage(image_eq)
80
81         # Calculate the beam-shape parameters
82         beam_data, beam_status = beamDetector.BeamShape(loc,
        image_binary)
83
84
85         # Use RansacFit to find the inliers
86         inliers, line_xy, image_inliers, theta_line = ransacFit.
        FindInliers(image_binary)
87
88
89         # Detect mean, max and min temperature in the tappingbeam
90         temp_max, temp_mean, temp_min = beamDetector.TempCalculation
        (array_temp, image_inliers)
91
92         # Convert to BGR format
93         image_inliers = cv2.cvtColor(np.array(image_inliers), cv2.
        COLOR_GRAY2BGR)
94
95         # Horizontally stack the images before sending them to the
        GStreamer pipeline
96         image_GST = np.hstack((image_thermal, image_inliers))
97
98     else:
99
100        # Thermal image side-by-side, if the template matching fails
101        image_GST = np.hstack((image_thermal, image_thermal))
102
103        # Initialize the remaining values
104        temp_max, temp_mean, temp_min = 0,0,0
105        inliers, line_xy, theta_line, beam_data, beam_status = 0, 0,
        0, 0, 0

```

```
106
107     # Write to SHM
108     out.write(image_GST)
109
110     # Save data to database, for every 5th iteration
111     if i >= 5:
112         # Time
113         timestamp = datetime.now().replace(microsecond=0)
114
115         # Update temperature data
116         database.update_temperature(( temp_max, temp_mean, temp_min,
117                                     timestamp ))
118
119         # Update image date
120         database.update_imagedata(( inliers, line_xy, theta_line,
121                                   beam_existence, beam_data, beam_status, timestamp ))
122
123         i = 0
124
125     i = i + 1
126
127     # Update existence parameter
128     beam_existence_old = beam_existence
129     beam_existence_old_old = beam_existence_old
```

C.1.2 IRCamera.py

```

1  | #! /usr/bin/env python3
2  | from ctypes.util import find_library
3  | import numpy as np
4  | import ctypes as ct
5  | import cv2
6  | import os
7  | import sys
8  | import time
9  |
10 | class IRCamera(object):
11 |     """
12 |     IRCamera object initializes the thermal camera and
13 |     returns the thermal image and the temperature array
14 |     """
15 |     def __init__(self,source):
16 |         """
17 |         Initialize camera variables
18 |         """
19 |         # create log dir if non existent
20 |         if not os.path.exists('./src/log'):
21 |             os.mkdir('./src/log')
22 |
23 |         if not os.path.exists('./src/images'):
24 |             os.mkdir('./src/images')
25 |
26 |
27 |         # load library
28 |         if os.name == 'nt':
29 |             #windows:
30 |             path_dll = os.path.join(source, "bin\\x64\\libirimager.dll"
31 |                                     )
32 |             self.libir = ct.CDLL(path_dll)
33 |
34 |             #init vars for Windows
35 |             self.pathXml = ct.c_char_p(b'./config/20022030.xml')
36 |             self.pathFormat = ct.c_char_p(b'./config/')
37 |             self.pathLog = ct.c_char_p(b'./log/logfilename')
38 |             print('==== Windows OS ====')
39 |
40 |         else:
41 |             print('DLL path:',source)
42 |             #linux:
43 |             self.libir = ct.cdll.LoadLibrary(ct.util.find_library("
44 |                                     irdirectsdk"))

```

```

45     path_xml = os.path.join(source, "config/20022030.xml" )
46     self.pathXml = ct.c_char_p(path_xml.encode())
47     self.pathFormat = ct.c_char_p()
48     path_log = os.path.join(source, "log/logfilename" )
49     self.pathLog = ct.c_char_p(path_log.encode())
50     print('==== Linux OS ====')
51
52
53     # init vars for thermal camera
54     self.palette_width = ct.c_int()
55     self.palette_height = ct.c_int()
56     self.thermal_width = ct.c_int()
57     self.thermal_height = ct.c_int()
58     self.serial = ct.c_ulong()
59
60     # instance of EvoIRFrameMetadata class
61     self.metadata = self.EvoIRFrameMetadata()
62
63     # init lib
64     self.retLib = self.libir.evo_irimager_usb_init(self.pathXml,
65         self.pathFormat, self.pathLog)
66     print('==== Init IR imager library ====')
67     if self.retLib != 0:
68         print("error at init")
69         exit(self.retLib)
70
71     # get the serial number
72     ret = self.libir.evo_irimager_get_serial(ct.byref(self.serial))
73     print('serial: ' + str(self.serial.value))
74
75     # get thermal image size
76     self.libir.evo_irimager_get_thermal_image_size(ct.byref(self.
77         thermal_width), ct.byref(self.thermal_height))
78     print('thermal width: ' + str(self.thermal_width.value))
79     print('thermal height: ' + str(self.thermal_height.value))
80
81     # init thermal data container
82     self.np_thermal = np.zeros([self.thermal_width.value * self.
83         thermal_height.value], dtype=np.uint16)
84     self.npThermalPointer = self.np_thermal.ctypes.data_as(ct.
85         POINTER(ct.c_ushort))
86
87     # get palette image size, width is different to thermal image
88     width duo to stride alignment!!!
89     self.libir.evo_irimager_get_palette_image_size(ct.byref(self.
90         palette_width), ct.byref(self.palette_height))
91     print('palette width: ' + str(self.palette_width.value))

```

```

86     print('palette height: ' + str(self.palette_height.value))
87
88     # init image container
89     self.np_img = np.zeros([self.palette_width.value * self.
90         palette_height.value * 3], dtype=np.uint8)
91     self.npImagePointer = self.np_img.ctypes.data_as(ct.POINTER(ct.
92         c_ubyte))
93
94     """
95     Initialize calibration variables
96     """
97     # Initilize camera parameters
98     self.f = 0.013 # focal length of the 029 lens on the Optris
99     PI400i
100
101     self.Sx = 384 # camera resolution in the x-axis (horisontal)
102     self.Sy = 288 # camera resolution in the y-axis (vertical)
103
104     # Camera intrinsic calibration matrix
105     self.mtx = np.array([[ -self.f/self.Sx, 0,
106         self.Sx/2],
107         [ 0, -self.f/self.Sy,
108         self.Sy/2],
109         [ 0, 0,
110         1]])
111
112     # Camera distortion calibration matrix
113     self.dist = 0
114
115     # Splits up calibration into making a map, and doing the
116     remapping in calibrate
117
118     # member function
119     # This is faster than doing cv2.undistort()
120     self.map1, self.map2 = cv2.initUndistortRectifyMap(
121         self.mtx,
122         self.dist,
123         np.eye(3),
124         self.mtx,
125         (self.Sx, self.Sy),
126         cv2.CV_32FC1
127     )
128
129     def status(self):
130         """
131         Returns a boolean value for the initialization status of the
132         camera
133         """
134

```

```

125         if self.retLib == 0:
126             status = True
127             print('==== IR camera ready ====')
128
129         else:
130             status = False
131             print('Error at init. Camera status:',status)
132
133         return status
134
135
136
137
138     def getThermal(self):
139         """
140         Function for returning the thermal image and temperature array
141         """
142
143         ret = self.libir.evo_irimager_get_thermal_palette_image_metadata
144             (self.thermal_width, self.thermal_height, self.
145              npThermalPointer, self.palette_width, self.palette_height,
146              self.npImagePointer, ct.byref(self.metadata))
147
148
149         if ret != 0:
150             print('error on evo_irimager_get_thermal_palette_image ' +
151                  str(ret))
152
153
154         # get the palette image
155         thermal_image = self.np_img.reshape(self.palette_height.value,
156                                             self.palette_width.value, 3)[:,:,:-1]
157
158         # get the thermal array
159         thermal_vector = self.np_thermal/10. - 100.
160
161         thermal_array = thermal_vector.reshape(self.thermal_height.value
162                                              , self.thermal_width.value)
163
164         return thermal_image, thermal_array
165
166     def calibrate(self, image):
167         """
168         Perform calibration of input OpenCV image
169         """
170         # Make copy of input image

```

```

166     # # Perform color calibration
167     # image_float = np.array(image, float) * self.gain_matrix
168
169     # # Clip to keep values between 0 and 255
170     # # Using [:] sets the value of object "image" without making a
        new object
171     # # i.e. just replaces in-object which does not need a return
        statement
172     # calibrated[:] = np.clip(image_float, 0, 255)
173
174     # Apply camera distortion calibration
175     calibrated = image.copy()
176     calibrated[:] = cv2.remap(calibrated, self.map1, self.map2, cv2.
        INTER_LINEAR)
177     return calibrated
178
179
180     class EvoIRFrameMetadata(ct.Structure):
181         """
182         Structure that contains additional frame information from the
            camera
183         """
184
185         # Define EvoIRFrameMetadata structure for additional frame info
186         _fields_ = [
187             ("counter", ct.c_uint),
188             ("counterHW", ct.c_uint),
189             ("timestamp", ct.c_longlong),
190             ("timestampMedia", ct.c_longlong),
191             ("flagState", ct.c_int),
192             ("tempChip", ct.c_float),
193             ("tempFlag", ct.c_float),
194             ("tempBox", ct.c_float),
195         ]
196
197
198
199
200     if __name__ == "__main__":
201
202         path = os.path.dirname(os.path.abspath(__file__))
203
204         # Crop area, tapping test
205         class Template():
206             x = 145
207             y = 40
208             w = 80

```



```
209         h = 230
210
211     xyTemplate = Template()
212
213     # instance of IRCamera class
214     irCamera = IRCamera(path)
215
216     # capture and display image till q is pressed
217     t, i = 0, 0
218     while chr(cv2.waitKey(1) & 255) != 'q':
219
220
221         # get thermal image and temperature array
222         image_thermal, array_thermal = irCamera.getThermal()
223
224         # Index thermal image array to create template image
225         image_template = cv2.cvtColor(image_thermal, cv2.COLOR_BGR2GRAY)
226         [xyTemplate.y:(xyTemplate.y + xyTemplate.h), xyTemplate.x:(
227             xyTemplate.x + xyTemplate.w)]
228
229         # Save images
230         cv2.imwrite('../src/images/frame{}.png'.format(i),
231             image_template)
232         print('Captured!')
233         i +=1
```

C.1.3 FeatureTracking.py

```
1
2 import os
3 import numpy as np
4 import matplotlib.pyplot as plt
5 import cv2
6 import time
7
8
9 class FeatureTracking(object):
10     """
11     Class for tracking the tapping beam, uses template matching finding
12     the tapping beam region.
13     """
14     def __init__(self,templatePath):
15         """
16         Initialize variables
17         """
18         self.templatePath = templatePath
19
20
21     def TemplateMatching(self,image):
22         """
23         Template matching for finding the specific image region where
24         the tapping beam is located.
25         Requires a template of the tapping beam, use Template.py to
26         create the desired template image.
27         """
28         # Read template
29         template_image = cv2.imread(self.templatePath)
30
31         # Convert template image to grayscale
32         template_image = cv2.cvtColor(template_image,cv2.COLOR_BGR2GRAY)
33
34         # Convert CV image to grayscale
35         image_gray = cv2.cvtColor(image, cv2.COLOR_BGR2GRAY)
36
37         # Get template height and width
38         template_w, template_h = template_image.shape[:,-1]
39
40         # Get image height and width
41         image_w, image_h = image_gray.shape[:,-1]
42
43         # Convert CV image to grayscale
44         image_gray = cv2.cvtColor(image, cv2.COLOR_BGR2GRAY)
```

```

44     # Perform match operations
45     res = cv2.matchTemplate(image_gray,template_image,cv2.
        TM_CCOEFF_NORMED)
46     # Specify a threshold for the matching
47     threshold = 0.8
48
49     # Store the coordinates of matched area in a numpy array
50     loc = np.where( res >= threshold)[::-1]
51
52     # Base of the segmented image
53     image_segmented = np.zeros(image_gray.shape,np.uint8)
54
55     if bool(loc[0].any()) is False:
56         loc = (0, 0, image_w, image_h)
57         beam_existence = 0
58
59         # Isolate the tapping ROI
60         image_segmented = image_segmented
61
62
63     else:
64         loc = (int(round(np.mean(loc[0]),0)),int(round(np.mean(loc
            [1]),0)),template_w, template_h)
65         beam_existence = 1
66         # Isolate the tapping ROI
67         image_segmented[loc[1]:(loc[1] + loc[3]), loc[0]:(loc[0] +
            loc[2])] = image_gray[loc[1]:(loc[1] + loc[3]), loc[0]:(
            loc[0] + loc[2])]
68
69
70     return loc, image_segmented, beam_existence
71
72
73     def BoundingBox(self,image,loc,theta):
74         """
75         Draw a bounding box over the tappingbeam grayscale image.
76         The coordinates for the bounding box is numbered ccw,
77         starting with the top left corner.
78         """
79
80         # Define top left corner, width and heigth
81         pt0, width, heigth = (loc[0],loc[1]), loc[2], loc[3]
82
83         # Calculate the absolute value of the tapping beam angle
84         absDelta = np.ceil(np.abs(heigth/np.tan(theta[0])))
85
86         # Correct the offset

```

```
87     if theta[1] < 90:
88         delta = absDelta
89     else:
90         delta = - absDelta
91
92     # Define corners
93     pt1 = [pt0[0], pt0[1]]
94     pt2 = [pt0[0] + delta, pt0[1] + height]
95     pt3 = [pt0[0] + width + delta, pt0[1] + height]
96     pt4 = [pt0[0] + width, pt0[1]]
97
98     # Create list of corners
99     corners = [np.array([ pt1, pt2, pt3, pt4 ], dtype = int)]
100
101     # Draw the contour
102     image_contour = cv2.drawContours(np.array(image), corners
103         , -1, (255, 255, 255), 2)
104
104     return image_contour
```

C.1.4 BeamDetector.py

```

1  import numpy as np
2
3
4
5  class BeamDetector(object):
6
7      def __init__(self, thresh_gain = 100, heighth_top = 0, heighth_bottom =
8          0):
9          """
10             Initialize the variables.
11             """
12             # BinaryImage
13             self.thresh_gain = thresh_gain
14
15             # BeamShape
16             self.heighth_top = heighth_top # starting position for the edge
17                 detection
18             self.heighth_bottom = heighth_bottom # djust stop position for the
19                 edge detetion
20
21     def BinaryImage(self, image):
22         """
23         Binary image thresholding based upon temperature/image
24         brightness.
25         This algorithm is based upon the idea that the tapping beam
26         always
27         exists in the brightest image pixels, within some margin.
28         """
29         # Base of the binary image
30         image_binary = np.zeros(image.shape, np.uint8)
31         image_white = np.uint8(255)
32
33         # Find the pixels with maximum brightness
34         i_mean = np.mean(image)
35         i_max = np.amax(image)
36         i_thresh = np.ceil(i_max - i_mean/i_max*self.thresh_gain)
37         indices = np.where(image >= i_thresh)
38
39         # print('Threshold:', i_thresh, 'Max:', i_max, 'Mean:', i_mean)
40
41         # Converts the coordinates
42         coordinates_x = np.transpose(indices[0])
43         coordinates_y = np.transpose(indices[1])
44
45         image_binary[coordinates_x, coordinates_y] = image_white

```

```
42     return image_binary
43
44
45
46     def HistogramEqual(self, image):
47         """
48         Function for normalizing the histogram
49         https://www.imageprocessing.com/2011/04/matlab-code-histogram-
50             equalization.html
51         """
52         # Create histogram vector
53         histogram = np.zeros(256)
54         buffer, _ = np.histogram(image,
55                                 bins=np.arange(256),
56                                 range=(0, 1))
57
58         histogram[0:buffer.size]=buffer
59
60         # Cumulative distrobution of the histogram
61         cdf = histogram.cumsum()
62
63         # Create masked array, excluding indices where the value is zero
64         cdf_m = np.ma.masked_equal(cdf,0)
65
66         # Scale the histogram to values between 0 and 255
67         cdf_m = (cdf_m - cdf_m.min())*255/(cdf_m.max()-cdf_m.min())
68
69         # Fill inn the blank indexes with the value = 0
70         cdf = np.ma.filled(cdf_m,0).astype('uint8')
71
72         # Create the new equalised image
73         image_eq = cdf[image]
74
75         return image_eq
76
77     def BeamShape(self, loc, image):
78         """
79         Slices the tapping beam into horizontal vectors with even
80             spacing,
81         detects the edges by convolving a filter with the image vector.
82         """
83         # Define top left corner, width and heighth
84         pt0, width, height = (loc[0],loc[1]), loc[2], loc[3]
85
86         # Isolate the pixels of the tappingbeam, found with template.
```

```

87     image_isolated = np.zeros((height,width))
88     image_isolated = image[pt0[1]:(pt0[1] + height), pt0[0]:(pt0[0]
      + width)]
89
90     # For local testing
91     # image_isolated[:,10:20] = 0
92     # image_isolated[:,30:40] = 0
93
94     # Increment vector for iterating through the image in the y-
      direction
95     y_increment = np.arange(self.height_top, (height + self.
      height_bottom), 10)
96
97     # Empty array for storing the y-position and the detected number
      of edges
98     beam_data = np.zeros((len(y_increment),2))
99
100    # Initialize counter variable
101    k = 0
102
103    # Iterating through the image in the y-direction, row-by-row.
104    for i in y_increment:
105
106        # Convolve the extracted image data with a Gaussian
          derivative filter
107        row = image_isolated[i,:]
108        row_convolve = np.convolve([1,0,-1], row)
109
110        # Find peaks in dataset, inspired by: https://tcoil.info/
          find-peaks-and-valleys-in-dataset-with-python/
111        row_convolve_peak = (np.diff(np.sign(np.diff(np.abs(
          row_convolve)))) < 0).nonzero()[0] + 1
112
113        # Count number of edges in row
114        edges = len(row_convolve_peak)
115
116        # Save data
117        beam_data[k,:] = np.array([i,edges])
118
119        # Update counter
120        k += 1
121
122    # Remove noise, only accept data between 0 and 8
123    indices = np.where( beam_data[:,1]>8 )
124    coordinates_x = np.transpose(indices[0])
125
126    # Set the invalid values to zero

```

```

127     beam_data[coordinates_x, 1] = 0
128
129     # Calculate the mean of the tappingbeam shape-values
130     beam_value_mean = np.mean(beam_data[:,1])
131
132     if 3 >= beam_value_mean > 1:
133
134         beam_status = 1 # Optimal shape
135
136     elif beam_value_mean > 3:
137
138         beam_status = 0 # Sparse shape
139
140     else:
141
142         beam_status = 2 # Fault, check beam_data matrix or adjust
            the y-increment vector in BeamDetector.BeamShape()
143
144     return beam_data, beam_status
145
146
147
148     def TempCalculation(self, array_thermal, image_binary):
149         """
150         Calculates the mean, max and min temperature of the tapping beam
151         .
152         """
153
154         # Find the pixel coordinates for the tapping beam
155         indices = np.where(image_binary == 255)
156
157         # Converts the coordinates
158         coordinates_x = np.transpose(indices[0])
159         coordinates_y = np.transpose(indices[1])
160
161         coordinates_y = np.delete(coordinates_y, np.where(coordinates_y
            >= 382))
162
163         # Empty array
164         temp_region = np.zeros(image_binary.shape, np.uint8)
165
166         # Isolate the tapping beam temperature
167         temp_region = array_thermal[coordinates_x, coordinates_y]
168
169         # Calcualte mean, max and min temperature
170         temp_mean = np.mean(temp_region)
171         temp_max = np.max(temp_region)

```



```
171 |         temp_min = np.min(temp_region)
172 |
173 |         return temp_max, temp_mean, temp_min
```

C.1.5 RansacFit.py

```

1 import numpy as np
2 import numba as nb
3 import cv2
4 from numba import jit
5 from numba.experimental import jitclass
6
7
8 spec = [('thresh',nb.float32),
9         ('iterations',nb.uint32),
10        ('samples',nb.uint32),
11        ('inliers',nb.uint32)]
12 @jitclass(spec)
13 class RansacFit(object):
14
15     def __init__(self, thresh = 3, iterations = 1000, samples = 4,
16                 inliers = 50):
17
18         """
19         Initialize the variables for RansacFit(thresh),
20         where thresh is the inlier threshold for the RANSAC algorithm.
21         """
22         self.thresh = np.float32(thresh)
23         self.iterations = np.uint32(iterations)
24         self.samples = np.uint32(samples)
25         self.inliers = np.uint32(inliers)
26
27     def InitJIT(self, data_size):
28
29         """
30         Initializes the JIT - compiler.
31         Run this function directly after the instansiation of the
32         RansacFit class.
33         Note that the data input to this function should be of the same
34         size and type
35         as the data that is to be used in the FindInliers function
36         """
37         # Create sample data
38         data = np.ones(data_size, dtype = np.uint32)
39
40         data[30:150,150:170] = np.uint32(255)
41         data[100:150,100:150] = np.uint32(255)
42
43         # Rund the Ransac function with sample data
44         initInliers, _, _, _ = self.FindInliers(data)
45
46         # If sucesfull, print to terminal

```

```

44     if initInliers is not None:
45         print('==== JIT compiled RansacFit.py ====')
46
47
48     def FindInliers(self, data):
49
50         """
51         Finds the inliers in a dataset based upon a y=ax+b line model.
52         Takes in a binary image of the segmented tappingbeam, returns
53         the
54         position for.
55         """
56
57         # Find the matrix positions where data == 255
58         indices = np.where(data == 255)
59
60         # Converts the coordinates
61         data_x, data_y = np.transpose(indices[1]), np.transpose(indices
62             [0])
63
64         # Create data matrix - flipped axis for using image coordinate
65         system
66         data_xy = np.column_stack((data_x,data_y))
67
68         # Robustly find inlier data with self written RANSAC algorithm
69         bestModel, bestInliers= self.fit_ransac(data_xy, max_iters =
70             self.iterations, samples_to_fit = self.samples,
71             inlier_threshold = self.thresh, min_inliers = self.inliers)
72
73         # Generate coordinates of estimated line model
74         line_x_min = np.uint32(np.min(bestInliers[:,0])) # lowest index
75         value
76         line_x_max = np.uint32(np.max(bestInliers[:,0])) # highest index
77         value
78
79         line_x = np.arange(start = line_x_min, stop = line_x_max, dtype
80             = np.float64) # arange integers from lowest to highest
81         length_x = len(line_x) # length of line
82         line_y = np.zeros(length_x, dtype = np.float64) # empty zeros
83         vector for y-value
84
85         bestModel_a = bestModel[0,0]
86         bestModel_b = bestModel[1,0]*np.ones(length_x, dtype = np.
87             float64)
88         line_y = bestModel_a*line_x + bestModel_b

```

```

81     # Calculate the absolute angle for the line model
82     # startPoint is supposed to be the point on the RANSAC'ed
      line
83     # that is closest to the tappinspout (top right corner).
84     # endPoint is supposed to be the point on the RANSAC'ed line
85     # at the bottom of the image.
86
87     if line_y[0] == np.max(line_y):
88         startPoint = (line_x[-1], line_y[-1])
89         endPoint = (line_x[0], line_y[0])
90
91     elif line_y[0] == np.min(line_y):
92         startPoint = (line_x[0], line_y[0])
93         endPoint = (line_x[-1], line_y[-1])
94
95     # Find the delta-distance between startPoint and endPoint in x-
      and y-direction
96     deltaX = (endPoint[0] - startPoint[0])
97     deltaY = (endPoint[1] - startPoint[1])
98
99     theta_deg = np.arctan2(deltaY,deltaX)*180/np.pi
100
101
102     # Base of the binary image
103     image_binary = np.zeros(data.shape, dtype = np.uint8)
104     image_white = np.uint8(255)
105
106     # Create binary image of the inliers
107     index_length = len(bestInliers[:,0])
108     index_x = np.zeros((index_length,1), dtype = np.uint32)
109     index_y = np.zeros((index_length,1), dtype = np.uint32)
110     index_x[:,0] = bestInliers[:,0]
111     index_y[:,0] = bestInliers[:,1]
112
113     # Iterate through the image matrix
114     for ii in range(index_length):
115         image_binary[index_y[ii,0], index_x[ii,0]] = image_white
116
117     image_binary = np.copy(image_binary)
118
119     return bestInliers, bestModel, image_binary, theta_deg
120
121
122
123     def fit_lsq(self, X, y):
124
125         """

```

```
126     Source: https://medium.com/@iamhatesz/random-sample-consensus -  
127         bd2bb7b1be75  
128     Fits model for a given data using least squares.  
129     X should be an mxn matrix, where m is number of samples, and n  
130         is number of independent variables.  
131     y should be an mx1 vector of dependent variables.  
132     """  
133     b = np.ones((X.shape[0], 1), np.uint32)  
134     A = np.hstack((X, b)).astype(np.float64)  
135     theta = np.linalg.lstsq(A, y.astype(np.float64), rcond=-1)[0]  
136  
137     return theta  
138  
139  
140  
141     def evaluate_model(self, X, y, theta, inlier_threshold):  
142         """  
143         Source: https://medium.com/@iamhatesz/random-sample-consensus -  
144             bd2bb7b1be75  
145         Evaluates model and returns total number of inliers.  
146         X should be an mxn matrix, where m is number of samples, and n  
147             is number of independent variables.  
148         y should be an mx1 vector of dependent variables.  
149         theta should be an (n+1)x1 vector of model parameters.  
150         inlier_threshold should be a scalar.  
151         """  
152  
153         X = X.copy()  
154         b = np.ones((X.shape[0], 1), np.uint32)  
155         y = y.copy()  
156         A = np.hstack((y, X, b))  
157         theta = np.append(-1., theta)  
158  
159         distances = np.abs(np.sum(A*theta, axis=1)) / np.sqrt(np.sum(np.  
160             power(theta[:-1], 2)))  
161         inliers = (distances <= inlier_threshold).astype(np.bool_)  
162         num_inliers = np.count_nonzero(inliers)  
163  
164         return num_inliers, inliers  
165  
166  
167     def fit_ransac(self, data, max_iters, samples_to_fit,
```

```

    inlier_threshold, min_inliers):
168     """
169     Source: https://medium.com/@iamhatesz/random-sample-consensus -
        bd2bb7b1be75
170     """
171     # Create X and y vector from the dataset
172     data_len = len(data[:,0])
173     X = np.zeros((data_len,1), dtype = np.uint32)
174     y = np.zeros((data_len,1), dtype = np.uint32)
175     X[:,0] = data[:,0]
176     y[:,0] = data[:,1]
177
178     # Declare variables for RANSAC algorithm
179     best_model = np.zeros((2,1), dtype = np.float64)
180     best_inliers = np.zeros((X.shape[0], 1), dtype = np.bool_)
181     best_model_performance = np.uint32(0)
182     num_samples = X.shape[0]
183
184
185
186     # Iterate through the data set with random points
187     for i in range(max_iters):
188         sample = np.random.choice(num_samples, size=samples_to_fit,
            replace=False)
189         model_params = self.fit_lsq(X[sample], y[sample])
190         model_performance, model_inliers = self.evaluate_model(X, y,
            model_params, inlier_threshold)
191
192         if model_performance < min_inliers:
193             continue
194
195         if model_performance > best_model_performance:
196             best_model = model_params
197             best_model_performance = model_performance
198             best_inliers[:,0] = model_inliers
199
200
201     # Find the index for each inlier, achieve proper array
        dimensions
202     best_inliers_index = np.zeros((best_model_performance, 1), dtype
        = np.uint32) # create zeros vector
203     best_inliers_index[:,0] = np.where(best_inliers)[0].astype(np.
        uint32) # transfer the inlier indexes into the new vector
204
205     inliers_x = np.zeros((best_model_performance,1), dtype = np.
        uint32) # create zeros vector
206     inliers_y = np.zeros((best_model_performance,1), dtype = np.

```

```
uint32) # create zeros vector
207
208     inliers_x[:] = X[best_inliers_index.reshape(
        best_model_performance)] # transfer image position of the
        inliers in x-direction
209     inliers_y[:] = y[best_inliers_index.reshape(
        best_model_performance)] # transfer image position of the
        inliers in y-direction
210
211     inliers_xy = np.hstack((inliers_x, inliers_y)) # combine the
        inliers into a nx2 array
212
213
214     return best_model, inliers_xy
```

C.1.6 Database.py

```

1  from sqlite3 import Error
2  from datetime import datetime
3  import numpy as np
4  import sqlite3
5  import io
6  import os
7
8  class Database(object):
9
10
11     def __init__(self, dbPath):
12         """
13         Initalize variables
14         """
15         self.dbPath = dbPath
16
17         # Register a new datatype
18         def adapt_array(arr):
19             """
20             http://stackoverflow.com/a/31312102/190597 (SoulNibbler)
21             """
22             out = io.BytesIO()
23             np.save(out, arr)
24             out.seek(0)
25             return sqlite3.Binary(out.read())
26
27         def convert_array(text):
28             out = io.BytesIO(text)
29             out.seek(0)
30             return np.load(out)
31
32         # Converts np.array to TEXT when inserting
33         sqlite3.register_adapter(np.ndarray, adapt_array)
34
35         # Converts TEXT to np.array when selecting
36         sqlite3.register_converter("array", convert_array)
37
38         # Temperature data table
39         temp_table = """ CREATE TABLE IF NOT EXISTS temperature (
40             id            integer PRIMARY KEY,
41             tempMax       float          NOT NULL,
42             tempMean      float          NOT NULL,
43             tempMin       float          NOT NULL,
44             timestamp     text           NOT NULL); """
45
46

```



```

47
48     # Image data table
49     image_table = """ CREATE TABLE IF NOT EXISTS imagedata (
50     id                integer PRIMARY KEY,
51     inliers           arr                                NOT NULL,
52     lineXY            arr                                NOT NULL,
53     lineAngle        float                              NOT NULL,
54     beamExcistence   float                              NOT NULL,
55     beamShape        arr                                NOT NULL,
56     beamStatus       float                              NOT NULL,
57     timeStamp        text                               NOT NULL); """
58
59
60
61     # create a database connection
62     self.conn = self.create_connection()
63
64     # create tables
65     if self.conn is not None:
66         # create temperature table
67         self.create_table(temp_table)
68
69         # create image data table
70         self.create_table(image_table)
71
72         print("==== Created connection to database =====")
73
74     else:
75         print("Error! cannot create the database connection.")
76
77
78     def create_connection(self):
79         """ create a database connection to a SQLite database """
80         conn = None
81         try:
82             conn = sqlite3.connect(self.dbPath, check_same_thread =
83                 False, detect_types=sqlite3.PARSE_DECLTYPES)
84             return conn
85
86         except Error as e:
87             print(e)
88
89         return conn
90
91     def create_table(self, create_table_sql):
92         """ create a table from the create_table_sql statement
93         :param conn: Connection object

```

```
93         :param create_table_sql: a CREATE TABLE statement
94         :return:
95         """
96         try:
97             c = self.conn.cursor()
98
99             c.execute(create_table_sql)
100
101         except Error as e:
102             print(e)
103
104     def update_temperature(self, data):
105
106         sql = ''' INSERT INTO temperature(tempMax, tempMean, tempMin,
107             timestamp)
108             VALUES(?,?,?,?) '''
109
110         cur = self.conn.cursor()
111         cur.execute(sql, data)
112         self.conn.commit()
113         return cur.lastrowid
114
115     def update_imagedata(self, data):
116
117         sql = ''' INSERT INTO imagedata(inliers, lineXY, lineAngle,
118             beamExcistence, beamShape, beamStatus, timestamp)
119             VALUES(?,?,?,?,?,?,?) '''
120
121         cur = self.conn.cursor()
122
123         cur.execute(sql, data)
124
125         self.conn.commit()
126         return cur.lastrowid
127
128     def select_data(self):
129
130         cur = self.conn.cursor()
131         cur.execute("SELECT * FROM temperature ORDER BY id DESC LIMIT 1"
132             )
133
134         rows_temperature = cur.fetchall()
135
136         cur.execute("SELECT * FROM imagedata ORDER BY id DESC LIMIT 5")
137
138         rows_imagedata = cur.fetchall()
```

```
137         return rows_temperature, rows_imagedata
138
139 if __name__ == '__main__':
140
141
142     database = Database(r'/home/elkem/GitLab/elkemvision/webapp/database
143                        /data.db')
144
145     _, beam_data = database.select_data()
146     beam_existence = beam_data[0][4]
147     beam_angle = beam_data[0][3]
148     print(beam_angle)
```

C.2 Human Machine Interface

C.2.1 mainFlask.py

```
1 |#!/usr/bin/env python
2 |
3 |from webapp import app
4 |
5 |
6 |if __name__ == '__main__':
7 |    app.run(host='0.0.0.0', debug=False)
```

C.2.2 home.py

```
1 |#!/usr/bin/env python
2 |
3 |from webapp import app, path
4 |from src import Database
5 |from flask import render_template, url_for, Response
6 |import numpy as np
7 |import cv2
8 |import io
9 |import random
10|import json
11|import time
12|from datetime import datetime
13|import os
14|
15|
16|
17|
18|# Connect to database
19|path_db = os.path.join(path, 'database', 'data.db' )
20|database = Database.Database(path_db)
21|
22|# Capture UDP stream
23|cap = cv2.VideoCapture("udpsrc port=5000 ! application/x-rtp ! queue !
   |    rtph264depay ! h264parse ! nvv4l2decoder ! nvvidconv ! videoconvert
   |    ! appsink")
24|
25|# Defines the
26|beam_angle_good = np.array([0,72])
27|beam_angle_bad = np.array([72,120])
28|
29|# Yield images
30|def frame_thermal():
31|    while True:
32|        ret, frame = cap.read()
33|        frame_split = frame[:,0:383]
34|        if frame_split is not None:
35|            ret, frame_split = cv2.imencode('.jpg', frame_split)
36|            frame_split = frame_split.tobytes()
37|            yield (b'--frame\r\n'b'Content-Type: image/jpeg\r\n\r\n' +
   |                frame_split + b'\r\n')
38|
39|def frame_binary():
40|    while True:
41|        ret, frame = cap.read()
42|        frame_split = frame[:,383:767]
43|        if frame_split is not None:
```

```

44         ret, frame_split = cv2.imencode('.jpg', frame_split)
45         frame_split = frame_split.tobytes()
46         yield (b'--frame\r\n'b'Content-Type: image/jpeg\r\n\r\n' +
47               frame_split + b'\r\n')
48
49 def frame_shape():
50     while True:
51         _, beam_data = database.select_data()
52         beam_existence = np.mean(np.array([beam_data[0][4], beam_data
53             [1][4], beam_data[2][4], beam_data[3][4], beam_data[4][4]]))
54         beam_status = np.mean(np.array([beam_data[0][6], beam_data
55             [1][6], beam_data[2][6], beam_data[3][6], beam_data[4][6]]))
56
57         if beam_existence == 1 and beam_status == 1:
58             frame = cv2.imread('webapp/static/HMI_beam_shape_optimal.png
59                 ',1)
60
61         elif beam_existence == 1 and beam_status == 0:
62             frame = cv2.imread('webapp/static/HMI_beam_shape_split.png'
63                 ',1)
64
65         elif beam_existence == 0:
66             frame = cv2.imread('webapp/static/HMI_beam_shape_stopped.png
67                 ',1)
68
69         else:
70             frame = None
71
72         if frame is not None:
73             ret, frame = cv2.imencode('.png', frame)
74             frame = frame.tobytes()
75             yield (b'--frame\r\n'b'Content-Type: image/jpeg\r\n\r\n' +
76                   frame + b'\r\n')
77
78 def frame_angle():
79     while True:
80         _, beam_data = database.select_data()
81         beam_existence = np.mean(np.array([beam_data[0][4], beam_data
82             [1][4], beam_data[2][4], beam_data[3][4], beam_data[4][4]]))
83         beam_angle = np.mean(np.array([beam_data[0][3], beam_data[1][3],
84             beam_data[2][3], beam_data[3][3], beam_data[4][3]]))
85
86         if beam_existence == 1 and beam_angle_good[0] < beam_angle <=
87             beam_angle_good[1]:

```

```

81         frame = cv2.imread('webapp/static/
82             HMI_beam_angle_free_pouring.png',1)
83     elif beam_existence == 1 and beam_angle_bad[0] < beam_angle <=
84         beam_angle_bad[1]:
85         frame = cv2.imread('webapp/static/HMI_beam_angle_sticking.
86             png',1)
87     elif beam_existence == 0:
88         frame = cv2.imread('webapp/static/HMI_beam_shape_stopped.png
89             ',1)
90     else:
91         frame = None
92
93     if frame is not None:
94         ret, frame = cv2.imencode('.png', frame)
95         frame = frame.tobytes()
96         yield (b'--frame\r\n' + b'Content-Type: image/jpeg\r\n\r\n' +
97             frame + b'\r\n')
98
99 @app.route('/')
100 def index():
101     """ Home template """
102     return render_template('home.html')
103
104
105 @app.route('/camera_feed_thermal')
106 def camera_feed_thermal():
107     """Video streaming route."""
108     return Response(frame_thermal(), mimetype='multipart/x-mixed-replace
109         ; boundary=frame')
110
111 @app.route('/camera_feed_binary')
112 def camera_feed_binary():
113     """Video streaming route."""
114     return Response(frame_binary(), mimetype='multipart/x-mixed-replace;
115         boundary=frame')
116
117 @app.route('/beam_status_image')
118 def beam_status_image():
119     """ Beam status image """
120     return Response(frame_shape(), mimetype='multipart/x-mixed-replace;

```

```
        boundary=frame')
121
122
123 @app.route('/beam_angle_image')
124 def beam_angle_image():
125     """ Beam angle image """
126     return Response(frame_angle(), mimetype='multipart/x-mixed-replace;
        boundary=frame')
127
128
129 @app.route('/beam-temp')
130 def beam_temp():
131     """ Temperature-data route """
132     def generate_temperature_data():
133         while True:
134             temp_data, _ = database.select_data()
135             json_data = json.dumps(
136                 {'time': temp_data[0][4], 'value': temp_data[0][1:4]})
137             yield f"data:{json_data}\n\n"
138             time.sleep(1)
139
140     return Response(generate_temperature_data(), mimetype='text/event-
        stream')
```


C.2.3 base.html

```
1 <!doctype html>
2 <html lang=en>
3
4 <head>
5     <!-- Bootstrap CSS -->
6     <link rel="stylesheet" href="static/bootstrap/css/bootstrap.min.css"
7         >
8     <title>{% block title %}{% endblock %}</title>
9 </head>
10
11 <body>
12     <nav class="navbar navbar-expand-lg navbar-light bg-light">
13         <div class="container-fluid">
14             <a class="navbar-brand" href="#"></a>
16             <button class="navbar-toggler" type="button" data-bs-
17                 toggle="collapse" data-bs-target="#navbarNav" aria-
18                 controls="navbarNav" aria-expanded="false" aria-label=
19                 "Toggle navigation">
20                 <span class="navbar-toggler-icon"></span>
21                 </button>
22                 <div class="collapse navbar-collapse" id="navbarNav">
23                     <ul class="navbar-nav">
24                         <li class="nav-item">
25                             <a class="nav-link active" aria-current="page" href=
26                                 "/">Home</a>
27                         </li>
28                         <li class="nav-item">
29                             <a class="nav-link disabled" href="#" tabindex="-1"
30                                 aria-disabled="true">Data</a>
31                         </li>
32                     </ul>
33                 </div>
34             </div>
35         </nav>
36         {% block home %}
37
38         {% endblock %}
39
40     <!-- Option 1: Bootstrap Bundle with Popper -->
41     <script src="static/bootstrap/js/bootstrap.bundle.min.js"></
42         script>
43
44     <!-- Option 2: Separate Popper and Bootstrap JS -->
```

```
39 |
40 |     <!-- <script src="https://cdn.jsdelivr.net/npm/@popperjs/core@2
      |         .5.4/dist/umd/popper.min.js" integrity="sha384-
      |         q2kxQ16AaE6UbzuKqyBE9/u/KzioAlnx2maXQHiDX9d4/zp80k3f+M7DPm+
      |         Ib6IU" crossorigin="anonymous"></script>
41 |     <script src="https://cdn.jsdelivr.net/npm/bootstrap@5.0.0-beta1/
      |         dist/js/bootstrap.min.js" integrity="sha384-
      |         pQQkAEnwaBkjpqZ8RU1fF1AKtTcHJwFl3pblpTlHXybJjHpMYo79HY3hIi4NKxyj
      |         " crossorigin="anonymous"></script> -->
42 |
43 |
44 |     </body>
45 |
46 | </html>
```

C.2.4 home.html

```

1  {% extends "base.html" %}
2
3  {% block title %} Home Page {% endblock %}
4
5  {% block home %}
6
7  <body>
8      <h1>Tapping Beam Monitor</h1>
9  </body>
10 <body>
11     <!-- Image stream-->
12     <div class="container">
13         <div class="row">
14             <div class="col-md-4">
15                 
16             </div>
17
18             <div class="col-md-4">
19                 
20             </div>
21
22             <div class="col-md-4">
23                 <div class="row">
24                     <div class="col-12"></div>
26                     <div class="col-12"></div>
28                 </div>
29             </div>
30         </div>
31 </body>
32
33 <!-- Temperature plot -->
34 <body>
35     <div class="container">
36         <div class="row">
37             <div class="col-12">
38                 <div class="card">
39                     <div class="card-body">
40                         <canvas id="canvas_temp"></canvas>
41                     </div>
42                 </div>
43             </div>
44         </div>

```

```

45     </div>
46 </div>
47 <!--suppress JSUnresolvedLibraryURL -->
48 <script src="https://cdnjs.cloudflare.com/ajax/libs/jquery/3.4.0/
    jquery.min.js"></script>
49 <!--suppress JSUnresolvedLibraryURL -->
50 <!-- <script src="https://cdnjs.cloudflare.com/ajax/libs/twitter-
    bootstrap/4.3.1/js/bootstrap.min.js"></script> -->
51 <!--suppress JSUnresolvedLibraryURL -->
52 <script src="https://cdnjs.cloudflare.com/ajax/libs/Chart.js/2.8.0/
    Chart.min.js"></script>
53
54 <!-- Chart JavaScript -->
55 <!-- <script src="static/js/chart.min.js"></script> -->
56
57 <script>
58     $(document).ready(function () {
59         const config = {
60             type: 'line',
61             data: {
62                 labels: [],
63                 datasets: [{
64                     label: ["Max temp."],
65                     backgroundColor: ['rgba(255, 99, 132, 0.2)'],
66                     borderColor: ['rgba(255, 99, 132, 1)'],
67                     data: [],
68                     fill: false,
69                 }, {
70                     label: ["Mean temp."],
71                     backgroundColor: ['rgba(54, 162, 235, 0.2)'],
72                     borderColor: ['rgba(54, 162, 235, 1)'],
73                     data: [],
74                     fill: false,
75                 }, {
76                     label: ["Min temp."],
77                     backgroundColor: ['rgba(255, 206, 86, 0.2)'],
78                     borderColor: ['rgba(255, 206, 86, 1)'],
79                     data: [],
80                     fill: false,
81                 }
82             ]},
83         options: {
84             responsive: true,
85             title: {
86                 display: true,
87                 text: 'Tappingbeam temperature'
88             }

```

```
89         tooltips: {
90             mode: 'index',
91             intersect: false,
92             enabled: false
93         },
94         hover: {
95             mode: 'nearest',
96             intersect: true
97         },
98         scales: {
99             xAxes: [{
100                 display: true,
101                 scaleLabel: {
102                     display: true,
103                     labelString: 'Time'
104                 }
105             }],
106             yAxes: [{
107                 display: true,
108                 scaleLabel: {
109                     display: true,
110                     labelString: 'Value'
111                 }
112             }]
113         }
114     };
115 };
116
117 const context = document.getElementById('canvas_temp').
118     getContext('2d');
119
120 const lineChart = new Chart(context, config);
121
122 const source = new EventSource("/beam-temp");
123
124 source.onmessage = function (event) {
125     const data = JSON.parse(event.data);
126     if (config.data.labels.length === 20) {
127         config.data.labels.shift();
128         config.data.datasets[0].data.shift();
129         config.data.datasets[1].data.shift();
130         config.data.datasets[2].data.shift();
131     }
132     config.data.labels.push(data.time);
133     config.data.datasets[0].data.push(data.value[0]);
134 }
```

```
135 |         config.data.datasets[1].data.push(data.value[1]);
136 |         config.data.datasets[2].data.push(data.value[2]);
137 |         lineChart.update();
138 |     }
139 | });
140 | </script>
141 | </body>
142 |
143 | {% endblock %}
```